Engineering Human Hepatic Tissue for Modeling Liver-Stage Malaria
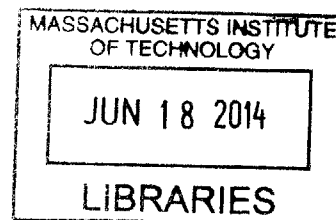
By

Shengyong Ng

B.S. Biomedical Engineering
The Johns Hopkins University, 2008

SUBMITTED TO THE DEPARTMENT OF BIOLOGICAL ENGINEERING IN PARTIAL FULFILLMENT OF
THE REQUIREMENTS FOR THE DEGREE OF

DOCTOR OF PHILOSOPHY IN BIOENGINEERING
AT THE
MASSACHUSETTS INSTITUTE OF TECHNOLOGY

JUNE 2014

Signature of Author: **Signature redacted**

Department of Biological Engineering
May 2, 2014

Certified by: **Signature redacted**

Sangeeta N. Bhatia, M.D., Ph.D.
John J. and Dorothy Wilson Professor of Health Sciences & Technology and Electrical
Engineering & Computer Science
Thesis Supervisor

Certified by: **Signature redacted**

Robert S. Langer, Sc.D.
David H. Koch Institute Professor
Thesis Supervisor

Accepted by: **Signature redacted**

Darrell J. Irvine, Ph.D.
Professor of Biological Engineering and Materials Science & Engineering
Thesis Committee Chair

1

Thesis Committee Members:

Charles M. Rice, Ph.D.
Maurice R. and Corinne P. Greenberg Professor in Virology, The Rockefeller University

Maria M. Mota, Ph.D.
Associate Professor, Instituto de Medicina Molecular, University of Lisbon

Engineering Human Hepatic Tissue for Modeling Liver-Stage Malaria

By
Shengyong Ng

Abstract

The *Plasmodium* liver stage is an attractive target for the development of antimalarial drugs and vaccines, as it provides an opportunity to interrupt the life cycle of the parasite at a critical early stage. However, targeting the liver stage has been difficult due to a lack of human liver models that robustly recapitulate host-pathogen interactions in a physiologically relevant cell type. Through the application of hepatic tissue engineering concepts and techniques, this thesis sought to develop advanced models of liver-stage malaria that will allow the facile interrogation of potential antimalarial drugs in primary human hepatocytes. In the first part of this work, we established liver-stage *Plasmodium* infection in an engineered microscale human liver platform based on micropatterned cocultures of primary human hepatocytes and supportive stromal cells, enabling medium-throughput phenotypic screens for potential antimalarial drugs in a more authentic host cell, and demonstrated the utility of this model for malaria vaccine testing. We further hypothesized and showed that recapitulation of a more physiologically relevant oxygen tension that is experienced by hepatocytes *in vivo* improved infection rates and parasite growth *in vitro*. Next, we demonstrated the feasibility of establishing liver-stage malaria infections in human induced pluripotent stem cell-derived hepatocyte-like cells (iHLCs), thus enabling the study of host genetic variation on liver-stage malaria infection and antimalarial drug responses. We also applied recently discovered small molecules to induce further hepatic maturation, thus increasing the utility of using iHLCs for antimalarial drug development. Finally, we designed and provided a proof-of-concept for a humanized mouse model of liver-stage malaria that involves the fabrication and ectopic implantation of PEG-cryogel-based engineered human artificial livers, and can be generated in a facile, rapid and scalable fashion for future preclinical antimalarial drug testing *in vivo*. The results of this research represent a three-pronged approach towards engineering scalable human liver models that recapitulate liver-stage malaria infection which may ultimately facilitate antimalarial drug discovery at various stages of the drug development pipeline.

Thesis Supervisor: Sangeeta N. Bhatia, M.D., Ph.D.
Title: Professor, Health Sciences and Technology/Electrical Engineering and Computer Science

Thesis Supervisor: Robert S. Langer, Sc.D.
Title: David H. Koch Institute Professor

Acknowledgements

I would first like to thank Sangeeta for taking me into the lab, for her constant encouragement over the years, and for always squeezing in time for informal drop-ins outside of her packed official schedule. She has allowed me the freedom to develop my interests and the choice to be as independent as I wish during my graduate school, yet readily provided incisive insights whenever I hit a snag and sought help, and constantly injected moral support from the sidelines in her own way. I also wish to thank my thesis co-adviser, Bob Langer, for believing in me and my thesis project, and for constantly reminding me that the work that goes into a PhD thesis should not be infinite. Thanks also to my thesis committee chair Darrell Irvine, and my committee members Charles Rice and Maria Mota, who have provided unwavering support from day one and an unstinting belief in my ability to achieve what I had proposed. It has been a pleasure and privilege to exchange ideas with and get feedback from Charlie during our annual joint lab pow-wows. Maria has been instrumental in introducing us to basic parasitological assays that we routinely use today, and more importantly, is a master malarialogist who is always bursting with new ideas and directions that contribute significantly to our research.

I have a lot to thank Sandra and Ani for, who comprise the malaria team in our lab. Sandra has not only been my mentor in lab, but also a mentor outside of lab, and indeed a mentor in life in general. She has always patiently shared a listening ear for my complaints about lab work or about life. One important lesson I have learnt from her is not to stress out over events whose outcome is beyond our predictive capabilities, or more specifically, not to take it personally when experiments fail. This philosophy is encapsulated in her maxim "It is what is it", which really means "It is what it is". Ani has been a key team player whose bubbly and dependable nature makes it a breeze to work with, and whose easy-going personality, composure and organization has tided us over many large-scale experiments in foreign lab environments.

Special thanks to Heather, who taught me many lessons on scientific communication, both verbal and written, and provided invaluable advice on my professional development, and thanks to Kelly, Rob, Kathleen, Alice, Dave, Ester, Gabe, Neetu and Greg for your mentorship at various stages of my graduate career and constantly reminding me of the bottom line of a PhD. Thanks Nate, Kartik, Cheri, Meghan, David, Kevin, Vyas, Justin, Alex, Andrew, Yin, Sabine, Tal, Arnout, Piyush, Nil, Arnav and Jaideep, whose friendship and intellectual prowess have contributed in many ways to my development while at LMRT. Thanks Lia, Mythili, Matt and more recently, Lian-Ee, for their due diligence in keeping our lab running smoothly in a never-ending race against our consumption of lab consumables. And thanks Sue, for keeping our lab accounts in the black and for all the things you do that keeps our lab wheels running but that remain largely invisible to the privileged and often blissfully unaware people in the main lab.

Many others have paved the way in my gradual development as a scientist over the decades. These include the Elisseeff lab at Johns Hopkins, where I worked with Winnette A. McIntosh, Stephen So and Jennie Wang, the Institute of Bioengineering and Nanotechnology, where I worked in the labs of Motoichi Kurisawa and Ruan Runsheng prior to and during my undergraduate years. In particular, I also wish to thank the following members in those labs for having kindly introduced me to the world of wet

Table of Contents

List of figures

Extracellular and intracellular parasites are labeled yellow and red, respectively. Nuclei visible with blue DAPI stain. (D) Quantification of small (<5μm) and large (>10μm) forms in *P. vivax*-infected MPCCs. (E) Representative double immunofluorescence stain (anti-CSP) of primary human hepatocytes infected with cryopreserved *P. falciparum* at day 15. Extracellular and intracellular parasites are labeled yellow and red respectively. 55

around groups of nuclei, and eventually surrounds individual merozoites. MSP-1-positive merosome-like structures are also observed breaking off from infected hepatocytes. Scale bars: 10µm. 61

11

Chapter 1: Background and Significance

1.1 Malaria

Malaria is a mosquito-borne infectious disease caused by eukaryotic protists of the genus *Plasmodium* in the *Apicomplexa* family. There are many *Plasmodium* species with different host specificities, with five major species that are known to infect humans: *P. falciparum, P. vivax, P. malariae, P. ovale* and *P. knowlesi. P. falciparum* and *P. vivax* are the most prevalent species, accounting for most of the estimated 250 million clinical cases per year[1,2]. While *P. falciparum* is the most lethal *Plasmodium* species, causing up to 1 million deaths per year[3], *P. vivax* accounts for the majority of the morbidity associated with malaria due to its relapsing nature[4]. The bite of an infected mosquito transmits sporozoites into the host. These sporozoites are rapidly sequestered in the hepatic sinusoids primarily due to electrostatic interactions with liver-expressed heparan sulfate proteoglycans[5,6], cross the sinusoidal endothelium and Space of Disse[7–10], and traverse several cells before finally invading a hepatocyte [11,12]. The formation of an exoerythrocytic form (EEF) in a host hepatocyte marks the start of the clinically silent but obligatory liver stage of malaria[13] **(Figure 1.1)**. The *Plasmodium* liver stage is characterized by massive replication and maturation of the parasite over a period of time that varies between 2 days for the rodent malaria parasites (*P. berghei, P. yoelii*) and up to 15 days in *P. malariae*. The liver stage of *P. falciparum* and *P. vivax* lasts 6 and 8 days respectively[14]. Development during the liver stage culminates in the generation of thousands of mature merozoites per initial EEF, which egress in sacs derived from the host cell membrane, known as merosomes[15], and proceed to infect erythrocytes, thus establishing the blood stage of malaria. The blood stage involves a cyclical multiplication of the parasite in red blood cells, which leads to the classical clinical symptoms associated with malaria, including recurrent fever and vomiting. This pathology often leads to severe disease in the form of anemia, cerebral malaria and acute respiratory distress, especially in *P. falciparum*-infected patients. In addition, *P. vivax* and *P. ovale* can generate dormant liver-stage forms called hypnozoites that persist beyond the clearance of the initial blood stage, and thus result in clinical relapses (or blood stage reinfections) after recovery from the initial episode[14]. Blood stage parasites mature into gametocytes in response to stimuli that are just beginning to be

better understood, and are transmitted to mosquitoes resulting in the propagation of the third and last stage of the parasite's life cycle.
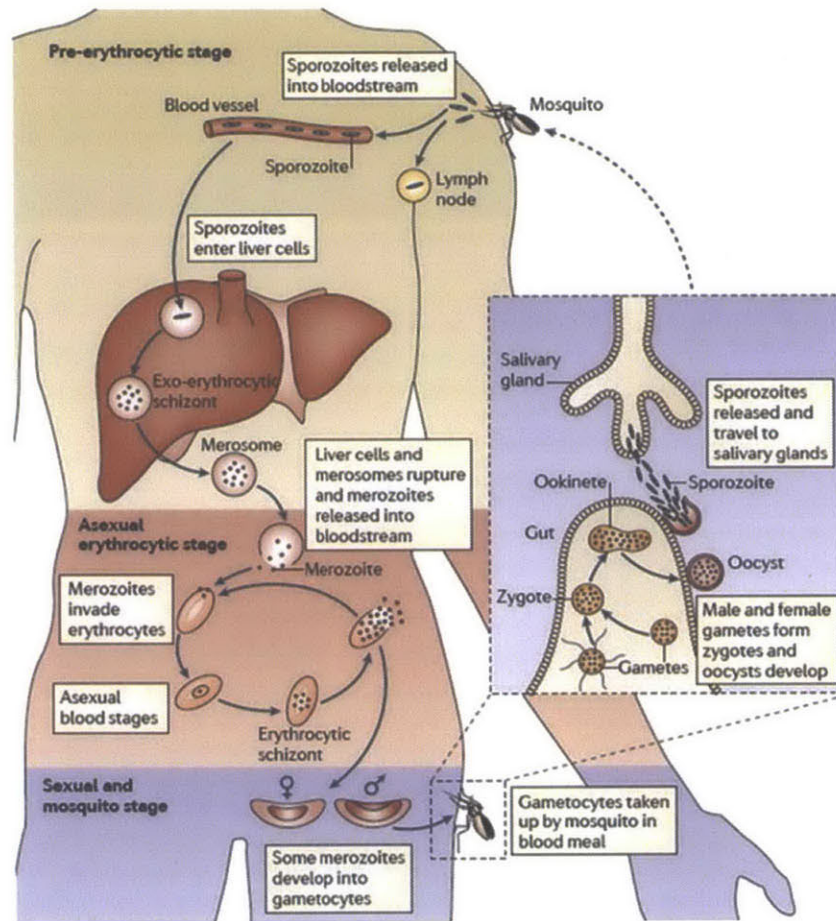
Figure 1.1 Life cycle of malaria

1.2 Liver-stage malaria as a target for drug and vaccine development

The liver stage of malaria is an attractive target for the development of anti-malarial drugs and vaccines for several reasons. Firstly, the relatively small number of sporozoites typically introduced into the host compared with the typical blood stage parasite load presents an opportunity for the complete clearance at the liver stage resulting in a clinical cure (defined as the lack of emergence of symptoms caused by the blood stage)[14]. Secondly, there is a limited number of parasite replication in the hepatic phase and hence a reduced likelihood for drug resistant forms to emerge. Thirdly, certain relapsing *Plasmodium* species like *P. vivax* and *P. ovale* form hypnozoites which lay dormant in the liver and can be activated at a future time

leading to the spontaneous appearance of secondary blood stage infections even after the resolution or clearance of the primary blood stage infection[16,17]. The existence of hypnozoites makes it particularly difficult to achieve permanent eradication of the malarial parasite from the host. Fourthly, the arrest of the liver stages allows for the possibility of causal prophylaxis (complete prevention of clinical symptoms that emerge in the blood stage) and also prevents transmission to the mosquito stages, which is an important step towards achieving malaria eradication. Fifthly, the exposure of the host to the entire repertoire of liver-stage parasite antigens is sufficient to induce a protective immune response against homologous strains of the parasite, suggesting the potential for the development of efficacious malaria vaccines that result in the growth arrest of the late *Plasmodium* liver stages [18–20] without the risk of developing clinical symptoms due to a blood-stage breakthrough.

1.3 Models for studying liver-stage malaria

The liver stage of mammalian malaria was first reported in 1948 in rhesus monkeys infected with *P. cynomolgi*[21], with the discoveries of the liver stages of the human malaria species following soon after[22,23]. However, the study of the liver stage was limited to non-human primates until the discovery of *Plasmodium* species in rats that could also infect laboratory rodent strains in the 1960s. It was almost 20 years later that liver stage malaria infection in cultured host cells *in vitro* was first reported[24], and various technical advances over the years have expanded the range and physiological relevance of host cells used to model liver-stage malaria *in vitro*, and increased the feasibility of developing more scalable models that are amenable to the modern paradigm of antimalarial drug discovery.

Unlike blood stage malaria parasites, which have a cyclical life cycle, liver stage parasites have a linear life cycle and cannot be continuously propagated. Therefore, the establishment of any liver-stage malaria model is ultimately dependent on the constant availability of *Plasmodium* sporozoites, which involves a substantial effort that involves the maintenance of mosquito colonies and the regular sourcing or production of infectious *Plasmodium* gametocytes. An additional biological complication arises due to the considerable variability in sporozoite numbers and sporozoite infectivity between batches. Recent efforts in adapting cryopreservation techniques for *Plasmodium* sporozoites may ease the dependence on a

constant sporozoite production schedule[18,25]. With the development of *in vitro* culture of *P. falciparum* blood stages, production of *P. falciparum* sporozoites is no longer limited by the availability of patient blood samples. However, *in vitro* culture of *P. vivax* blood stages has yet to be achieved, which limits the production of *P. vivax* sporozoites for supporting experimental models of liver-stage *P. vivax*.

In vitro models of liver-stage malaria

The establishment of *in vitro* models of liver-stage malaria is further complicated by the generally low infection efficiency of hepatocytes with *Plasmodium* sporozoites. The earliest *in vitro* models of liver-stage malaria involved the infection of a human embryonic lung cell line, WI-38[24], or human hepatoma cell line, HepG2[26], with *P. berghei*, a rodent malaria species. This was followed by the infection of primary rat hepatocytes by two rodent malaria species, *P. berghei*[27] and *P. yoelii*[28]. Subsequently, complete liver-stage development of two human malaria species (*P. falciparum*, *P. vivax*) that resulted in the release of infectious merozoites was achieved in primary human hepatocytes[29,30].

Primary human hepatocytes, the authentic host cell for the parasite, are normally quiescent (i.e. non-dividing) in vivo and therefore preferred. However, limited availability and the difficulty in maintaining their differentiated phenotype has limited their use. Renewable cell sources such as human hepatoma cell lines HepG2 and Huh-1/2 have been attempted but have largely resulted in arrested liver-stage development[31,32], with the exception of *P. vivax* in HepG2[33]. The recent discovery of a human hepatoma cell line, HHS-102[34] and an immortalized human hepatocyte cell line, HC-04[35], that support full liver-stage development of both *P. falciparum* and *P. vivax* has expanded the repertoire of *in vitro* models for the study of the liver stage human malaria, but these cell lines do not fully recapitulate the physiology of primary hepatocytes, such as the quiescent cell state, polarization, and drug detoxification enzymes for metabolism of antimalarials. Similarly, to address specific biological questions innate to the hepatocyte (e.g. innate immunity or intracellular redox status), a hepatic cell type that maintains a phenotype that is closest to the native hepatocyte *in vivo* will be ideal. The extension of *in vitro* models of liver-stage malaria to such applications is predicated upon the development of improved *in vitro* models of the human liver that can maintain the survival of

17

primary human hepatocytes and a wide array of hepatocyte-specific functions *in vitro* (see section 1.5 for an overview to hepatic tissue engineering techniques that have been developed to improve primary hepatocyte phenotypic maintenance *ex vivo*).

Cell Type	Name	*Plasmodium* species
Human hepatoma	HepG2	**P. vivax; P. ovale**[*]; *P. berghei*
	Huh-1/2	**P. falciparum**[*]; *P. berghei; P. yoelii*
	Huh-7	*P. berghei*
	HHS-102	**P. falciparum**
Human immortalized hepatocytes	HC-04	**P. falciparum; P. vivax**; *P. berghei; P. yoelii;*
Human embryonic lung	WI38	**P. falciparum**[*]; **P. vivax**[*]; *P. berghei*
Primary human hepatocytes		**P. falciparum; P. vivax; P.ovale;** *P. berghei; P. yoelii*

Table 1.1. *In vitro* models of malaria. *: incomplete development

In vivo models of liver-stage malaria

Despite major advances achieved by *in vitro* culture of liver stage malaria, certain immunological and pathophysiological questions can only be addressed *in vivo*. Humans are ultimately the ideal system to investigate liver-stage *Plasmodium* infection, especially with the recently popularized concept of controlled human malaria infections (CHMI) by sporozoite challenge or blood-stage challenge[36–39], which has already been applied to evaluate a pre-erythrocytic vaccine based on cryopreserved irradiated whole sporozoites[40]. However, due to the costs and logistical challenges involved, the CHMI model will probably be used in the setting of early-stage clinical safety trials for drugs or vaccines and is unlikely to supplant other *in vivo* models for the academic investigation of more fundamental biological processes related to liver-stage malaria pathophysiology and for the more broad-based preclinical screening of potential antimalarial drugs and vaccines that result from prior *in vitro* phenotypic screens.

Chimpanzees experimentally infected with *P. falciparum* or *P. vivax* are currently the only model that recapitulates the full liver and continuous blood stages of *P. falciparum* or *P. vivax* infections[41,42], and hence constitute the biological gold standard for preclinical drug and

vaccine efficacy testing, but there are tremendous costs, logistical and ethical considerations in their use. Smaller non-human primate models like *Aotus* and *Saimiri* are also infectible with various strains of *P. falciparum*[43,44], *P. vivax*[45,46] and *P. knowlesi*[47], but these experimental models are less robust than the chimpanzee model, require significant adaptation of wild-type strains in a laboratory setting and are also subject to increasingly significant sourcing issues due to diminishing availability of these primates[44].

Rodent models of malaria that utilize different combinations of laboratory rodent hosts with rodent *Plasmodium* species are the workhorse among experimental *in vivo* models of liver-stage malaria[48], and numerous studies have elucidated specific host-parasite combinations that can mimic aspects of the human malaria parasites in the human host such as cerebral malaria and malaria-induced acute lung injury[49-52]. Nevertheless, a crucial question has been raised as to the relevance of those phenotypic similarities between rodent and human malaria models due to their potentially different underlying mechanisms of action[49]. To increase the relevance of rodent models towards modeling human malaria *in vivo*, a recent approach has been to genetically engineer chimeric rodent *P. berghei* parasites that express human malaria antigens such as *P. falciparum* circumsporozoite protein (PfCS), which have been used to test whether antibodies against PfCS induced by active immunization or passively transferred would protect mice against PfCS-transgenic *P. berghei* sporozoite challenge [53]. Transgenic approaches can also be used to humanize components of the rodent host to better recapitulate mechanisms of human malaria pathogenesis in a small animal model. For example, the expression of humanized receptors on mouse endothelial cells to sequester PfCS parasites may allow the modeling of blood stage cytoadherence, which is a major putative cause of clinically lethal cerebral malaria[54].

When the goal of using rodent models for antimalarial drug discovery is taken into consideration, the differences in the drug resistance mechanisms that have developed in rodent and human malaria species[55] present an additional conundrum in terms of the ability to extrapolate efficacy data that was gleaned from rodent malaria models to the human malaria species. Furthermore, an additional factor that is not usually considered in the liver-stage malaria field is the potential difference in drug metabolism pathways between human and

rodent livers[56]. These species-dependent metabolism pathways can result in the potential major human metabolites passing undetected in laboratory rodent models and result in a lack of predictivity of preclinical rodent models for potential idiosyncratic drug-induced liver injury (DILI), multi-organ drug toxicity due to human liver-specific metabolic by-products, and adverse drug-drug interactions with existing FDA-approved drugs [57]. One way to address this problem and still reap the benefits of a small animal model is to develop humanized mice with human liver components, which is reviewed in the following section.

1.4 Humanized mice

Human liver chimeric mice

Certain human pathogenic diseases in which the pathogen demonstrates a high cellular and species specificity for human hepatocytes, like the hepatitis B, C and D viruses and human malaria (e.g. *P. falciparum*, *P. vivax*), have hitherto been modeled only in non-human primates. Mice with chimeric human livers were generated to enable the study of these human hepatotropic pathogens in a small animal model.

A second motivation for the development of human liver chimeric mice is their potential ability to model human-specific drug metabolism, which is poorly replicated in rodents due to interspecies differences in the drug metabolism pathways in rodent and human hepatocytes[56,57]. Humanized liver chimeric mice have been generated by various genetic or transplantation approaches which are reviewed in this section.

Genetically humanized mice

Various genetic approaches have been employed to manipulate the mouse genome to create transgenic mice that express human-specific genes[58]. A variety of genetically humanized mouse models have been developed for various components of the hepatic drug metabolism pathway, including xenobiotic receptors like constitutive androstane receptor (CAR), phase 1 detoxification enzymes of the cytochrome P450 (CYP) family like CYP2D6[59,60] and CYP3A4[61], and phase 2 conjugating enzymes like UDP glucuronosyltransferase (UGT) 1A[62] and phase 3 transporters like multidrug resistance protein (MRP) 2[63]. Due to the inherent limitations of humanizing only a single gene among the 57 CYP members in human livers, there have been

recent attempts to introduce multiple human drug metabolism genes into mice to create more complex humanized mice[64].

Mice have also been genetically humanized to express human proteins that are known to be necessary for the infection of liver cells by hepatotropic pathogens. For example, hepatitis C virus (HCV) entry into hepatocytes depends on the hepatic expression of four entry factors, of which only two (CD81, occludin) needs to be the human-specific protein[65]. Based on this observation, transgenic mice that selectively express human CD81 and human occludin were generated and shown to be infectible with HCV[65] and support complete viral replication *in vivo*[66].

Ectopic transplantation models

A demonstration of the transplantation approach involved the ectopic transplantation of human liver fragments into the ear pinna or under the kidney capsule of either lethally irradiated mice that were reconstituted with SCID mouse bone marrow cells (Trimera model) [67,68] or non-obese diabetic/severe combined immunodeficiency (NOD/SCID) mice[69], but a major limitation of this approach is the limited availability of fresh human donor liver tissue and its rapid loss of viability *ex vivo*.

A variation on the direct transplantation of human liver fragments involved isolating primary human hepatocytes from human liver and either directly injecting the hepatocytes in suspension under the kidney capsule of FH117 SCID mice[70], or embedding the hepatocytes in Matrigel and transplanting it under the kidney capsule of NOD/SCID mice[71], but a major problem with primary human hepatocyte transplantation models are the short-term viability of the transplanted hepatocytes[72].

Genetic liver injury / hepatocyte repopulation models

A different approach towards creating a human liver compartment in a mouse involved the development of genetically engineered mice that have an immunocompromised background to prevent the rejection of human cells, and that undergo mouse liver injury so as to create a niche that facilitates the transplantation with and repopulation of the depleted mouse liver by primary human hepatocytes. This approach leverages the unique capability of

the primary hepatocyte to proliferate in response to regeneration stimuli that arise in an injured liver. The first example of this approach was the albumin-uroplasminogen activator (uPA) transgenic mouse, which exhibits spontaneous liver injury due to constitutive expression of the hepatotoxin urokinase plasminogen activator (uPA) under the albumin promoter[73]. These uPA mice can be rescued by transplanting primary mouse hepatocytes from a different mouse, which repopulate the diseased recipient liver[74]. The introduction of an immunodeficient SCID background into the uPA mouse (uPA-SCID) allows the transplantation and engraftment of primary human hepatocytes[75]. However, the uPA-SCID mice are difficult to breed and must be transplanted with hepatocytes within a very narrow window of time (within 1-3 weeks after birth) due to the subsequent lethality of uPA-induced hepatotoxicity[76].

Subsequently, three different liver-injury mouse models were developed with the main advantage being that the mouse liver injury is inducible. The first of these to be developed is based on a targeted genetic knockout of the liver-specific fumarylacetoacetate hydrolase (*Fah*) gene, which causes a defect in the tyrosine catabolic pathway and results in the accumulation of hepatotoxic metabolites in the liver, and is lethal to neonates in mice[77]. This lethality can be prevented by administering 2-(2-nitro-4-trifluoro-methylbenzoyl)-1,3 cyclohexanedione (NTBC) to block the first steps of the tyrosine catabolism pathway upstream of FAH. Similarly to the uPA-SCID mice, $Fah^{-/-}$ mice can survive NTBC withdrawal if FAH-expressing wild-type primary mouse hepatocytes are transplanted into the $Fah^{-/-}$ mice and repopulate the recipient mouse liver[78]. The genetic crossing of $Fah^{-/-}$ mice with $Rag2^{-/-}/\gamma c^{-/-}$ mice that lack mature B cells, T cells and NK cell resulted in the $Fah^{-/-}/Rag2^{-/-}/\gamma c^{-/-}$ (FRG) mouse model that enabled the transplantation and engraftment of primary human hepatocytes without immune rejection[79,80]. More recently, two transgenic models were developed, the TK-NOG[81] and AFC8[82] models, which are based on the inducible expression of the herpes simplex virus thymidine kinase or FK508-caspase 9 fusion protein, respectively, by administering ganciclovir or AP20187, respectively. Interestingly, the AFC8 model involved not only the injection of human fetal hepatocytes, but also human CD34$^+$ hematopoietic stem cells (HSCs) and fetal thymus cells which resulted in the engraftment of a human immune system in addition to a human liver

compartment[82]. A common feature of these three inducible liver-injury mouse models is the relatively long engraftment time of several months and variable chimerism[79,81,82].

Ectopic transplantation
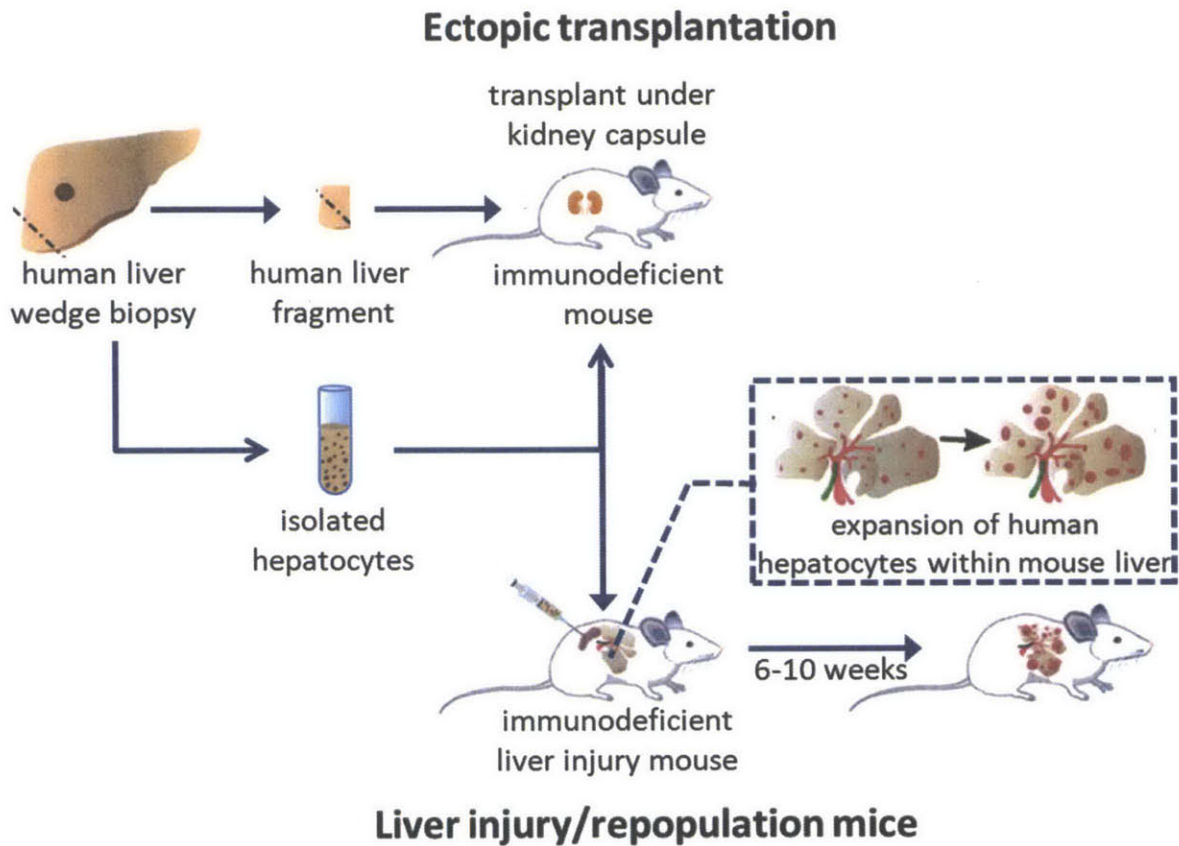
Figure 1.2 General strategies for generating mice with human liver compartments

Human liver chimeric mice for modeling hepatotropic diseases

As described earlier, there is currently one genetically humanized mouse model expressing human CD81 and human occludin that supports the complete viral life cycle of HCV[66].

Among the ectopic hepatic tissue transplantation approaches, the HCV-Trimera model was expressly developed for modeling HCV infections *in vivo*. The HCV-Trimera model involves the ex vivo exposure of the human liver fragments to HCV prior to transplantation under the kidney capsule of irradiated mice that had previously received a bone marrow transplant from a SCID mouse[67], and exhibited serum viremia that is responsive to inhibitors of the HCV internal

ribosomal entry site (IRES) or monoclonal antibodies against the HCV envelope protein E2[68]. A similar model involves the injection of HCV into NOD/SCID mice that were previously transplanted with human liver tissue fragments under the kidney capsule, and could support detectable levels of HCV RNA in the serum up to 4 weeks after inoculation with the virus[69]. Among the two purified primary hepatocyte transplantation approaches reported to date, the complete viral life cycle of HBV was reported in the NOD/SCID model with the demonstration of HDV super-infection[71], while the FH117 SCID model (involving the injection of primary hepatocytes under kidney capsule) supported infection with the liver-stages of *P. falciparum* with mature liver-stage schizonts expressing prototypical late liver-stage antigens such as merozoite surface protein 1[70].

To date, the mouse liver injury - human hepatocyte repopulation models have been the most widely applied to modeling human hepatotropic infections in small animals[83,84]. This is largely due to their relatively stable humanization (once established) compared to the earlier-reported ectopic transplantation models, and that these models do not require the use of cryopreserved hepatocytes that can be plated after thawing, and therefore can be generated using a larger pool of cryopreserved donor hepatocyte lots that can only be used in suspension.

Humanized uPA-SCID mice support hepatitis B[85] and C[86–90] virus infection, hepatitis D virus super-infection in HBV-infected mice[91] and human cytomegalovirus[92] infection. HCV-infected uPA-SCID mice have also been shown to validate the antiviral activity of two compounds already known to be effective in clinical trials: interferon a2b and an anti-protease agent (BILN-2061)[87]. Humanized uPA-SCID mice also support infection protozoan infections such as *P. falciparum*[93,94], with the expression of late liver-stage markers such as merozoite surface protein-1 (MSP-1) and erythrocyte binding antigen-175 (EBA-175) culminating in the production of merozoites that could be isolated and were infectious for human erythrocytes *in vitro*[94].

Humanized FRG mice also support infection with HBV[95], HCV[95] and *P. falciparum*[96]. Notably, the FRG model was able to support development of the late liver-stages of *P. falciparum*, with the expression of merozoite surface antigens like MSP-1, EBA-175, AMA-1

concomitant with the formation of merozoites and their subsequent release in merosomes. Moreover, when the FRG mice were backcrossed to the NOD background, the resultant FRG/NOD mice were able to support short-term human erythrocyte repopulation in addition to *P. falciparum* liver-stage infection. Remarkably, complete *P. falciparum* liver-stage development in mice was demonstrated for the first time using this FRG/NOD model, with the egression of mature *P. falciparum* merozoites from humanized livers culminating in their invasion of human erythrocytes *in vivo*[96].

Humanized AFC8 mice were originally developed to model chronic hepatitis C virus infection in a small animal, and its ability to support liver-stage malaria infection is unknown[54]. The TK-NOG model has also not been reported to support infection with human hepatotropic pathogens to date.

Despite the potential for mouse liver injury - human hepatocyte repopulation models for modeling human hepatotropic infectious diseases, the relatively long engraftment time, variable chimerism, and the requirement for liver injury for humanization present significant challenges to the scaling up of these models for preclinical drug development. On the other hand, the comparative ease of mouse model generation and the potential scalability to large cohort sizes are attractive advantages of the ectopic transplantation approach, but the delivery and persistence of isolated primary human hepatocytes in an appropriate ectopic site is a major issue. The application of biomaterials and hepatic tissue engineering techniques may help to alleviate the problems with the ectopic transplantation approach, and will be a major theme in the later part of the thesis.

As many of the existing human liver chimeric mouse models are able to recapitulate liver-stage malaria infection, they offer the potential for studying *in vivo* host-parasite interactions in much greater depth than possible *in vitro*, especially with the advent of humanized mouse models that contain a human immune system. The benefits of combining existing human liver chimeric mouse models and mice containing human immune systems are discussed in the following section[76,97].

Type of humanization	Mouse model	Pathogen
Ectopic	FH117 SCID + PHHs (kidney capsule)	*P. falciparum*[70]
	NOD/SCID + PHHs in matrigel (kidney capsule)	HBV/HDV[71]
	HCV-Trimera (SCID mouse bone marrow + human liver tissue, kidney capsule)	HCV[67,68]
	NOD/SCID + human liver tissue (kidney capsule)	HCV[69]
Liver injury/PHH repopulation	uPA-SCID	*P. falciparum*[93,94], HCV[86–90], HBV[85], HBV/HDV[91], CMV[92]
	FRG	*P. falciparum*[96], HBV[95], HCV[95]
	AFC8	HCV[82]

Table 1.2: Human liver chimeric mouse models of infectious disease. PHHs = primary human hepatocytes.

Dual humanized mice with a human immune system and a human liver compartment and potential applications to liver-stage malaria

Mice with human immune systems (HIS) offer several potential applications including the modeling of human pathogenic infection of cells of the HIS, testing therapeutic interventions against blood borne human pathogens, studying the human immunological response to blood borne human pathogens and characterizing the immune response against vaccine/adjuvant formulations[98]. Generally, HIS mouse models involve the transplantation of fetal or neonatal human hematopoietic progenitor cells and/or human peripheral blood cells into severely immunocompromised mice, such as those bearing a *scid* mutation or a recombinase (*Rag2*) deficiency (which lack T and B cells) in conjunction with an interleukin receptor common gamma chain knockout ($\gamma c^{-/-}$) (which lack functional NK cells)[99,100]. A major limitation of such mice is the inability to support the maturation of the transplanted human hematopoietic progenitor cells into all the differentiated lineages of a mature human immune system. An additional strategy that is commonly utilized to support the engraftment of transplanted human cells is the genetic humanization of mice to allow the expression of human cytokines[101,102]. To confer additional relevance of the HIS response to human pathogens introduced into the model, genetically humanized mice that express human major

histocompatibility complex (MHC), human antibodies as well as human T-cell receptors on mouse host cells have also been engineered[58,103]. Humanized HIS mice have been used to model various aspects of EBV and HIV infection, and have demonstrated their potential as surrogate preclinical models for the development of effective vaccines as well as challenge models for blood borne human pathogens[98].

It would be potentially useful to introduce a HIS component to human liver chimeric mice to create dual humanized mouse models that could enable immunological studies in human liver-specific diseases. With liver-stage malaria, such a dual humanized mouse model would 1) make it possible to recapitulate both liver and blood stages of human malaria in a small animal model, 2) enable the study of the human adaptive immune response to malaria infection of human hepatocytes, and 3) be useful as a small animal challenge model for vaccine candidates against liver-stage human malaria. The AFC8 mouse model is an example of a dual humanized mouse model containing both a HIS and a human liver compartment. Due to the co-engraftment of a human immune system in addition to a human liver compartment, AFC8 mice not only support hepatocyte infection with HCV, but also demonstrate virus-specific T-cell responses, liver inflammation and fibrosis[82]. Therefore, in addition to the potential for modeling both the liver stage of malaria and the transition to the blood stages, which has already been achieved in FRG mice[96], the AFC8 model also offers the prospect of supporting continuous cyclical blood stage malaria infection *in vivo*, which opens up opportunities for modeling various aspects of blood stage malaria pathogenesis that are unique to the human disease e.g. cytoadherence and its relationship to clinically significant cerebral malaria and separately, and also enables the testing of the efficacy of potential antimalarial vaccines[54]. The achievement of continuous blood stage human malaria infection in a dual humanized mouse would create the exciting possibility of a second transition from the blood stage to the sexual stage in the mosquito via mosquito bites of the malaria-infected mice, thus completing the entire human malaria life cycle in a small animal. However, the AFC8 model has a relatively low liver repopulation rate, which may make it less efficiently infected with liver-stage malaria parasites, as a certain degree of humanization is required to result in detectable liver stage burdens[96]. The humanization process is also slow in the AFC8 model, like other liver injury/hepatocyte

repopulation models. It would therefore be ideal to develop alternative methods to rapidly humanize mice with a human liver compartment that can be infected with liver-stage malaria, especially in mouse backgrounds that are known to support HIS engraftment.

1.5 Hepatic tissue engineering

A major aim of hepatic tissue engineers is the development of cell-based therapies for liver disease, especially in patients with end-stage liver failure and for whom the only viable clinical treatment is a liver transplant. These cellular therapies encompass approaches that provide temporary support, such as extracorporeal bioartificial liver (BAL) devices as well as more permanent adjunct interventions such as cellular transplantation, transgenic xenografts, and implantable hepatocellular constructs. Prior work in the hepatic tissue engineering field has generated a variety of models of the human liver which, in addition to contributing towards the long-term goal of creating new therapeutic treatment modalities for liver disease, has also opened up opportunities to study liver biology and liver pathophysiology. Due to the complex array of functions performed by the healthy liver, including detoxification, synthetic and metabolic processes, the maintenance of a differentiated hepatocellular phenotype is a basic yet crucial requirement for any successful hepatocellular therapy or model.
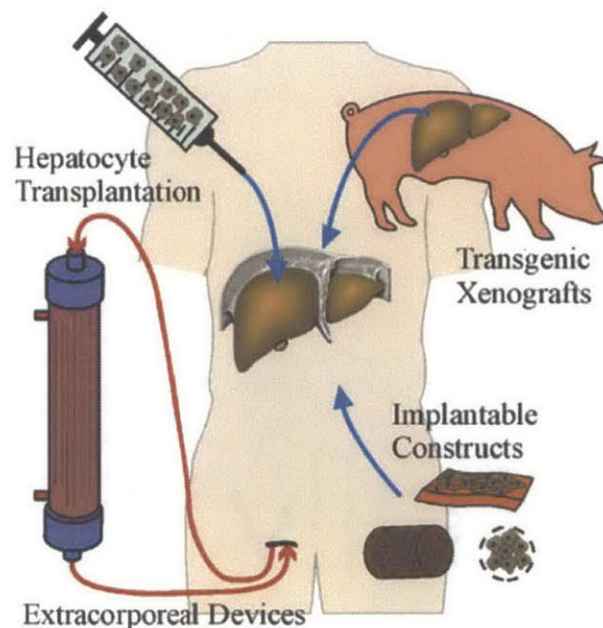
Figure 1.3 Cell-based therapies for liver disease and failure

Cell sources for hepatic tissue engineering

Despite holding great promise, liver cell-based therapies has been hindered from clinical application by the propensity for primary hepatocytes isolated from the human liver to rapidly lose their differentiated phenotype and function *in vitro*[104]. The unstable ex vivo hepatic phenotype is compounded by the paucity of human liver tissue as a source of primary human hepatocytes and the limited potential for mature primary hepatocytes to proliferate ex vivo[105]. As such, alternative cell sources have been explored, each with its own strengths and weaknesses.
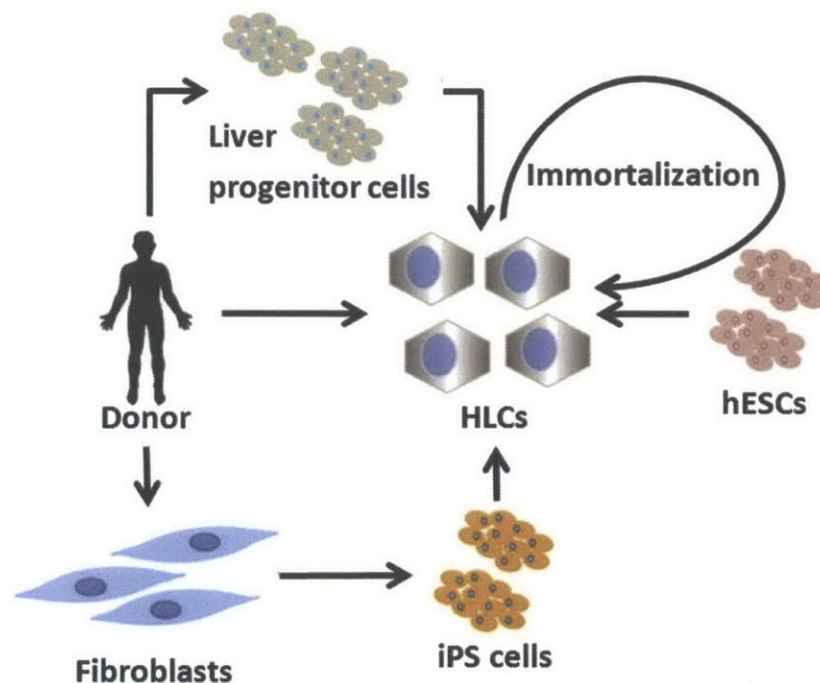
Figure 1.4 Cell sources for hepatic tissue engineering

Immortalized human hepatocyte cell lines like HepG2 (human hepatoblastoma), HepaRG, or immortalized fetal human hepatocytes, have been proposed as readily available surrogates for hepatic tissue. However, they lack the full functional capacity of primary adult hepatocytes and present a risk of oncogenic transformation after transplantation.

A variety of fetal and adult progenitor cells have been explored as potential hepatocyte sources. Human fetal hepatoblasts and human embryonic liver cells are liver precursor cells at different stages of development that both exhibit a bipotential differentiation capacity towards

either hepatocytes or bile duct epithelial cells and exhibit proliferative potential *in vitro*, but both are associated with significant sourcing issues. To date, efforts to find liver-resident cells with similar progenitor properties in the adult liver have not been successful.

Pluripotent stem cells have the potential to give rise to cell types of all three germ layers, including differentiated cells like hepatocytes. Multiple protocols have been described that enable the directed differentiation of human embryonic stem (hES) cells into hepatocyte-like cells *in vitro*. More recently, the discovery that fully differentiated human adult cells, like skin cells, could be reprogrammed to an undifferentiated, pluripotent state called human induced pluripotent stem (iPS) cells, and can be subsequently differentiated into hepatocyte-like cells *in vitro*, has overcome some of the ethical and logistical issues associated with hES cells. Pluripotent stem cell-derived hepatocytes exhibit both the phenotypic and functional characteristics associated with hepatocytes, though the resulting differentiated cells exhibit a more fetal state of maturation compared to adult human hepatocytes[106]. This technical advance has opened up the possibility of generating large populations of hepatocyte-like cells *in vitro* for hepatic tissue engineering applications.

Cell Source	Critical Issues
Primary hepatocytes Human (adult or fetal), xenogeneic	Sourcing, expansion, phenotypic instability, immunogenicity, safety (xenozoonotic)
Immortalized hepatocyte lines Tumor-derived, SV40, telomerase, spontaneously immortalized	Range of functions, genomic instability, safety (tumorigenicity)
Stem Cells Embryonic, liver progenitors (hepatoblasts, oval cells), other lineages (HSC, MAPC), induced pluripotent stem cells, direct reprogramming to hepatocytes	Sourcing, differentiation efficiency, phenotypic instability, immunogenicity, safety (tumorigenicity)

Table 1.3: Cell sources for hepatic tissue engineering.

In vitro human liver models

The development of *in vitro* human liver models was driven by the need to predict human responses to potential drugs in terms of hepatic metabolism profile, inhibition or induction of hepatic drug metabolism enzymes, drug-drug interactions and hepatotoxicity *in vitro* prior to preclinical and clinical studies. *In vitro* human liver models can also facilitate the study of liver biology, and have increasingly been adapted to the study of liver pathophysiology, including liver-specific pathogenic diseases.

An extensive range of *in vitro* liver model systems has been developed, including perfused whole organs and wedge biopsies, precision cut liver slices, immortalized liver cell lines, isolated primary hepatocytes in suspension or cultured on surfaces, isolated organelles, membranes or enzymes and recombinant systems expressing specific drug metabolism enzymes. While perfused whole organs, wedge biopsies, and liver slices maintain many aspects of the normal *in vivo* microenvironment and architecture, they typically suffer from very short-term viability (< 24 hours) and limited nutrient/oxygen diffusion to inner cell layers. Purified liver fractions and single enzyme systems are routinely used in high-throughput systems to identify enzymes involved in the metabolism of new pharmaceutical compounds, but lack the complete spectrum of gene expression and cellular machinery required for recapitulating more complex liver-specific functions like inducibility of hepatic cytochrome P450 activity. Liver cell lines derived from hepatoblastomas or immortalized primary human hepatocytes generally exhibit abnormal levels and repertoire of hepatic functions, perhaps most notably, the divergence of constitutive and inducible levels of cytochrome P450 enzymes. Models employing isolated primary hepatocytes are generally considered to be the most physiologically relevant, but the difficulty in maintaining their hepatocyte-specific functions *in vitro* has been a major stumbling block in the utility of such models. As such, substantial work has gone into developing methods to improve the survival and hepatocyte phenotypic maintenance *in vitro*.

The development of improved *in vitro* human liver models based on primary human hepatocytes can be guided by an understanding of the precisely defined tissue architecture

within the liver. The liver is an intrinsically complex three-dimensional (3D) environment, with cords of hepatocytes in close juxtaposition with the various liver-derived and non-liver-derived nonparenchymal cells and with gradients of extracellular matrix and soluble factors. Several microenvironmental cues have been incorporated into *in vitro* models of primary human hepatocytes to simulate the *in vivo* microenvironment of the hepatocyte, including soluble factors, cell-extracellular matrix (ECM) interactions, cell-cell interactions and 3D cellular architecture.

The supplementation of culture medium with physiological factors such as hormones, corticosteroids, growth factors, vitamins, amino acids, trace elements, or non-physiological small molecules such as phenobarbital and dimethylsulfoxide have all been shown to modulate hepatocyte function. Oxygen tension has also been shown to modulate hepatocyte function, since primary hepatocytes have oxygen consumption rates much higher than the average cell type and are therefore especially sensitive to hypoxia-induced damage. Since hepatocytes are anchorage-dependent epithelial cells, the impact of ECM composition and topology on hepatocyte phenotype *in vitro* has been widely studied. Many ECM coatings (most commonly type I collagen) have been shown to enhance hepatocyte attachment to the substrate, but this is generally insufficient to curtail the subsequent loss of hepatocyte function. Studies involving complex ECM mixtures have utilized biologically derived mixtures such as matrigel[107,108] and liver-derived biomatrix[109], or a combinatorial ECM microarray to identify specific ECM combinations that improve hepatocyte function compared to monolayer cultures on collagen I[110]. The topology of ECM presentation can also influence hepatocyte phenotype, as shown by the culture of hepatocytes that are sandwiched between two layers of type I collagen gel, which exhibit desirable morphology with polarized bile canaliculi, and maintain stable hepatocyte functions for several weeks[111,112]. Various studies employing cocultures of hepatocytes and nonparenchymal cells have highlighted the importance of heterotypic cell-cell interactions on hepatocyte phenotypic maintenance. Notably, the nonparenchymal cell type involved can either be liver-derived[113] or non-liver-derived[114], and can even be from a different species[114]. The 3D organization of hepatocytes has also been extensively explored as a strategy to maintain hepatocyte function. Various techniques, including non-adhesive or positively-

charged surfaces, rotational or rocking cultures, and encapsulation in macroporous scaffolds have been developed to encourage hepatocyte spheroid formation, which has led to improved hepatocyte survival and functions over standard monolayer culture of hepatocytes on collagen. Potential mechanisms underlying these effects include an increased degree of homotypic cell-cell contacts among hepatocytes, the retention of a three-dimensional cytoarchitecture, and the three-dimensional presentation of cell-secreted ECM molecules around the hepatocyte spheroids. Hepatocyte aggregates or spheroids may also be encapsulated in biomaterials or cultured in bioreactors to further control cell-cell interactions, provide additional cell-matrix interactions, or recapitulate physiologically relevant gradients of soluble factors.

The adaptation of microtechnology tools from the semiconductor industry to hepatic tissue engineering has also led to the development of tools that enable a finer control over cellular interactions and the miniaturization of biomedical assays. In the context of the liver, this has led to the ability to dynamically and temporally control cell-cell interactions[115,116], and spatially control tissue microarchitecture[104]. In particular, a photolithographic cell patterning technique has enabled the formation of micropatterned co-cultures in which hepatocyte islands of controlled diameters were surrounded by supporting nonparenchymal cells[104,117]. This pattern was miniaturized into a multiwall format using soft lithography techniques and has resulted in micropatterned cocultures that are optimized for human hepatocyte function by controlling the balance between homotypic (hepatocyte-hepatocyte) and heterotypic (hepatocyte-nonparenchymal) cell-cell interactions[118]. The maintenance of optimal hepatic function is highly dependent on hepatocyte island size and spacing. This platform has been utilized extensively for both drug development and pathogen model systems, as discussed in detail in the next section.

Drug and disease model systems.

The development of phenotypically stable *in vitro* models of primary human hepatocytes has opened up new avenues to study human liver-specific processes that were previously inaccessible with relatively short-lived and phenotypically unstable primary hepatocyte models. This is exemplified by the application of micropatterned cocultures that support primary human hepatocyte function to modeling various aspects of human-specific

drug metabolism, including drug-mediated modulation of CYP450 expression and activity, drug-drug interactions and chronic and acute hepatotoxicity[118-120]. The stabilization of primary human hepatocytes in the micropatterned coculture platform has also facilitated the studies of human hepatotropic pathogens like HCV, as demonstrated by the establishment of persistent HCV infection for the first time *in vitro*[121], and could be potentially applied to other hepatotropic pathogens like the hepatitis family of viruses and liver-stage malaria.

Implantable engineered human liver models

The development of implantable engineered human liver models was motivated by the need to ameliorate existing cell transplantation strategies, which suffer from inefficient seeding and engraftment, loss of hepatocyte survival, and a lack of clinical benefit[122] (REF). Implantable engineered hepatic tissues are typically fabricated by encapsulating hepatocytes in biomaterials *in vitro* prior to *in vivo* implantation. A variety of materials have been used to culture hepatocytes in 3D microenvironments *in vitro*, including naturally derived and synthetic materials. Naturally-derived biomaterials include collagen[123], peptides[124], fibrin[125,126], heparin[127], alginate[128,129], chitosan[130,131], hyaluronic acid[130], cellulose[132], decellularized liver matrix[133], whereas synthetic materials include polyethylene glycol (PEG)[134,135], poly(lactic-co-glycolic acid) (PLGA)[136,137], poly-L-lactic acid (PLLA)[138], polyethylene terephthalate (PET)[139], polycaprolactone (PCL)[140]. Chemical[141,142] and biochemical modification of these biomaterials with bioactive moieties like growth factors[143], adhesive peptides[134] or sugars[144-146] and composites[130] of biomaterials are often explored as strategies to improve hepatocyte attachment and maintain hepatocyte function. These biomaterials have been used in various forms like hydrogels[134], sponges[136], electrospun nanofibers[147] or woven meshes with varying degrees of spatial control over cellular location within the biomaterial ranging from random encapsulation in bulk hydrogels[134], controlling hepatocyte aggregate size via biomaterial porosity[123,148], microstructured molding[149], photopatterning[135], dielectrophoretic patterning, or 3D bioprinting[150].

The therapeutic potential of various implantable engineered human liver models can be evaluated by implanting them in mouse models[136,149,151,152], with the degree of hepatocyte survival and human hepatic functional maintenance of the implants after implantation used as

a preclinical indicator for potential clinical benefit. Beyond preclinical evaluation, implantation of engineered human liver tissue may also provide complementary or alternative *in vivo* models of human liver metabolism and pathophysiology to existing humanized-liver mouse models. As reviewed above, the most successful humanized mouse models currently available depend on significant genetically engineered host liver injury occurring during the humanization process and take several months to be established[84]. By revisiting the concept of ectopic transplantation of primary human hepatocytes, but with the additional application of hepatic tissue engineering techniques to stabilize and maintain hepatic function prior to and after implantation and the exploration of new implantation sites in mice, implantable tissue-engineered human livers were recently developed that offer an alternative humanization method to existing genetic liver injury/hepatocyte repopulation models[152]. In this model, primary human hepatocytes are cocultured with a stromal cell *in vitro* prior to co-encapsulation in a biofunctionalized poly(ethylene glycol) (PEG) hydrogel with a liver endothelial cell line, and the resulting engineered human artificial liver is implanted intraperitoneally in mice. The presence of juxtacrine and paracrine signals from the two stromal and endothelial cell types contributed to the stabilization of differentiated hepatic phenotype for at least two weeks *in vivo* and resulted in an engraftment efficiency of 92% within a week of implantation[152]. Due to the ability of PEG to delay the host rejection of transplanted tissues[153], these engineered tissues are able to survive in mice with an immune-competent background (e.g. Swiss Webster or C57/BL6 mice) and the humanized mice were used for modeling human-specific drug metabolism, drug-drug interactions, and drug-induced liver injury[152].

1.6 Thesis overview

The overall goal of this thesis is to develop advanced *in vitro* and *in vivo* models of liver-stage malaria for the interrogation of potential antimalarial drugs for efficacy in a physiologically relevant host cell type, primary human hepatocytes. Towards this goal, this dissertation employs advances in cell sources and hepatic tissue engineering to address limitations in existing human liver-stage malaria models such as the difficulty in maintaining hepatic survival and function *in vitro* and *in vivo*, inefficient infection of primary human hepatocytes with *Plasmodium* sporozoites *in vitro*, the inability to study the effect of host

genetic background on *Plasmodium* infection and drug responses, as well as the issues associated with generating scalable humanized mouse models that are infectible with liver-stage malaria in a facile manner. In **Chapter 2**, we describe the establishment of liver-stage *Plasmodium* infection in a microscale human liver platform based on micropatterned cocultures of primary human hepatocytes and supportive stromal fibroblasts. We demonstrate its ability to model long-term liver-stage infections, and its potential utility in enabling phenotypic screens for potential antimalarial drugs and vaccine testing in a more authentic host cell type. We further hypothesized that perturbation of the *in vitro* hepatic microenvironment using physiologically relevant cues like oxygen tension and innate immune modulation can improve primary hepatocyte infection rates and *Plasmodium* parasite growth and maturation *in vitro*. In **Chapter 3**, we describe the establishment of liver-stage *Plasmodium* infection in human induced pluripotent stem cell (iPSC)-derived hepatocyte-like cells, which is not only a renewable source of hepatocytes but also enables future studies of the effect of host genetic variation on liver-stage *Plasmodium* biology and potential antimalarial drug responses. We further apply recently discovered small molecules to induce further hepatic maturation *in vitro*, thus increasing the relevance of using these cells for antimalarial drug development and studying liver-stage malaria biology. In **Chapter 4**, we describe an implantable model of liver-stage malaria that involves a synthetic biomaterial environment that is engineered with the minimal microenvironment necessary for the maintenance of primary human hepatocyte survival and infectibility with *Plasmodium*, and apply it towards providing a proof of concept that humanized mouse models of liver-stage human malaria can be generated in a facile, rapid and scalable fashion for preclinical drug testing *in vivo*. Ultimately, the results of this research represent a three-pronged approach towards engineering scalable human liver-stage malaria models that could facilitate antimalarial drug discovery at various stages of the drug development pipeline.

Chapter 2: Engineering a Microscale Human Liver Platform for Modeling Liver-Stage Malaria *In vitro*

2.1 Introduction

Despite major advances in the prevention and treatment of malaria, this disease continues to be a major global health problem in human populations with ~ 250 million cases and nearly 1 million deaths every year. Currently, there is a renewed interest and focus on global malaria eradication, and it is now widely recognized that existing tools are insufficient to meet this goal[154,155]. In particular, the clinical options that target the liver stages of the parasite life cycle are inadequate. There is only one licensed drug that eliminates hypnozoites, only a few drugs that target liver-stage parasites, and no licensed malaria vaccines. This problem has been exacerbated by the emergence of drug resistance and the inability to treat some populations with primaquine, the only currently approved drug with anti-hypnozoite activity[156]. The *Plasmodium* liver stage is an attractive therapeutic target for the development of both anti-malarial drugs and vaccines, as it provides an opportunity to interrupt the life cycle of the parasite at a critical early stage. Therefore, screening platforms that model the *in vivo* *Plasmodium* liver stage could be used to advance the pipeline for antimalarial drug development and to validate promising liver stage vaccine candidates[157,158].

Studies of rodent *Plasmodium* pathogens (*P. berghei* and *P. yoelii*) have provided important insights, due in part to the capacity to conduct both *in vitro* and *in vivo* assays[159–161]. Nonetheless, there are essential differences between the rodent and human parasites, such as their antigenic variation and mechanisms of host cell invasion[55,162], and crucial species-dependent differences between the drug metabolism activities of rodent and human livers[56]. In a similar vein, although our understanding of the liver stage of human malaria, mainly *P. falciparum* and *P. vivax*, is based in large part on the infection of human hepatoma cell lines [26,34,157,163,164], and several *in vitro* models of liver-stage human malaria based on hepatic cell lines have been applied to antimalarial drug screening, these cell lines display abnormal proliferation, aberrant signaling, dysregulated gene expression, altered host responses to infection, and inadequate CYP450 and drug metabolism activity, and thus may not accurately recapitulate human hepatocyte biology. Furthermore, *in situ* observation of pathogen

development in liver cell lines is typically obscured after 6 days in culture, due to the continued proliferation of infected cells[165].

Primary cultured human hepatocytes that exhibit more physiologic human liver functions can support the development of the liver forms of *P. falciparum* and *P. vivax*[29,30,160,166,167], but are rarely employed and difficult to translate to screening platforms due to limited cell availability and challenges in maintaining their functional phenotype over extended periods of time *in vitro*[104]. There is evidence that mimicking the *in vivo* hepatic microenvironment, such as by adding cell-cell interactions, cell-matrix interactions and controlling tissue microarchitecture can improve *in vitro* models of the liver[111,118,168,169]. This is exemplified by micropatterned cocultures (MPCCs) of primary human hepatocytes and supporting stromal fibroblasts, which result in stable hepatocyte function, including albumin secretion, urea production and cytochrome P450 levels, for several weeks compared to hepatocytes alone[118]. This microscale human liver platform has been found to be more predictive than existing *in vitro* liver models for generating and identifying human drug metabolites, drug-induced liver toxicity, and supports the persistent replication of hepatitis C virus[119,121,170]. Therefore, this model shows promise as a basis for developing an improved liver-stage malaria screening platform in primary human hepatocytes. The availability of large cryopreserved lots of primary human hepatocytes also means that donor-dependent interexperimental variability can be minimized, which is advantageous for a screening platform. Nonetheless, reproducible access to sporozoites is also critical to achieve a practical system. Cryopreservation of large reproducible batches of aseptic sporozoites has also now been established for both *P. vivax*[163] and *P. falciparum*[157] sporozoites.

Although the stabilization of hepatic phenotype in MPCCs is predicted to improve liver-stage malaria infection rates in primary human hepatocytes, *in vitro* models of liver-stage malaria have historically demonstrated low infection efficiencies[30,35] and suboptimal parasite growth and development compared to *in vivo* models[96]. One feature of the *in vivo* hepatic microenvironment that is rarely considered in *in vitro* liver-stage malaria models is the presence of a range of oxygen tensions in the hepatic sinusoid[171], which is thought to be a factor that contributes to hepatic zonation, a compartmentalization of functions along the axis of

perfusion[172,173]. Previous studies have shown that exposing mixed populations of primary rat hepatocytes to physiological gradients of oxygen tension can induce compartmentalization *in vitro*, render the cells selectively susceptible to zonal hepatotoxins[174,175], and recapitulate the zonated patterns of carbohydrate-metabolizing enzyme gene expression *in vitro*[171,172,176]. Therefore, *in vitro* liver-stage malaria culture platforms may be improved by altering microenvironmental oxygen concentrations.

Outside the liver, ambient oxygen concentrations have a broad spectrum of biological impact, influencing diverse pathways from homeostasis to development[177]. The role of oxygen has been explored in a range of infectious diseases. For instance, hyperoxia reduces certain bacterial and *Apicomplexan* infections *in vitro* or *in vivo*[178–180], whereas hypoxia promotes hepatitis C virus infection *in vitro*[181] and *Trypanosoma lewisi* infections *in vivo*[182]. In the malaria field, previous studies have probed the effect of atmospheric oxygen on parasitemia in rodent and avian disease models. In particular, *P. berghei*-infected rats or *P. cathemerium*-infected canaries subjected to hypoxia exhibited increased levels of parasitemia[182,183], whereas hyperoxia decreased *P. berghei* parasitemia[184,185] and prevented early death caused by experimental cerebral malaria in the *P. berghei*-ANKA mouse model[185]. Furthermore, continuous *in vitro* culture of the blood stages of *P. falciparum* was first achieved by reducing atmospheric oxygen levels[186], and subsequent studies have characterized this microaerophilic nature of blood stage *P. falciparum*[187]. These prior observations suggest that oxygen concentrations may influence liver-stage malaria parasite survival and growth *in vitro*.

Another feature of the *in vivo* hepatic microenvironment that has not been recapitulated in existing *in vitro* models is the immunoprivileged status of the liver[188,189] that is mediated by immunosuppressive molecules and hepatic expression of co-inhibitory receptors that usually help to prevent inadvertent organ damage, but have been exploited by successful hepatic pathogens like hepatitis B and C virus and liver-stage malaria[190]. Little is known about the liver's innate immune response to malaria, but recent findings in rodent malaria models demonstrate that the type I interferon pathway is involved in the detection of *Plasmodium* RNA during liver-stage malaria infection *in vivo*[191]. Although liver-stage malaria infection *in vivo* is limited by the type 1 interferon response due to the recruitment of immune cells, it is unclear

whether the innate immune response of hepatocytes contributes to any inhibition or clearance of liver-stage infection. Prior work in our lab has shown that the viral infection of MPCCs is associated with the induction of interferon stimulated gene expression in hepatocytes and correlates with the spontaneous clearance of infection *in vitro*. Persistent viral infection could be achieved by inhibiting the innate immune response of primary human hepatocytes.

In this first part of this chapter, we demonstrate the feasibility of integrating cryopreserved human hepatocytes in MPCC with cryopreserved *P. falciparum* and *P. vivax* sporozoites to form an *in vitro* platform that supports the liver stages of human malaria infection. This platform offers the potential for automation based on several factors, including preselection of cryopreserved human hepatocyte and sporozoite batches to standardize infection rate, a machine-learning algorithm that enables an automated imaging-based readout of immunofluorescent staining, and the capacity to generate a positive Z factor in response to drug exposure. The 96-well, medium-throughput format requires less reagents (drugs, sporozoites) than larger footprint *in vitro* assays or *in vivo* assays. Collectively, our data document the development and characterization of a highly-reproducible, medium-throughput microscale human liver platform that may aid in the development of safe and efficacious antimalarial drugs and liver-stage vaccines.

In the second part of this chapter, we explored the effect of two microenvironmental perturbations on liver-stage malaria infection in primary human hepatocytes in MPCCs: oxygen tension and innate immune status. We first studied the influence of cell surface oxygen on liver stage malaria infection of primary human hepatocytes, using the MPCC model for hepatocyte culture that is phenotypically stable, responsive to ambient oxygen and supports the liver stage of malaria. Using this model system and a mathematical framework to estimate the cell surface oxygen partial pressures (pO_2) under a variety of experimental manipulations, we show that oxygen has a profound impact on the *Plasmodium* liver stage. In particular, both infection efficiency and development of EEFs can be perturbed by altering cell surface oxygen concentrations. We identified an optimal cell surface oxygen level for maximizing infection and demonstrate that host HIF-1α is at least partially responsible for this response. We also characterize the innate immune response of primary human hepatocytes to *Plasmodium* liver-

stage infection, and explore the role of innate immune inhibition on liver stage malaria parasite infection and growth.

2.2 Results

Platform establishment and demonstration of applications

Functional characterization of micropatterned, cryopreserved primary human hepatocytes

In order to establish an MPCC *in vitro* culture of primary human hepatocytes (**Figure 2.1A**) suitable for *Plasmodium* infection, we screened cryopreserved hepatocytes from several individual patient donors to identify those that met the following criteria: 1) selective adhesion to collagen type I; 2) maintenance of a functional hepatocyte phenotype for up to 3 weeks, as assessed by albumin expression, urea production and CYP450 activity; and 3) expression of the previously identified *Plasmodium* host entry factor, CD81[192]. We identified eight lots of cryopreserved human hepatocytes that were plateable on collagen I and that displayed typical hepatocyte morphology, including the presence of bile canaliculi (**Figure 2.2**). Seven of these lots demonstrated functional capacity in culture, as quantified by their production of albumin and urea, and also exhibited CYP450 activity for up to 3 weeks (**Figure 2.1B**). We next quantified the expression of the host entry factor CD81 on hepatocytes from each of the seven lots at the day of infection. Four of these lots (Donors 2, 3, 7 and 8) expressed high levels of CD81 by immunofluorescence (**Figure 2.1D**).
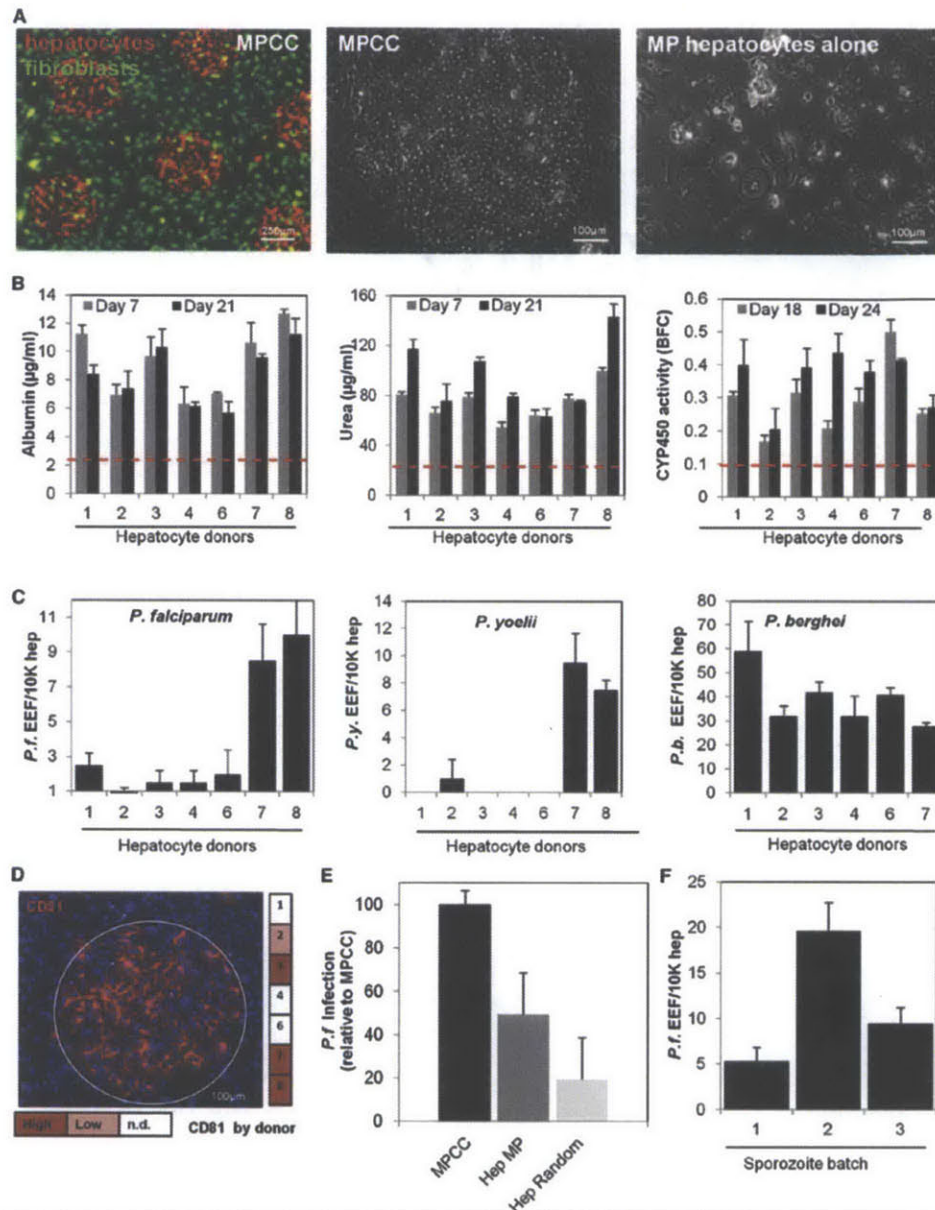
Figure 2.1. Functional Characterization of Cryopreserved Human Hepatocytes in Micropatterned Cocultures and Cryopreserved *Plasmodium* falciparum Sporozoites. (A) Morphology of primary human hepatocytes in micropatterned cocultures (left; hepatocytes, red and fibroblasts, green). Representative coculture of hepatocytes with (middle) and without (right) fibroblasts 18 days post seeding. (B) Albumin secretion, urea synthesis, and CYP450 activity in MPCCs of different donors. Red dashed lines indicate the average level observed in 6-day hepatocyte monocultures. (C) *P. falciparum*, *P. yoelii*, and *P. berghei* infection across donors. (D) Representative CD81 immunofluorescence staining at day 4 post seeding (left). Heat map indicates relative CD81 expression per donor as measured by IF (right; n.d., not detected). (E) *P. falciparum* infection in hepatocyte monocultures, micropatterned (MP), or randomly distributed (Random) relative to infection in MPCCs. 10,000 hepatocytes were plated in each case. (F) Levels of infection by three sporozoite batches in a single hepatocyte donor. Error bars represent SD. See also Figure 2.2.

42

Infection of primary human hepatocyte MPCCs with *P. falciparum*

To test whether primary hepatocytes stabilized by culturing in MPCCs can be infected with *P. falciparum*, we exposed MPCCs to cryopreserved *P. falciparum* sporozoites (NF54) (**Figure 2.3A, B**). We confirmed productive infection in all 7 donors by staining for HSP70 expression. However, a wide range of infection rates were observed between lots (**Figure 2.1C, left panel**). Specifically, at day 3 post-infection, the number of HSP70+, *P. falciparum* infected hepatocytes was much higher in donor 7 and 8 samples relative to the other tested lots. Hepatocytes from donors 7 and 8 were selected for further characterization of the model. We also examined the susceptibility of the same donor samples to productive infection by two different rodent species of *Plasmodium*. As shown in **Figure 2.1C, middle panel**, donor 7 and 8 also exhibit the highest levels of *P. yoelii* infection. However, this correlation was not observed in *P. berghei* (**Figure 2.1C, right panel**). Overall, infection with *P. berghei* was higher compared with *P. falciparum* and *P. yoelii*, with donor 1 showing slightly higher infection with *P. berghei* than the other donors. Interestingly, high CD81 expression was necessary, but not sufficient, to support robust infection by *P. falciparum* (**Figure 2.1C, D**). We next evaluated three different batches of cryopreserved *P. falciparum* sporozoites. As seen in **Figure 2.1F**, this experiment confirmed productive infection using sporozoites from three cryopreserved batches. However, infection efficiencies varied across batches. Based on higher infection levels, sporozoites from batch 2 were selected for further characterization of the model. Importantly, we observed higher infection rates when hepatocytes were cultured in the MPCC format as opposed to standard, unpatterned monocultures (**Figure 2.1E**, Hep Random). MPCCs remained susceptible to *P. falciparum* infection for many weeks after they were patterned; however, infection rates are optimal at day 2 after patterning (data not shown).
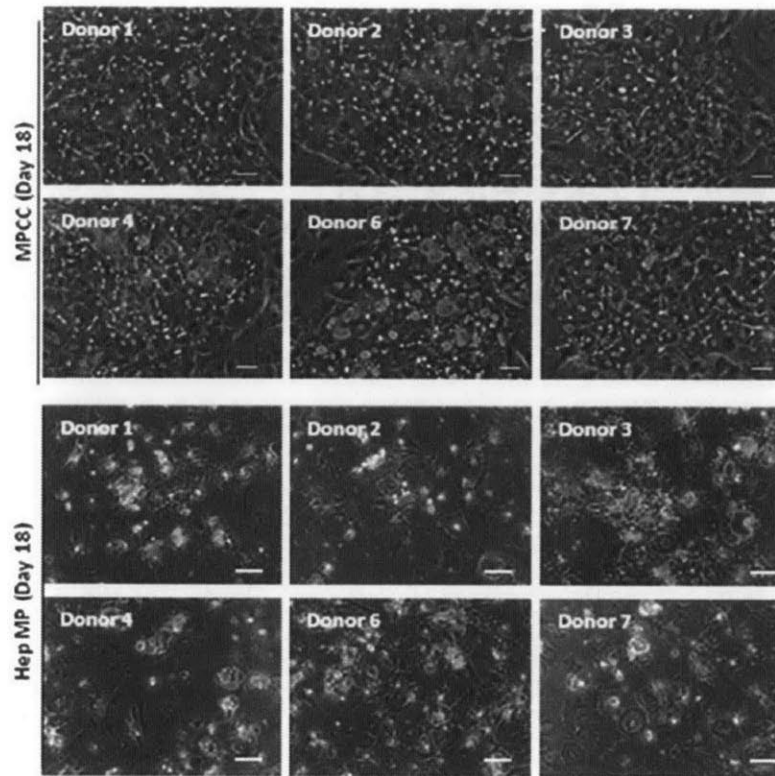
Figure 2.2. Morphology of Cryopreserved Human Hepatocytes, related to Figure 2.1. Morphology of cryopreserved human hepatocytes from different donors in micropatterned cocultures (day 18 post-seeding).

Recapitulation of entire *P. falciparum* liver stage in MPCCs

Having established that *P. falciparum* can infect MPCCs, we next sought to establish whether the entire liver stage could be reproduced *in vitro* using this combination of cryopreserved *P. falciparum* sporozoites and MPCC of cryopreserved human hepatocytes. The viability of the cryopreserved *P. falciparum* sporozoites was evaluated by assessing their gliding motility (**Figure 2.3C**) and by their capacity to traverse cells using a cell wounding assay[11]. On average, the addition of 37,000 motile cryopreserved *P. falciparum* sporozoites to 10,000 patterned hepatocytes resulted in 3% rhodamine-positive traversed cells (**Figure 2.3D**). To quantify the ability of the *P. falciparum* sporozoites to invade hepatocytes, *P. falciparum*-treated MPCCs were fixed 3 hours post-infection[193]. On average, 10% of hepatocytes contained intracellular cryopreserved *P. falciparum* sporozoites (**Figure 2.3E**). The human hepatocyte infection rate, based on the percentage of cells containing HSP70-expressing parasites at day 3 post-infection was 0.2% (**Figure 2.3J**). Notably, at this same time point, fresh sporozoites

44

achieved infection rates that were 7- to 13-fold higher (**Figure 2.6A**). Representative images of the HSP70-expressing parasites at day 3 and day 5 are shown in **Figures 2.3F and 2.3G**.
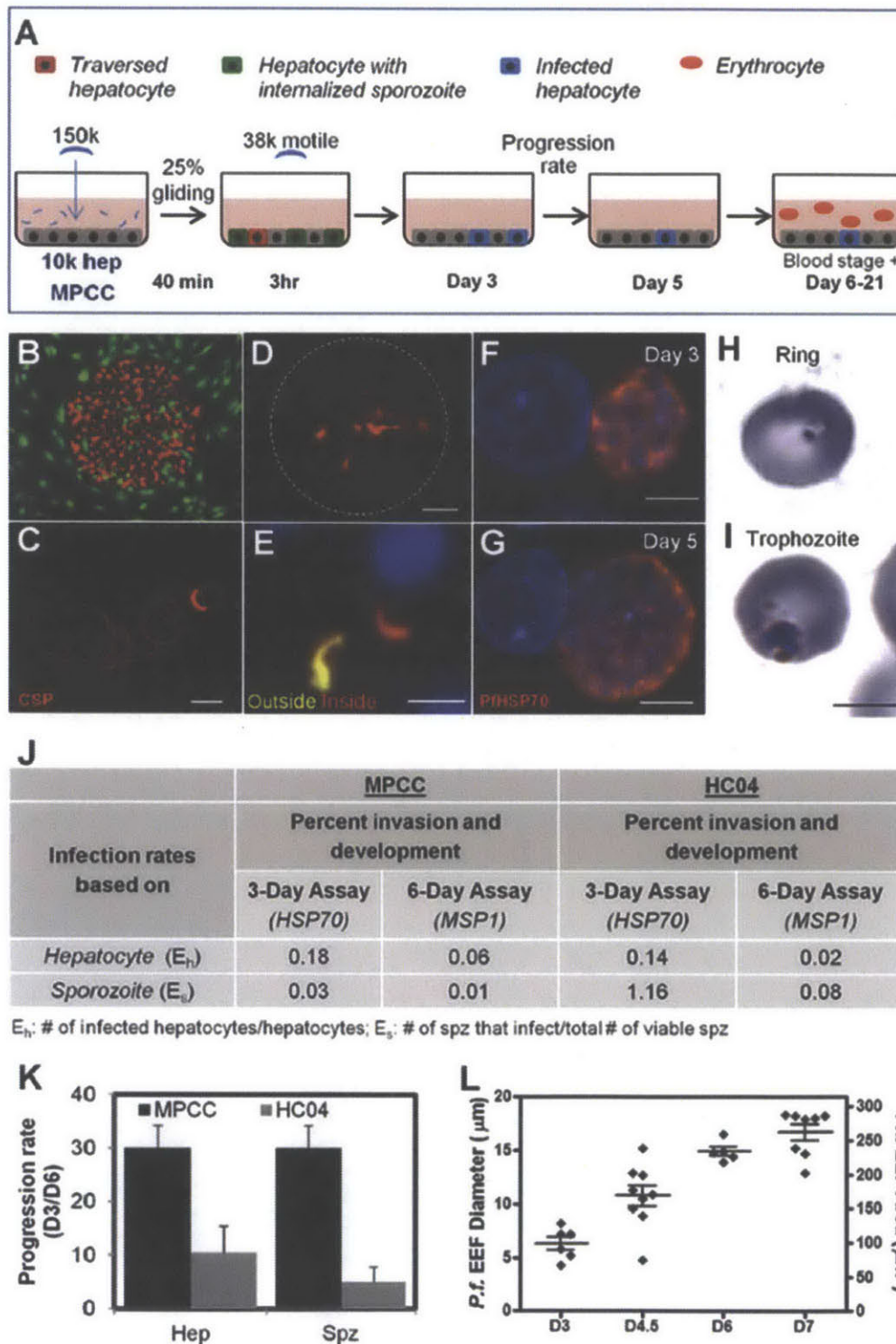
Figure 2.3. Liver-Stage Recapitulation in Primary Human Hepatocyte MPCCs. (A) Schematic of *P. falciparum* infection assay. (B) Typical morphology of primary human hepatocytes in MPCCs

(hepatocytes, red; fibroblasts, green). (C) Representative image of *P. falciparum* sporozoites gliding. CSP immunostaining was used to visualize trails. Quantification based on the average fraction of sporozoites that perform at least one circle. (D) Cell traversal ability of *P. falciparum* sporozoites as visualized by dextran-positive staining of primary human hepatocytes. (E) Representative double immunofluorescence stain (anti-PfCSP, both before and after cell permeabilization) of *P. falciparum*-infected MPCCs. Extracellular and intracellular sporozoites are labeled with yellow and red, respectively. Nuclei are visible with blue DAPI stain. (F and G) Representative images of *P. falciparum* in human primary hepatocytes at days 3 (F) and 5 (G) post infection. Parasites are identified by anti-PfHSP70 staining (red). (H and I) Infection of human RBCs by merozoites released from infected liver-stage culture. Representative images of Giemsa-stained RBCs in the ring stage (H) and the trophozoite stage (I). (J) Infection rates using MPCC primary human hepatocytes or HC04 hepatoma cells, calculated based on the plated number of sporozoites or hepatocytes. (K) Progression rate from day 3 to day 6 in MPCC and HC04 calculated as infection rate of day 6 O infection rate of day 3 3 100 (based on hepatocytes and sporozoites). (L) Schizont size distribution at days 3, 4.5, 6, and 7. Scale bar = 5 mm (F–I), 10 mm (C and E), or 100 mm (D). Error bars represent SEM.

The maturation of parasites derived from cryopreserved *P. falciparum* was assessed using three parameters: 1) immunostaining the infected cultures with antibodies against two proteins first expressed during late liver stages, PfEBA-175 (erythrocyte-binding antigen, 175 kDa) and PfMSP-1 (merozoite surface protein 1), which indicate full development of the respective schizonts inside the hepatocytes into merozoites; 2) the size of HSP70-expressing schizonts relative to previous reports of *P. falciparum* schizont size during liver stage development; and 3) the progression rate, calculated as the percentage of schizont-bearing cells at day 6 relative to day 3. At day 5 post-infection, cryopreserved sporozoites express both PfEBA-175 and PfMSP-1 (**Figure 2.4C**). The parasites we observed were similar in size to what has been reported in other *in vitro* settings (10 – 15 μm at day 5)[29,166], but smaller than those reported *in vivo*[23,96,194], (**Figure 2.3L and 2.4B**). Importantly, we demonstrated that the rate at which parasites progressed to the schizont stage between day 3 to day 6 post-infection was higher in infected MPCCs (33%) relative to the commonly used hepatoma line HC04 (14%) (**Figure 2.3K**).

Finally, to demonstrate that hepatic schizonts derived from cryopreserved *P. falciparum* sporozoites could achieve full maturity and release infective merozoites, red blood cells were added to the hepatocyte cultures at day 6 post-infection. After 10 days, Giemsa staining revealed infection of erythrocytes by *P. falciparum* merozoites (**Figure 2.3H, I**).
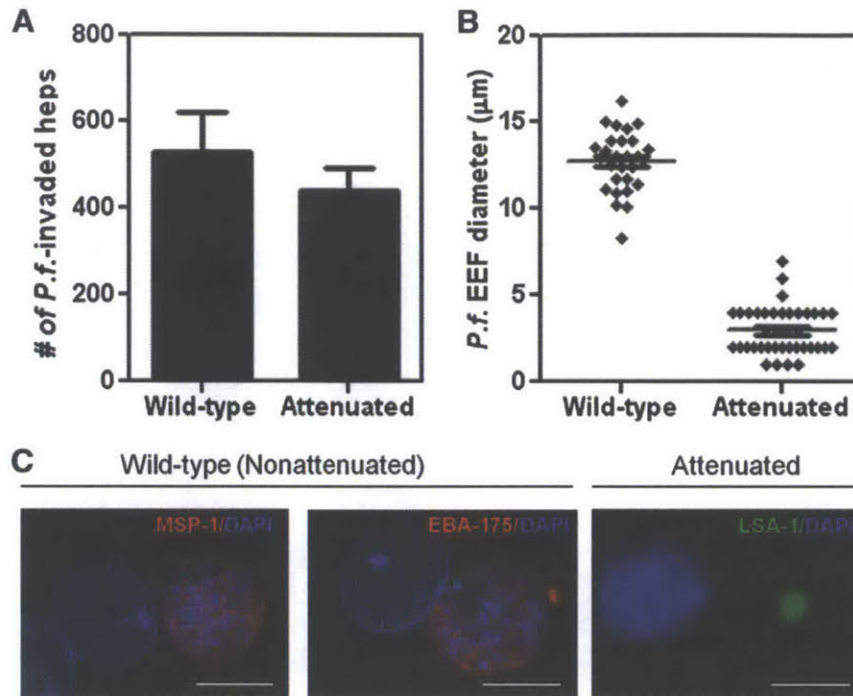
Figure 2.4. Comparison of Live-Attenuated versus Wild-Type Parasites for Candidate Vaccine Evaluation. (A) Number of infected hepatocytes observed after wild-type (nonattenuated) and attenuated cryopreserved sporozoite infection. (B) Size distribution of wild-type and attenuated parasites in MPCCs after 5 days of culture. (C) Representative images of parasites at day 5 post infection. Wild-type parasites are identified by anti-MSP-1 and anti-EBA-175 staining. Attenuated parasites are identified by anti-LSA-1 staining. Nuclei are visualized with DAPI (blue). Scale bar = 10 mm. Error bars represent SEM.

Assessing progression of attenuated *P. falciparum* for vaccine applications

The ability of the MPCCs to recapitulate the entire liver stage of *P. falciparum in vitro* highlights the potential to use this platform to study the biology of *P. falciparum* infected hepatocytes. For example, this capability should enable the assessment of candidate pre-erythrocyte malarial vaccines that are based on live attenuated parasites[18,166,195].

To illustrate the potential use of MPCCs in vaccine development, we compared the infection capacity of a pre-erythrocytic malaria vaccine candidate comprised of cryopreserved, live-attenuated *P. falciparum* sporozoites to that of cryopreserved non-attenuated (wild-type) *P. falciparum* sporozoites. Entry of the attenuated parasites was evaluated relative to the function of non-attenuated parasites. As seen in **Figure 2.4A**, entry by both groups of parasites

was similar. Late liver-stage development was evaluated at day 5 post-infection. Immunofluorescence staining with EBA-175 and MSP-1 antibodies detected mature schizonts only in MPCCs infected with the non-attenuated sporozoites, whereas MPCCs infected with the live-attenuated sporozoites were positive only for the early liver-stage antigen, LSA-1 (**Figure 2.4C**). As expected, schizonts that were established by the non-attenuated sporozoites were larger than the immature forms established by the attenuated sporozoites, where the hepatic stage development is arrested. **Figure 2.4B** shows a scatter plot of the range of EEF sizes generated by each group.

Development of a semi-automated, medium-throughput platform for antimalarial applications

We next explored the utility of the MPCCs as a potential anti-malarial drug screening platform. The hepatocyte serves both as the site of antimalarial drug metabolism (or bioactivation) and the host for the parasite. Thus, phenotypic stability of the hepatocyte phenotype and a full drug metabolism repertoire has the potential to capture a full range of drug responses such as efficacy, drug-drug interaction and toxicity[196]. MPCCs were established in a 96 well format, infected with *P. falciparum,* and treated with the canonical malaria drug, primaquine. The impact of the drug was evaluated based on its ability to reduce parasite infection relative to control cultures in a multi-day dose. As seen in **Figure 2.5A and 2.5B**, the IC_{50} for primaquine was approximately $1\mu M$ for *P. falciparum* during 3 days in culture. The IC_{50} for *P. falciparum* in the MPCC was lower compared to the IC_{50} obtained using unpatterned, monocultures of the hepatoma cell line, HC04 (**Figure 2.5A, B**). Primaquine is known to act via bioactivation to active daughter metabolites in the liver[197]. Thus, the clearance of the parent compound can be used as a proxy for the level of bioactivation in culture. We monitored depletion of primaquine in MPCCs, primary hepatocyte monocultures (Hep only) and the HC04 cell line over two days by high-performance liquid chromatography and found that MPCCs most efficiently cleared primaquine over this time frame (**Figure 2.5C**). We next compared the expression level of 83 human-specific drug metabolism genes in order to assess whether the observed macroscopic differences in parent compound depletion correlates with the drug
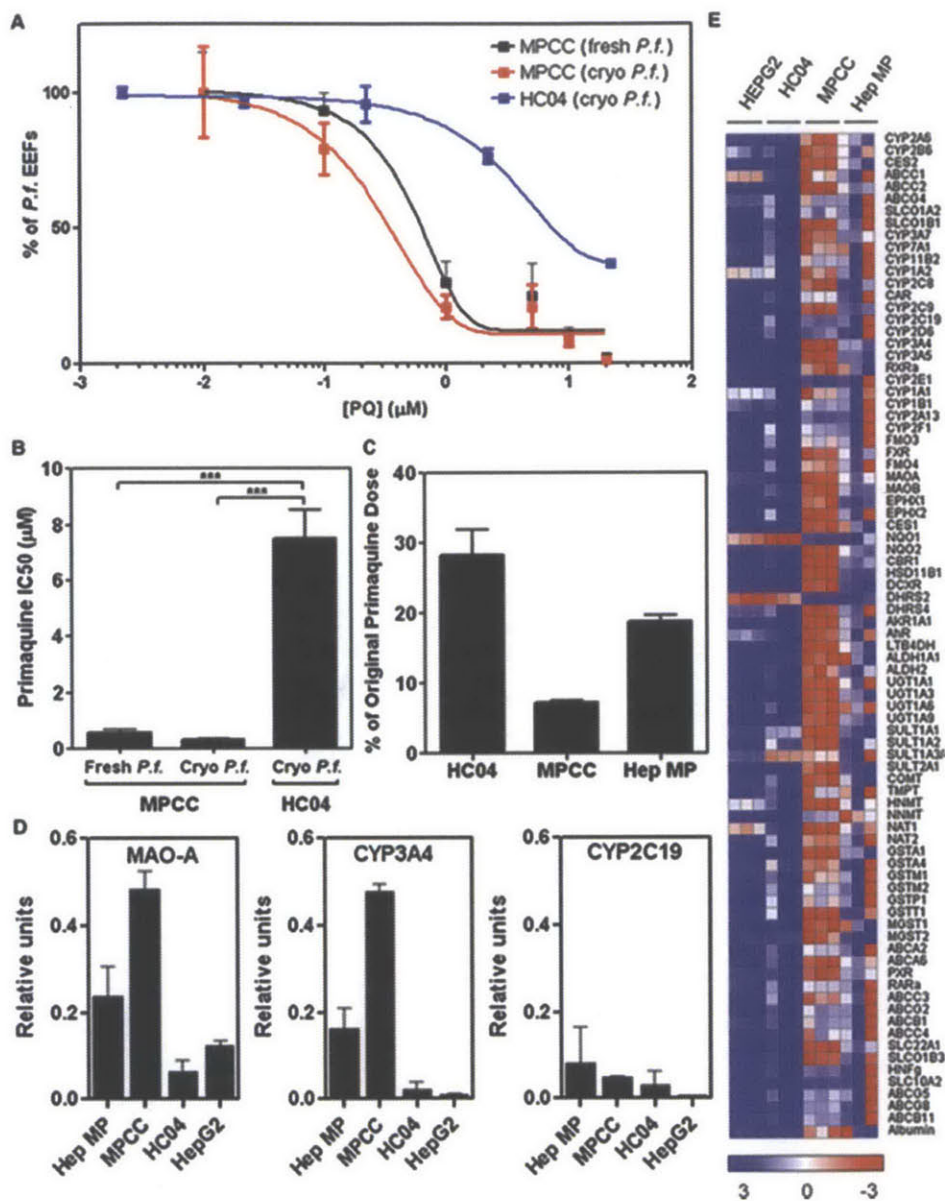
Figure 2.5. Utility of Medium-Throughput Human Hepatocyte Platform to Identify Lead Compounds. (A) Primaquine treatment of MPCCs or HC04 infected with fresh or cryopreserved sporozoites. (B) IC50 of primaquine in MPCCs versus HC04 (p = 0.0002 by one-way ANOVA; ***p < 0.001 by Tukey's multiple comparison test). (C) Primaquine metabolism by HC04, MPCCs, and patterned monocultures of primary human hepatocytes (Hep MP) quantified by liquid chromatography tandem mass spectrometry (LC-MS/MS). (D) Relative expression of three putative metabolism genes implicated in primaquine metabolism. (E) Heat map displays of LMA-Luminex analysis for 83 human-specific drug metabolism genes. Columns represent triplicate loadings of RNA extracted from HEPG2, HC04, MPCC, and Hep MP. Gene expression relative to average of control gene transferrin, and heat maps are row normalized. Error bars represent SEM. See also Figure 2.7.

metabolism repertoire of these model systems. In general, the bulk of hepatocyte drug metabolism genes were expressed at higher levels in the MPCCs **(Figure 2.5E)**. Of the three major enzymes involved with primaquine metabolism, two of the three were expressed at higher levels in MPCC than the other systems. In particular, monoamine oxidase A (MAO-A) which is thought to account for over 75% of primaquine metabolism, was expressed at a level 4-fold higher than hepatoma cell lines, suggesting that the platform may offer a more predictive system with which to assay candidate drug performance, including studies of mechanism of action.
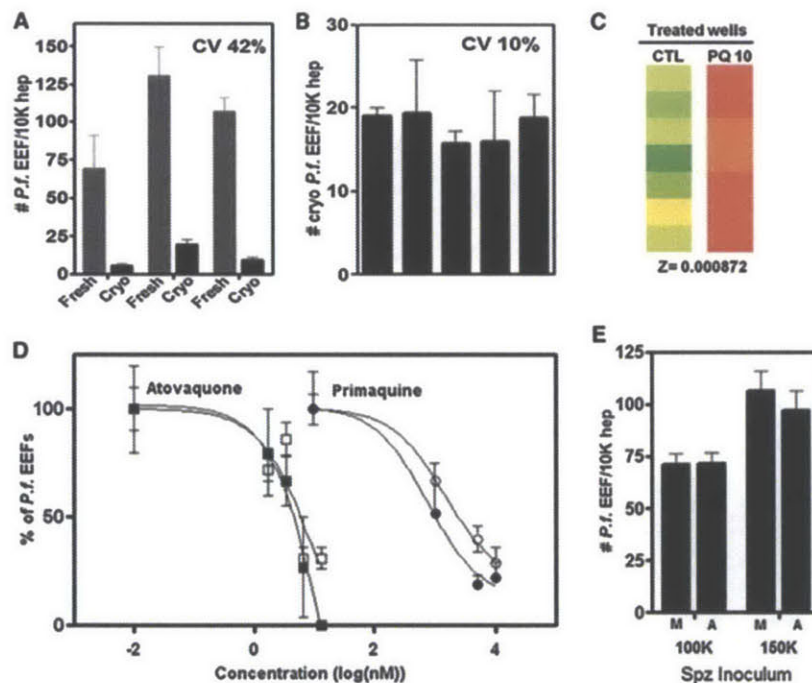
Figure 2.6. Adapting the Format to Drug Screening. (A) Interexperimental variability measured by the coefficient of variation (CV) and infection rate using fresh and cryopreserved sporozoites from three different batches. (B) Interexperimental variability measured by the coefficient of variation (CV) and infection rate using cryopreserved sporozoites from the same batch. (C) Heat map indicating levels of infection (green, highest EEF numbers; red, lowest EEF numbers) observed in seven representative control or primaquine-treated wells. Comparison yields positive Z factor. (D) *P. falciparum* infection with primaquine or atovaquone in two independent experiments performed on different days. (E) *P. falciparum* infection in MPCCs following two doses of fresh sporozoites determined by manual counts (indicated by M) or image analysis automation (indicated by A). Error bars represent SEM. See also Figure 2.8.

Next, to further adapt the microliver platform for medium-throughput screens, we characterized several critical parameters. As seen in **Figures 2.6A and 2.6B,** we found that day-to-day variability of hepatocyte infection using the same batch of cryopreserved sporozoites could be minimized (coefficient of variation [CV] = 10%) when compared to the range of infection rates obtained using 3 independent batches of fresh sporozoites (CV = 42%). Next, a positive Z factor (Z'>0), which indicates confidence in separating two normally distributed populations, was obtained when primaquine-treated wells (10 µM) were compared to control cultures (**Figure 2.6C**). In addition, the reproducibility of the phenotypic assay was assessed by establishing consistent dose-dependent inhibitory effects of two different drugs at three different concentrations in 2 independent experiments (atovaquone and primaquine) (**Figure 2.6D**). Furthermore, the magnitude of the inhibitory impact of primaquine was consistent across two independent human hepatocyte donors (**Figure 2.7**). Finally, we established and validated an automated image analysis read-out using this platform, following the infection of MPCCs with two different doses of sporozoites. As shown in **Figure 2.6E** and **Figure 2.8**, the number of parasites detected by automated image acquisition and analysis closely matches the counts obtained using conventional manual fluorescence microscopy.
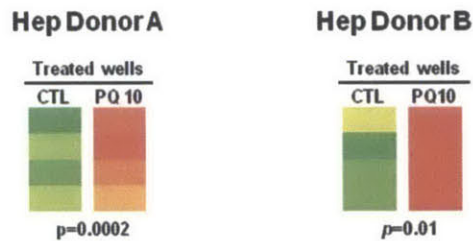
Figure 2.7. Inhibitory Effect of Primaquine , **Related to Figure 2.5 Inhibitory effect of primaquine (PQ) using two different hepatocyte donors.**
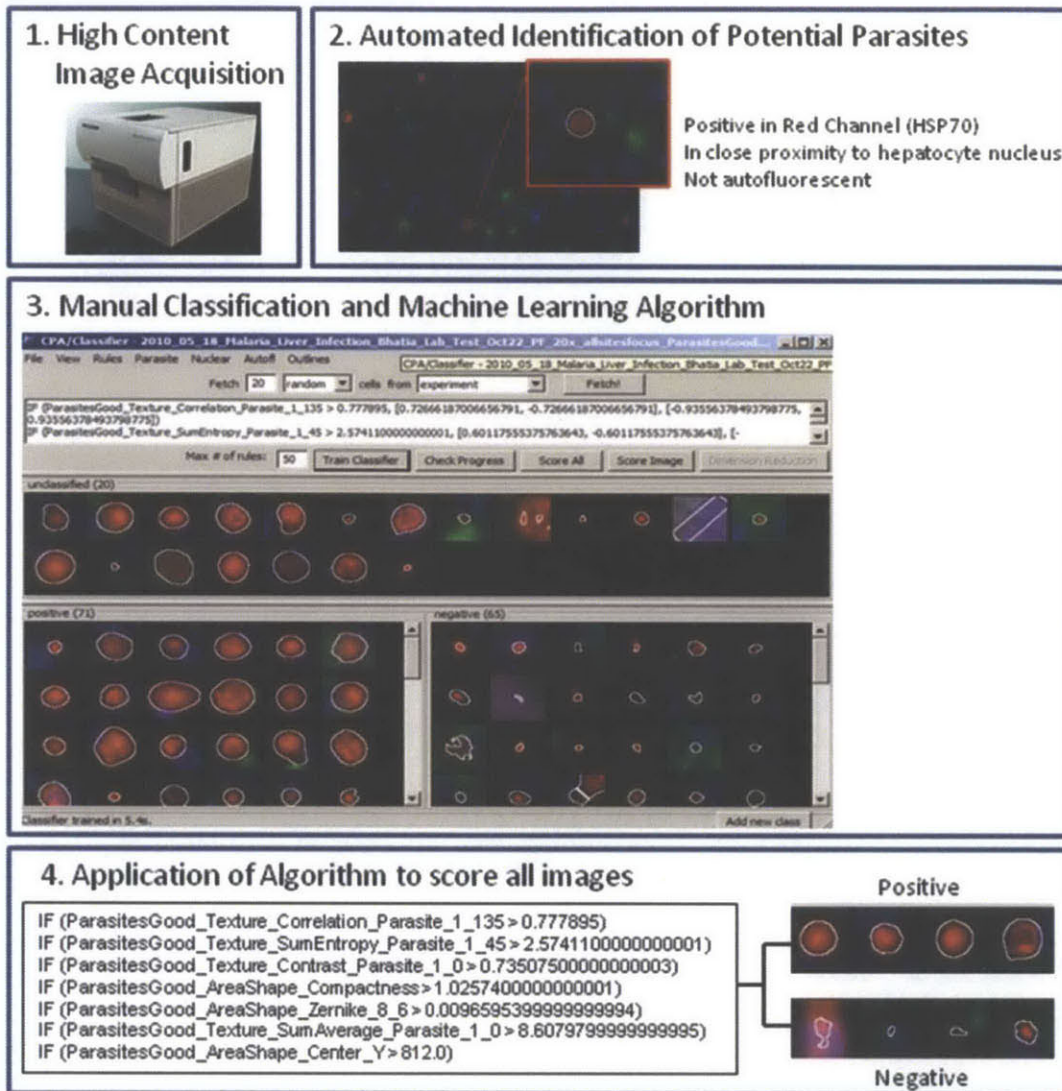
Figure 2.8. Image Automation Workflow, related to Figure 2.6. Images of 96 well plates are acquired using high content screening microscopes and analyzed by Cell Profiler (Broad Institute). Parasites are visualized through immunofluorescent staining of the HSP70 protein. Images of potential parasites are manually classified using Cell Profiler, which then learns the algorithm to score all images.

Infection of MPCCs with *Plasmodium vivax*

Plasmodium vivax differs from *P. falciparum* in several important ways. A key feature of *P. vivax* that underlies its persistence in the population is that the liver acts as a reservoir for dormant hypnozoites or 'small forms'[16,198]. These hypnozoites can reactivate after weeks, months, or even years, depending on the strain of *P. vivax*[199–201]. However, due to a lack of

model systems available to investigate this elusive organism, the biology of the dormant form of *P. vivax* is underexplored.

Based on our ability to establish the liver stage of *P. falciparum* in MPCCs, to maintain the hepatocyte phenotype for 4-6 weeks, and the observation that some strains of *P. vivax* can reactivate over a similar time scale, we next explored the feasibility of establishing the liver stages of *P. vivax* in MPCC over time. As for the *P. falciparum* experiments, the viability of the cryopreserved *P. vivax* sporozoites was evaluated by assessing their gliding motility prior to each experiment (**Figure 2.9A**). We explored several strains of *P. vivax* including Chesson, a strain known to efficiently form dormant forms and to reactivate at shorter time scales [202,203]. Cultures were infected and then fixed at various time points and stained for CSP. Using immunofluorescence microscopy, we analyzed the size distribution and localization of the *P. vivax* forms over a three week period. We readily observed *P. vivax* liver forms in MPCC, including mature, liver-stage schizonts larger than 20μm found at day 6 post-infection (**Figure 2.9B, C and 2.10A, B**). In addition, a population of smaller PvCSP-positive forms (<5μm) was detected within MPCCs at all time points, particularly identifiable at 6 and 21 days post-infection. (**Figure 2.9A, B and 2.10A-C**). The infection efficiency, based on the percentage of hepatocytes containing big and small PvCSP-positive forms at day 6 post-infection was 0.013% and 2%, respectively (**Figure 2.10D**). Similar numbers of small forms were observed up to day 21 (data not shown). Importantly, 85% of the small forms observed were intracellular, based on immunostaining performed before and after permeabilization (**Figure 2.10C**). In contrast, cultures infected with *P. falciparum* contained very few small forms after 15 days in culture, and those were predominantly extracellular (**Figure 2.10E**). These *P. vivax* small forms may represent the dormant hypnozoite stage of the parasite life cycle, which is responsible for clinical relapses in *P. vivax* malaria patients; however, further characterization will be required to substantiate this hypothesis. Both small and large forms were observed when other strains of fresh and frozen *P. vivax* sporozoites were examined (**Figure 2.10A and data not shown**). Finally, we demonstrated that the MPCC system can support maturation of hepatic *P. vivax* schizonts, based on the detection of the late-stage antigen PvMSP-1 at day 12 post-infection (**Figure 2.10B**).
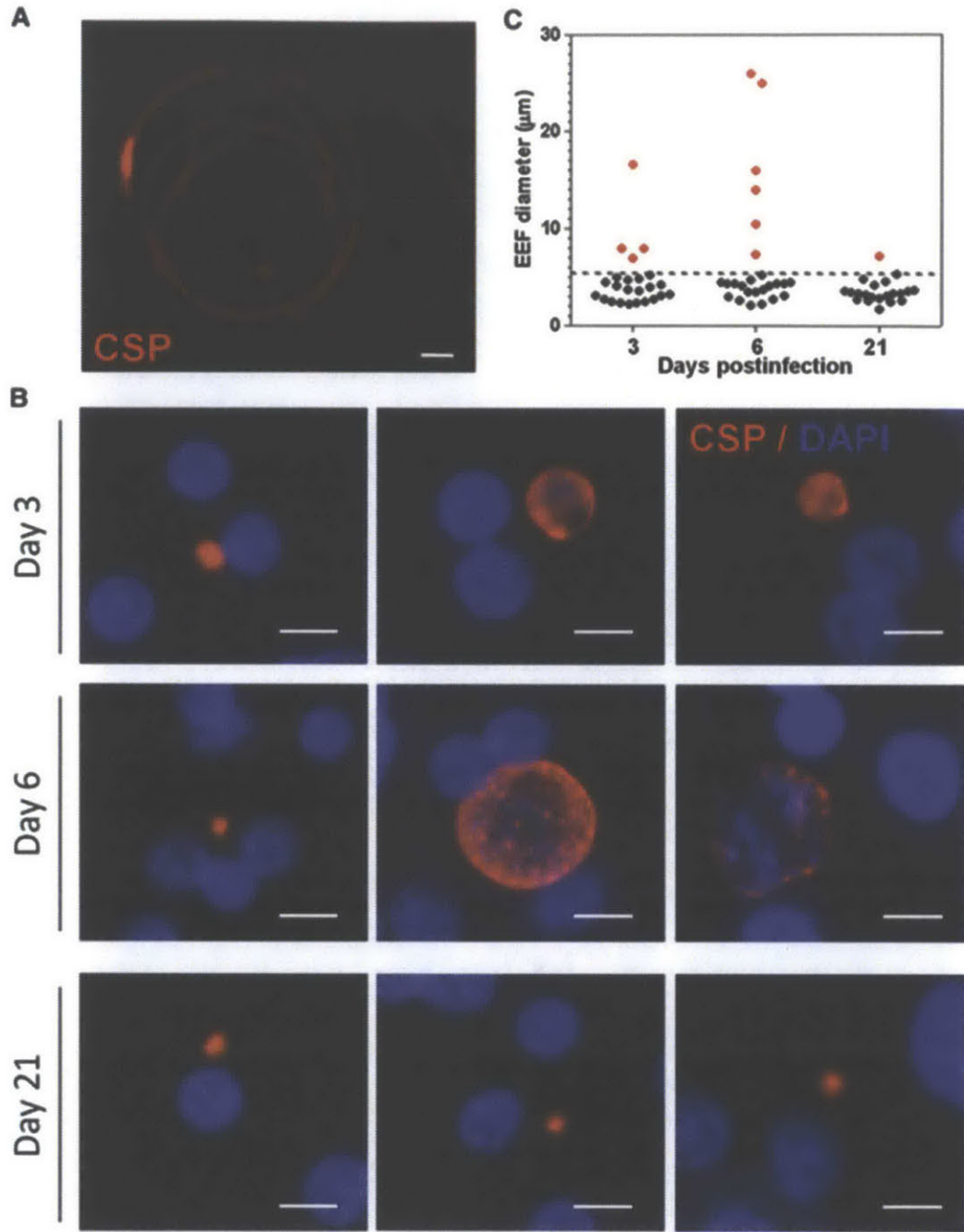
Figure 2.9. Infection with *Plasmodium* vivax. (A) Representative image of PvCSP-stained *P. vivax* (Chesson) sporozoites gliding. (B) Representative images of PvCSP-positive parasites over time. Scale bar = 10 mm. (C) Size distribution of *P. vivax* parasites in MPCCs over time. Red, all observed parasites bigger than 5 mm; black, 20 representative forms smaller than 5 mm. See also Figure S4.

	P.vivax (day 6 p.i)
Total big forms[a] / 10K Hep	1.3 ± 0.2 (0.013%)
Total small forms observed / 10K hep[$]	200 ± 25 (2%)
% of all small forms inside	85%
% of all small forms outside	15%

[a] big forms defined as DAPI+ forms >10µm
[$] all small forms observed <5µm
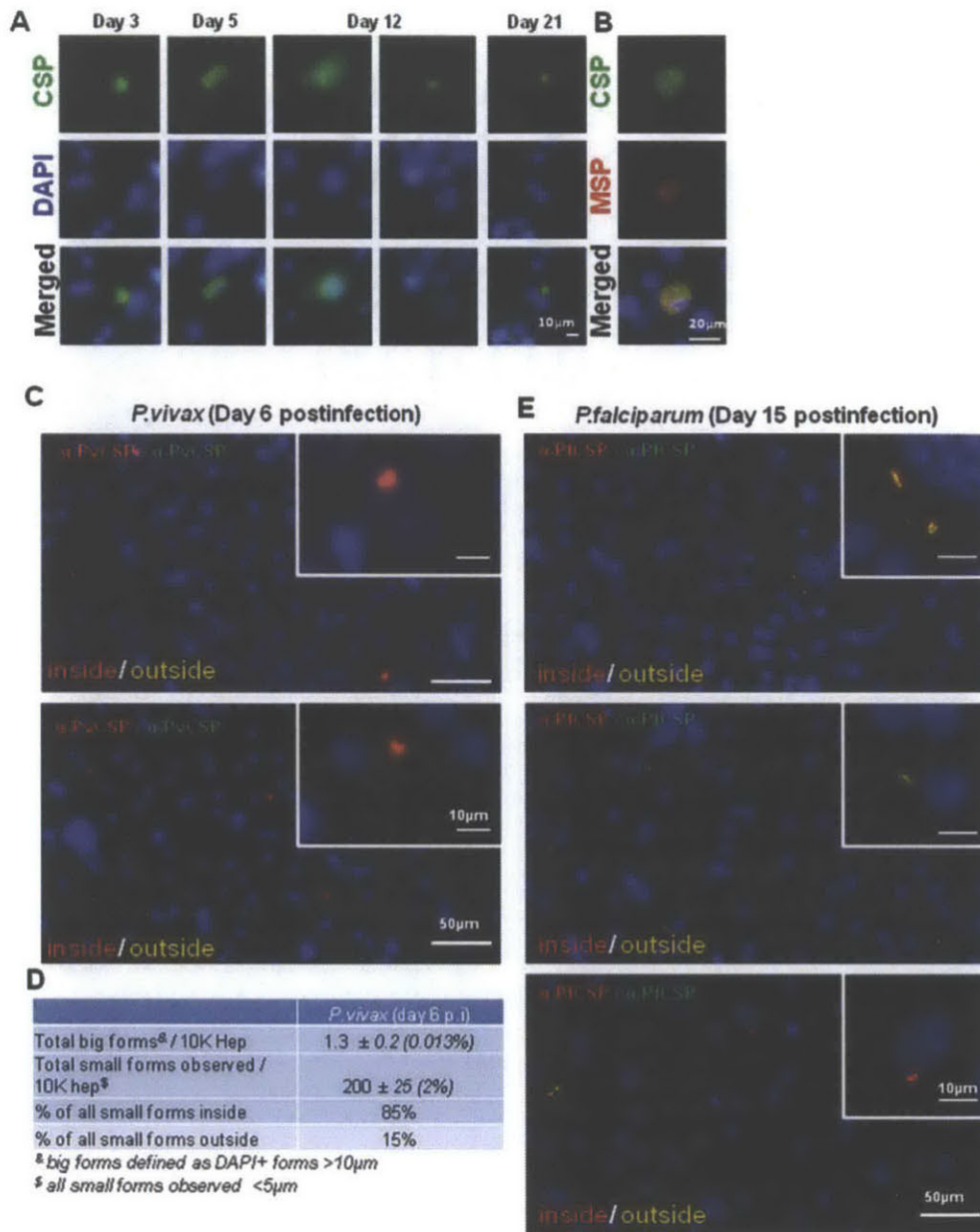
Figure 2.10. *Plasmodium vivax* **Infection Characterization** , Related to Figure 2.9. Infection with *Plasmodium* vivax (India VII). (A) Representative images of parasites at day 3, 5, 12 and 21 post-infection. Parasites are identified by anti-PvCSP staining. Scale bar: 10µm. (B) Detection of MSP-1 protein at day 12 post-infection. (C) Representative double immunofluorescence stain (anti-CSP) of primary human hepatocytes infected with cryopreserved *P. vivax* at day 6 post-infection. Extracellular and intracellular parasites are labeled yellow and red, respectively. Nuclei visible with blue DAPI stain. (D) Quantification of small (<5µm) and large (>10µm) forms in *P. vivax*-infected MPCCs. (E) Representative double immunofluorescence stain (anti-CSP) of primary human hepatocytes infected with cryopreserved *P. falciparum* at day 15. Extracellular and intracellular parasites are labeled yellow and red respectively.
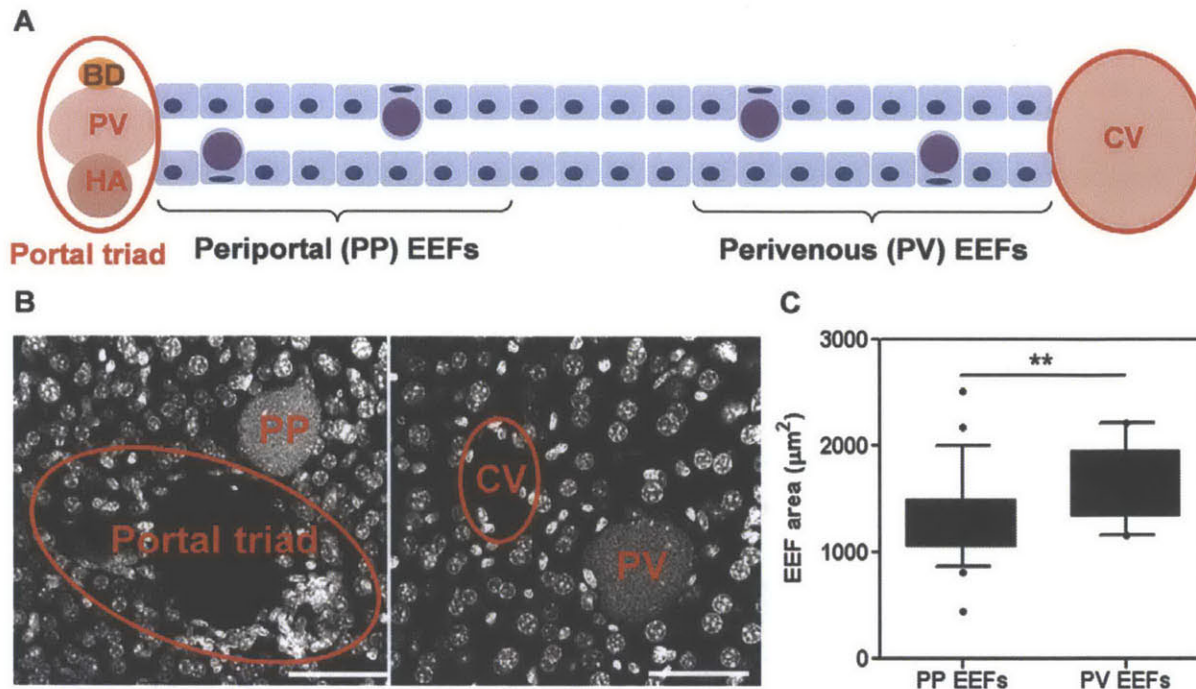
Figure 2.11. *Plasmodium* **EEF Development Correlates with Hepatic Oxygen Gradients** *In Vivo* . (A) Schematic of liver sinusoid denoting the definition of periportal (PP) EEFs and perivenous (PV) EEFs used for EEF size quantification. (B) 50-μm liver slices were stained with DAPI, and confocal *z*-stacks were made of GFP-expressing *P. yoelii* EEFs within 8 hepatocyte lengths of either the portal triad (periportal) or the central vein (perivenous) for which the maximal *XY* area could be determined within the slice. (C) Maximal *XY* areas of *P. yoelii* perivenous or periportal EEFs (as defined for A) at 46 hours post-infection in murine liver; **P<0.01, two-tailed *t*-test. Scale bar: 50 μm. PV, portal vein; BD, bile duct; HA, hepatic artery; CV, central vein.

In vivo **EEF development correlates with hepatic oxygen gradients**

Oxygen tensions in the hepatic sinusoids vary from 30 – 75 mmHg between the perivenous and periportal regions respectively[171]. To investigate whether this variation in oxygen concentration exerts an influence on liver stage *Plasmodium* infection *in vivo*, C57BL/6 mice were infected with GFP-expressing *P. yoelii* sporozoites, a host-parasite combination that supports robust liver stage infection[204], and their livers were collected 46h post-infection. Two populations of *P. yoelii* exoerythrocytic forms (EEFs) were defined to test the hypothesis that the hepatic sinusoidal variation of oxygen concentration correlates with EEF growth. EEFs were defined as periportal EEFs if they were found within 8 cell-lengths of the hepatic portal triad,

and perivenous EEFs if they were found within 8 cell-lengths of the hepatic central vein (**Figure 2.11A**). This definition minimizes the likelihood of an EEF being simultaneously defined as periportal and perivenous, taking into consideration that the number of hepatocytes between the portal triad and the central vein of a mouse liver is approximately 20. Immunohistochemical analysis of infected liver sections (**Figure 2.11B**) revealed that the maximal size of perivenous *P. yoelii* EEFs were significantly larger than periportal *P. yoelii* EEFs (**Figure 2.11C**), suggesting that oxygen concentrations could be a parameter that influences liver stage *Plasmodium* infection of primary hepatocytes *in vitro*.

Ambient hypoxia increases survival and growth of liver-stage malaria parasites in primary human hepatocyte MPCCs

To investigate whether hypoxia influences *P. berghei* infection of human liver cells *in vitro*, MPCCs were maintained at 4% O_2 for 24 hours before infection. A 3 hour exposure to *P. berghei* sporozoites was followed by an additional 48 hours of hypoxic culture, at which point infection efficiency was determined based on HSP70 immunofluorescence. The number of *P. berghei* EEFs per hepatocyte island was elevated in response to hypoxic incubation of primary human hepatocytes before, during and after infection (**Figure 2.12A**). A significant upward shift in the size distribution of *P. berghei* EEFs in hypoxic cultures compared to normoxic cultures was also observed (**Figure 2.12C, E**). This pattern of improved infectivity was observed in more than one lot of cryopreserved primary human hepatocytes (**Figure 2.12A, 2.13A**) and also in HepG2 cells (**Figure 2.13C**). Hypoxia-treated hepatocytes exhibited a similar increase in susceptibility to *P. yoelii* infection (**Figure 2.12B, D, F, 2.13B**), suggesting that the observed effect of hypoxia is not restricted to a particular *Plasmodium* spp..
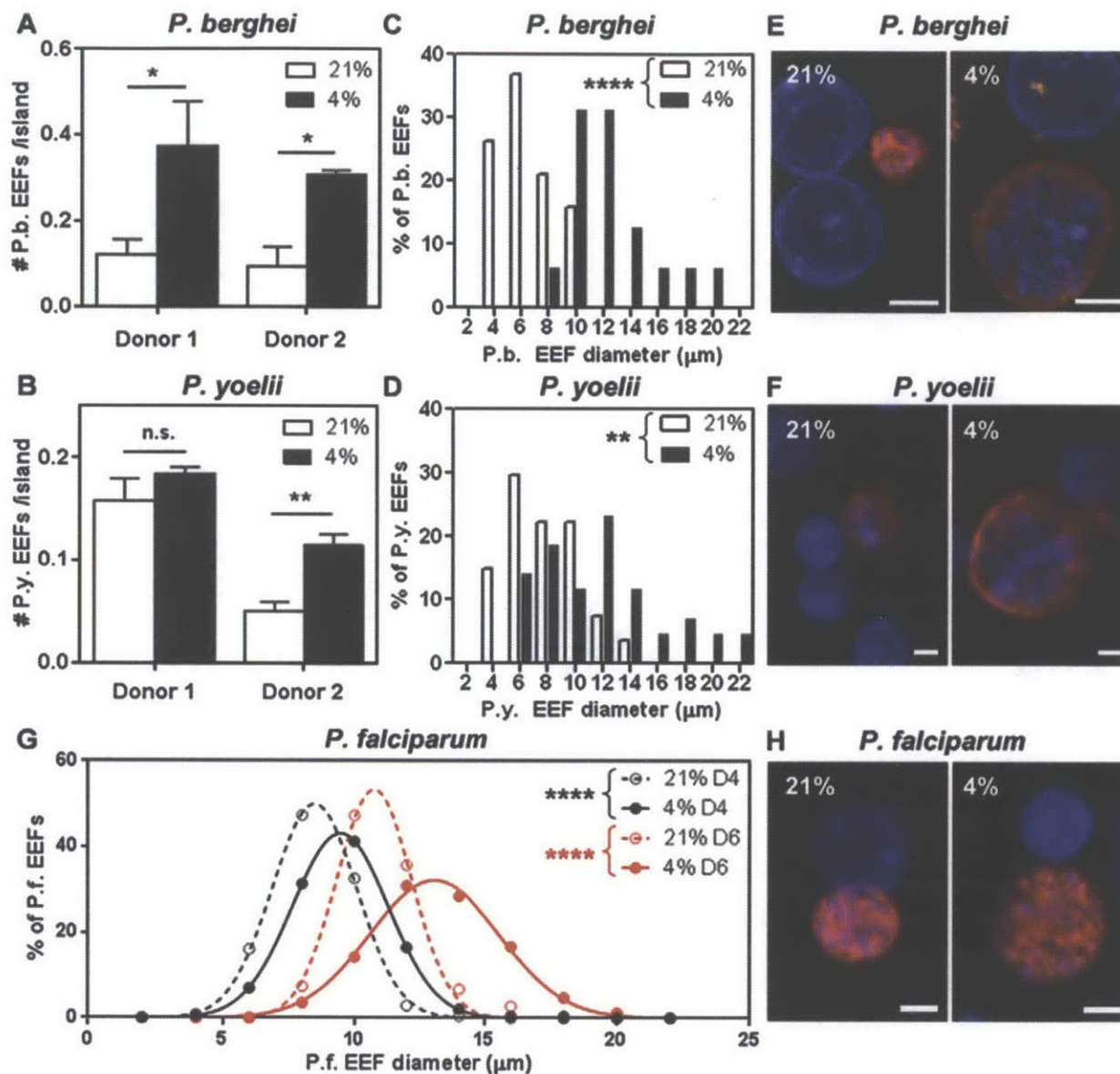
Figure 2.12. Ambient Hypoxia Increases Liver-stage Malaria Infection *In Vitro*. (A,B) Ambient hypoxia (4% O2) increases the number of *P. berghei* and *P. yoelii* EEFs in PHH MPCCs at 48 hours post-infection. (C,D,G) Ambient hypoxia (black symbols or bars, 4% O2) increases the EEF size distribution of *P. berghei* and *P. yoelii* at 48 hours post-infection and *P. falciparum* at 4 and 6 days post-infection in PHH MPCCs compared with normoxia (white symbols or bars, 21% O2). (E,F,H) Representative immunofluorescence images of *P. berghei*, *P. yoelii* EEFs at 48 hours post-infection, and *P. falciparum* EEFs at 6 days post infection at either ambient 21% or 4% O2. EEFs were stained for *Plasmodium* HSP70 (clone 2E6 for *P. berghei* and *P. yoelii*, clone 4C9 for *P. falciparum*). Scale bars: 5 μm. *$P<0.05$, **$P<0.01$, ****$P<0.0001$; two-tailed t-test.

Since *P. berghei* liver stage infections mature at 55-65 hours post-infection *in vitro*[205], *P. berghei* EEF sizes were quantified at 56 hours and 65 hours post-infection to address the possibility that hypoxia could be speeding up parasite development instead of increasing the potential for parasite growth. *P. berghei* EEFs were larger in hypoxic cultures at 48, 56 and 65 hours post-infection (**Figure 2.13F**). Furthermore, the number of *P. berghei* EEFs per hepatocyte island was consistently higher in hypoxic cultures at 48, 56 and 65 hours post-infection (**Figure 2.13E**). Given that both EEF numbers and sizes are larger in hypoxic cultures throughout the late liver stages of *P. berghei*, this suggests that the total number of potential merozoites is larger under hypoxia compared to normoxia. Consistent with this prediction, the number of nuclei in *P. berghei* EEFs at 65 hours post-infection was significantly higher in hypoxic cultures compared to the normoxic control (**Figure 2.13H**). *P. berghei* EEFs were also able to develop normally under hypoxia, as shown by the expression of the mid-liver-stage marker, PbMSP-1, at 65 hours post-infection and the appearance of various EEF morphologies characteristic of late liver-stage EEFs (**Figure 2.14**). Moreover, the percentage of MSP1-positive *P. berghei* EEFs is significantly higher in hypoxic cultures at 56 and 65 hours post-infection (**Figure 2.13G**), suggesting that the EEFs progress into the later phases of the liver stage more successfully under hypoxia.

Importantly, the effect of hypoxia on EEF size translated to the human *Plasmodium* species, *P. falciparum*, as ambient hypoxia increased the size of *P. falciparum* EEFs in hepatocytes at both 4 and 6 days post-infection (**Figure 2.12G, H**). However, the number of *P. falciparum* EEFs did not increase in hypoxic cultures maintained at 4% O_2 (**Figure 2.13D**).
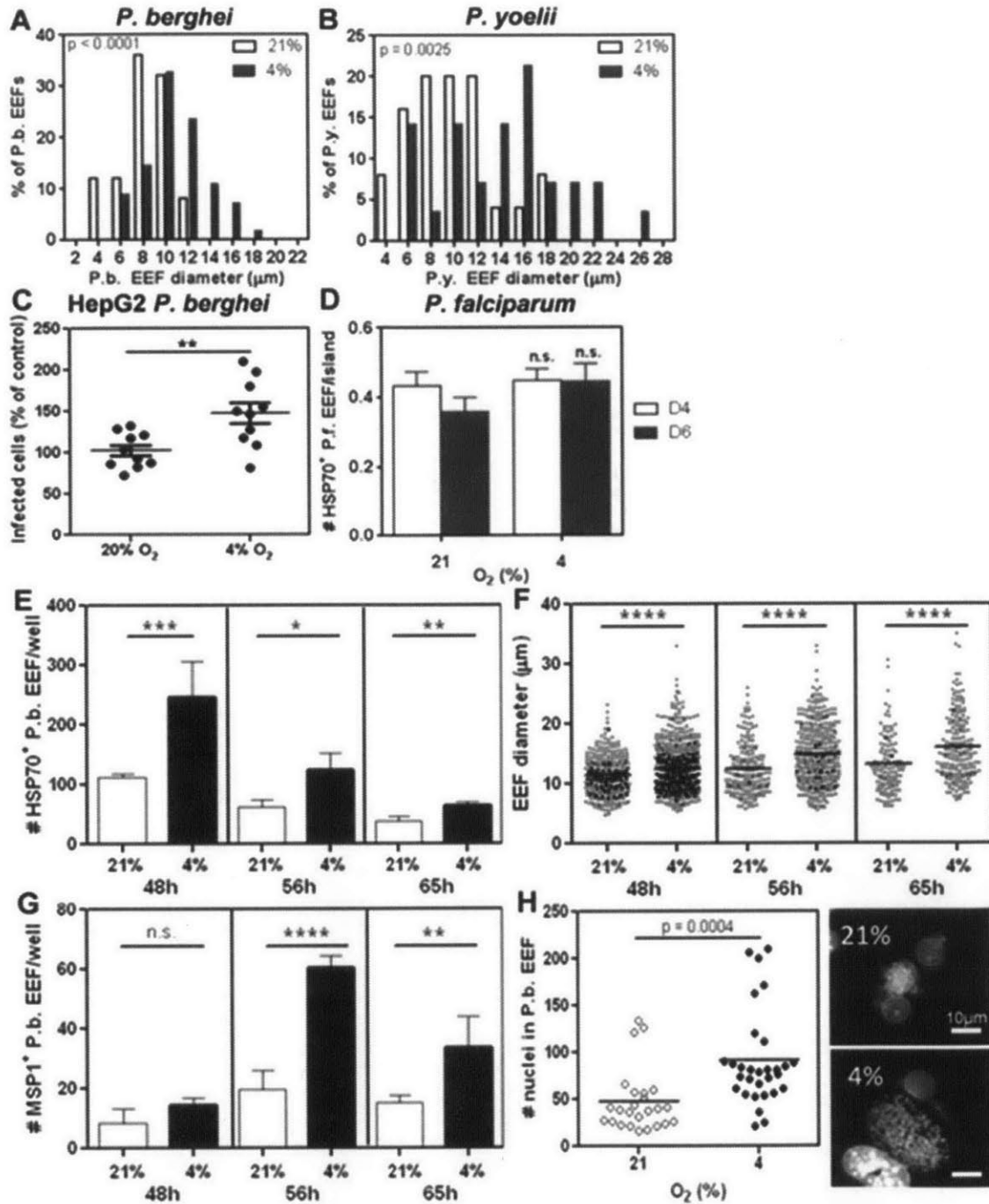
Figure 2.13: Effect of Ambient Hypoxia on Liver-stage Malaria Infection in Primary Human Hepatocytes. Ambient hypoxia (4% O_2) increases the (A) *P. berghei* and (B) *P. yoelii* EEF size distributions at 48h post-infection in primary human hepatocyte micropatterned cocultures in a second hepatocyte donor. $p < 0.0001$ and $p = 0.0025$ respectively, two-tailed t-test. (C) Ambient hypoxia (4% O_2) increases *P. berghei* infection in human hepatoma HepG2 cells at 48h post-infection. (D) Ambient hypoxia (4% O_2) does not increase *P. falciparum* infection in in primary human hepatocyte micropatterned cocultures at day 4 and day 6 post-infection. Culture of

primary human hepatocyte micropatterned cocultures at ambient hypoxia (4% O_2) during infection (E) increases the number of *P. berghei* EEFs at 48h, 56h and 65h post-infection compared to normoxia (21% O_2), * $p < 0.05$, ** $p < 0.01$, *** $p < 0.001$, two way ANOVA with Bonferroni Multiple Comparison Test, F = 32.1, DoF = 1, p = 0.0001 for the effect of O_2, (F) increases the *P. berghei* EEF size distribution at 48h, 56h and 65h post-infection compared to normoxia (21% O_2), **** $p < 0.0001$, two-tailed t-test, (G) increases the number of MSP1$^+$ *P. berghei* EEF at 56h and 65h post-infection. ** $p < 0.01$, **** $p < 0.0001$, two way ANOVA with Bonferroni Multiple Comparison Test, F = 63.5, DoF = 1, $p < 0.0001$ for the effect of O_2 and (H) increases the number of *P. berghei* nuclei per EEF at 65h post-infection. ** $p < 0.01$, two-tailed t-test. Scale bars: 10µm.
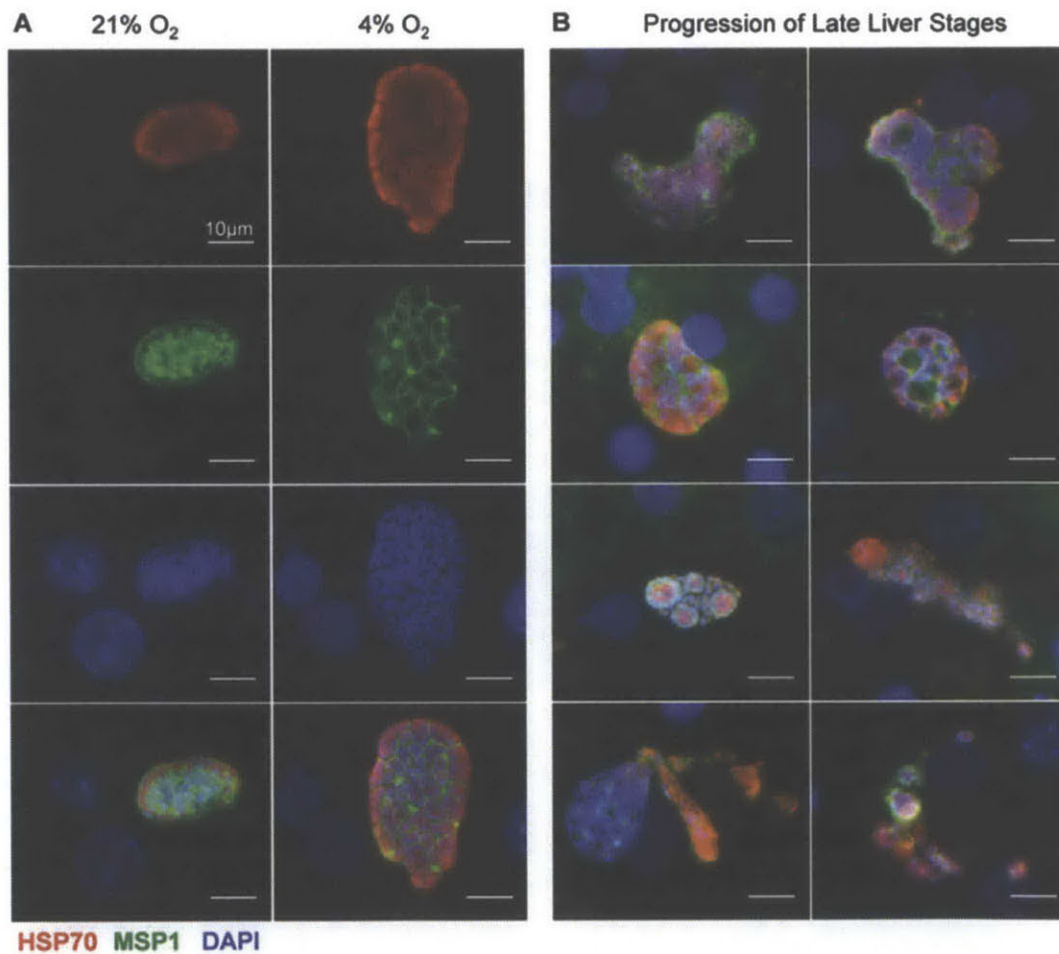
Figure 2.14: Late Liver-stage *Plasmodium* Development Under Ambient Hypoxia. (A) *P. berghei* EEFs at 65 hpi express PbHSP70 (red) and PbMSP-1 (green) at normoxia (21% O_2) or hypoxia (4% O_2). (B) Various stages of normal late liver-stage EEF development is observed at hypoxia. MSP-1 is initially expressed on the parasite membrane around all the parasite nuclei, then forms invaginations around groups of nuclei, and eventually surrounds individual merozoites. MSP-1-positive merosome-like structures are also observed breaking off from infected hepatocytes. Scale bars: 10µm.

Optimization of cell surface oxygen tension for *in vitro* liver-stage malaria infection

Given the observed impact of prolonged exposure to a reduced oxygen concentration, we sought an optimal set of conditions that might maximize the elevated infection of primary human hepatocytes (PHHs). By applying a mathematical model of diffusion and reaction solved at steady-state conditions[206] to PHH MPCCs (**Figure 2.15A, 2.16**), it was estimated that the typical cell surface pO_2 when cultures are incubated at normoxia ranges from $110 - 130$ mmHg (**Table 2.1**). In contrast, *in vivo* blood pO_2 (not at the cell surface) ranges from $30 - 75$ mmHg in the hepatic sinusoid[171]. Therefore, culture at ambient hypoxia may improve liver stage malaria infection by reducing cell surface pO_2 to a more physiologically relevant level. To test this hypothesis, a Hypoxyprobe™ assay that incorporates a hypoxic marker, pimonidazole hydrochloride[207], was conducted to compare the cell surface pO_2 in PHHs incubated at either normoxia or ambient hypoxia. Consistent with our hypothesis, incubation of PHHs at ambient hypoxia results in an increase in Hypoxyprobe™ staining relative to normoxia-cultured MPCCs (**Figure 2.15B**), confirming that ambient hypoxia indeed results in a decrease in cell surface pO_2 experienced by the hepatocytes.

Hepatocyte format	Predicted cell surface pO_2 (mmHg)
MPCC at normoxia (P_{air} = 21%)	$110 - 130$
MPCC at ambient hypoxia (P_{air} = 4%)	$5 - 10$
Hepatic sinusoid *in vivo*	$30 - 75$ (periportal – perivenous)[171]
Monolayer at normoxia (P_{air} = 21%)	$0.1 - 10$[29,167,208,209]

Table 2.1: Compilation of predicted cell surface pO_2 in different culture formats in primary hepatocyte *in vitro* culture models.

Cell surface pO_2 of MPCCs can also be altered by modifying parameters such as media height and hepatocyte density (**Figure 2.15A**). The model predicts that cell surface pO_2 decreases as media height increases (**Figure 2.16B**). Indeed, elevating the media height in wells of normoxic cultures resulted in an increase in Hypoxyprobe™ staining at the cell surface (**Figure 2.17A, B**). The greater media height also led to increased numbers of *P. berghei* EEFs at 48 hours post-infection (**Figure 2.17C**), collectively supporting the hypothesis that the effects of

ambient hypoxia on *in vitro* liver stage malaria infection efficiencies are mediated by a decrease in the effective cell surface pO_2 experienced by the hepatocytes.

Modeling also predicts that cell surface pO_2 will decrease as cell density increases (**Figure 2.15C, 2.16A**). However, modifications to hepatocyte density in a conventional monolayer culture may also influence infection efficiency due to the resulting changes in hepatocyte survival, polarization and morphology, rather than in response to changes in cell surface pO_2. To vary hepatocyte density while preserving the homotypic interactions necessary for hepatocyte survival and functional maintenance, the density of the hepatocyte island patterning was varied in MPCCs. These modifications led to perturbations of the cell surface pO_2 as predicted by the model, based on Hypoxyprobe™ staining results (**Figure 2.15C**). The simultaneous variation of both hepatocyte island density and atmospheric oxygen level permits fine-tuning of cell surface oxygen levels that span 4 orders of magnitude. Infections with *P. yoelii* across this range of conditions yield a monotonic increase in total EEFs as cell surface pO_2 decreases (**Figure 2.15E**). However, a threshold cell surface pO_2 is observed at 5 − 10 mmHg, below which the number of mature EEFs (> 10µm) decreases as cell surface pO_2 declines (**Figure 2.15D**). This biphasic relationship between the number of mature EEFs and cell surface pO_2 suggests that there is an optimal cell surface pO_2 for maximizing the number of mature EEFs in infected MPCCs. The combination of the optimal hepatocyte island density under ambient hypoxia (4% O_2) which gives rise to the optimal cell surface pO_2 of 5 − 10 mmHg was hence used for subsequent experiments.
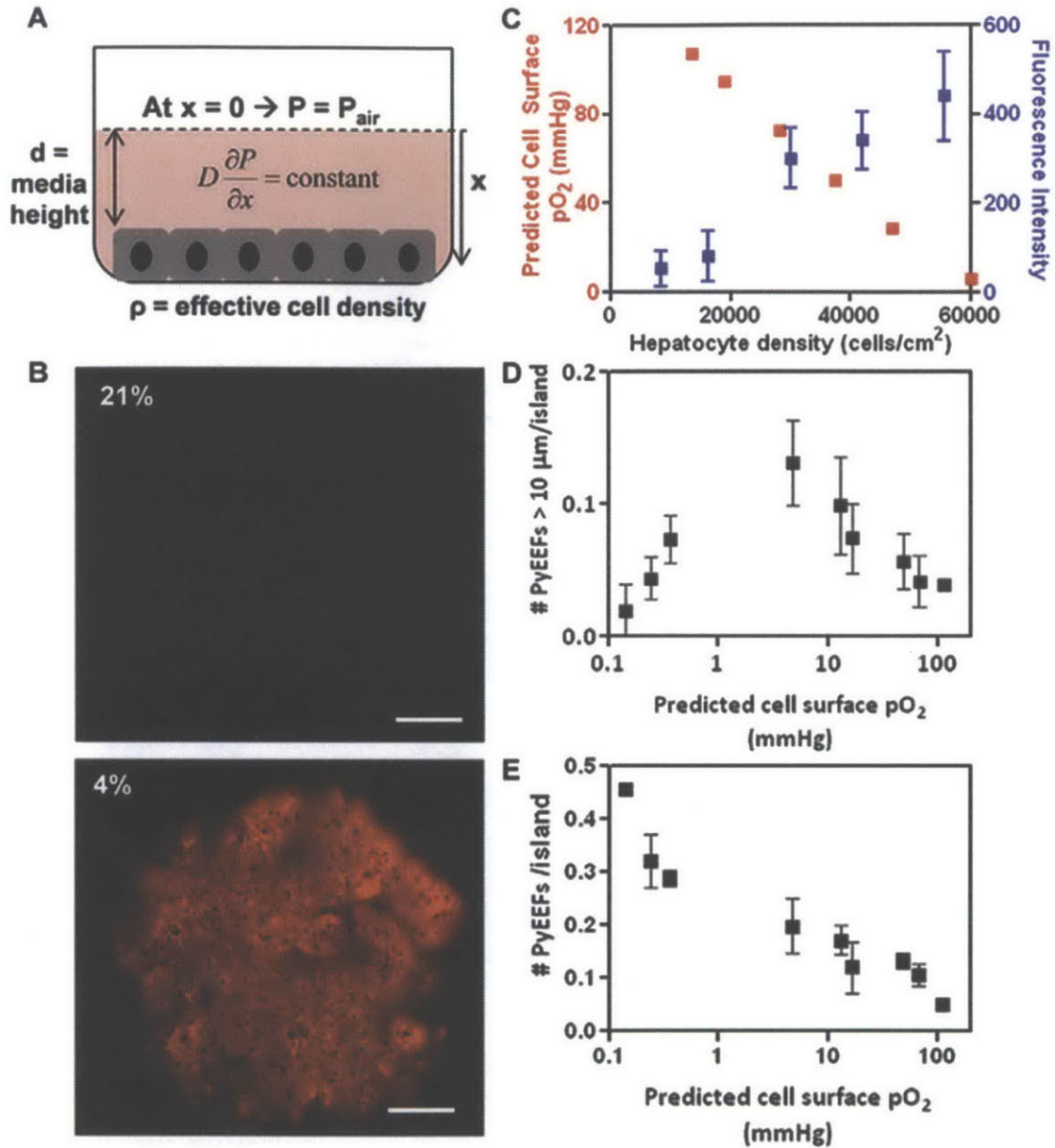
Figure 2.15. Optimal pO₂ Exists for Development of Mature *Plasmodium* EEFs. (A) Schematic of steady state diffusion-reaction model with three parameters that determine cell surface oxygen concentration: atmospheric pO_2 (P_{air}), height of medium and cell density.(B) Validation of effect of atmospheric pO_2 on cell surface pO_2 by Hypoxyprobe™ staining. Hypoxyprobe™ forms covalent adducts with thiol groups at $pO_2 < 10$ mmHg. (C) Modulation of cell surface pO_2 by varying effective cell density as predicted by the model (red), and Hypoxyprobe™ fluorescence intensity (blue). (D,E) Modulation of cell surface pO_2 by simultaneously varying both atmospheric pO_2 and effective cell density results (D) in a biphasic relationship between the number of well-developed *P. yoelii* EEFs and the predicted cell surface pO_2 and (E) in a monotonic relationship between the total number of *P. yoelii* EEFs versus predicted cell surface pO_2 in PHH MPCCs at 48 hours post-infection. Scale bars: 100 μm.

Model formulation

$$\frac{\partial P}{\partial t} = D\,\frac{\partial^2 P}{\partial x^2} + R$$

$$\frac{\partial P}{\partial t} = 0 \quad \text{and} \quad R = 0 \ \text{(in the bulk)}$$

$$\therefore \quad \frac{\partial^2 P}{\partial x^2} = 0 \ \rightarrow \ D\,\frac{\partial P}{\partial x} = \text{constant}$$

Boundary conditions:

1) O_2 uptake governed by Michaelis-Menten kinetics

$$-D\frac{\partial P}{\partial x} = \frac{V\rho P}{k(K_m + P)} \quad \text{at } x=d$$

2) Constant atmospheric oxygen

$$P = P_{air} \quad \text{at } x = 0$$

Symbol	Model parameter	Value used in model
D	Diffusivity of O_2 in water at 20°C	2×10^{-5} cm^2/s[1]
V	O_2 uptake rate of primary hepatocyte	4×10^{-7} nmol/s/cell[1]
ρ	Effective cell density	$8.4 \times 10^3 - 5.6 \times 10^4$ cells/cm^2
K	O_2 solubility in water	1.71 nmol/mL/mmHg[1]
Km	Partial pressure at half-maximal O_2 uptake rate	0.5 mmHg[1]
P_{air}	Atmospheric partial pressure of O_2	30 mmHg (4%) or 140 mmHg (21%)
d	Medium height	0.14 – 0.76 cm

[1]Yarmush, M. L., et al. (1992). Ann N Y Acad Sci **665**: 238-252
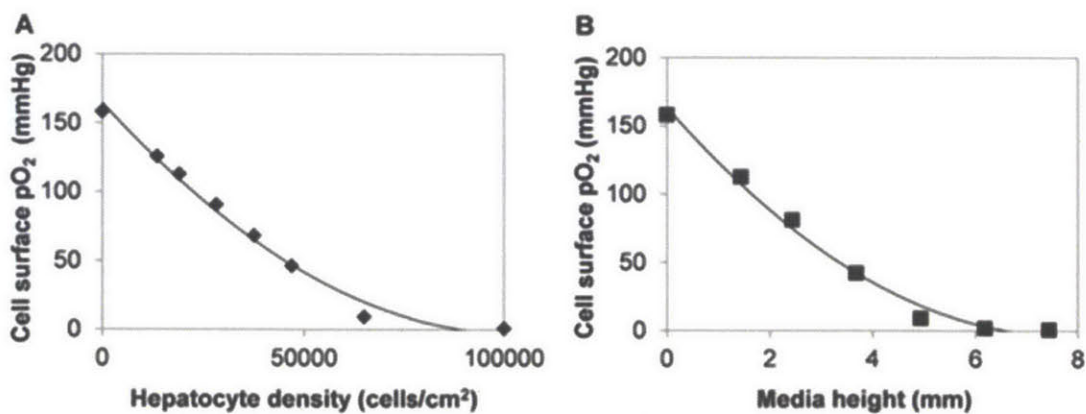
Figure 2.16: Diffusion – reaction model of cell surface pO$_2$. Mathematical model employed in the study. Table of parameter values used in this study. Graphs showing the modulation of cell surface pO$_2$ by (A) effective cell density and (B) media height as predicted by the mathematical model.
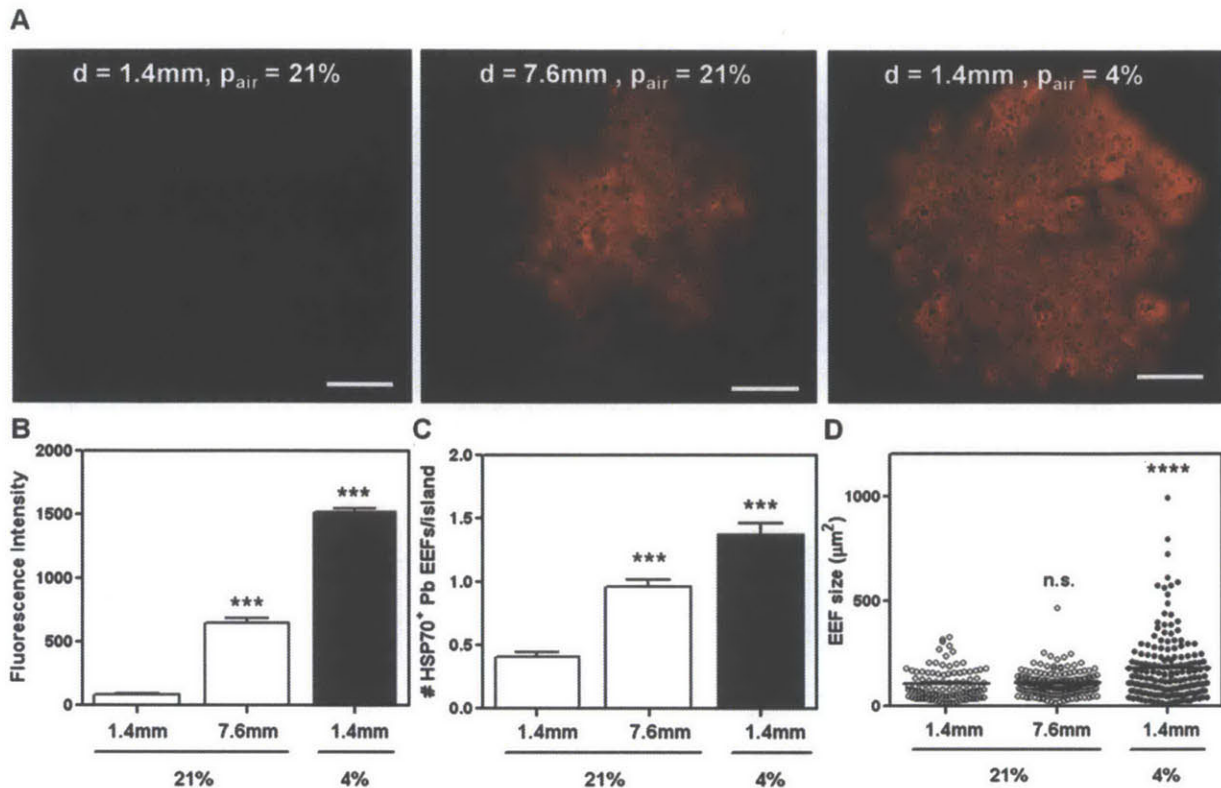
Figure 2.17: Modulation of Cell Surface pO_2 by Variation in Medium Height. (A) Increasing medium height at normoxia increases cell surface pO_2, as determined by Hypoxyprobe staining (red). (B) Quantification of Hypoxyprobe fluorescence intensity. (C) Decreasing cell surface pO_2 by increasing medium height increases *P. berghei* infection efficiencies in PHH MPCCs, but has no effect on EEF size distribution (D). *** $p < 0.001$, **** $p < 0.0001$, one way ANOVA with Tukey's Multiple Comparison Test. Scale bars: 100 μm.

Kinetics of hypoxic treatment alters liver-stage malaria infection *in vitro*

The hypoxia experiments performed thus far have exposed the PHH MPCCs to hypoxia throughout the 24h before infection, during infection (0 – 3h) and after infection (3 – 48h), termed the priming, invasion, and development phases, respectively. To assay whether improved infectivity requires each of these three phases of hypoxic treatment, MPCCs were incubated at ambient hypoxia over varying portions of the assay (**Figure 2.18A**). Increased numbers of EEFs at 48 hours post-infection were only observed when the infected MPCCs were cultured under hypoxia during the invasion and development phases (**Figure 2.18B**, conditions

A, B, E). In contrast, MPCCs pre-treated with hypoxia before infection and subsequently returned to normoxia (**Figure 2.18B**, conditions C, D) did not exhibit an increase in EEF number. These findings suggest that hypoxia treatment improves late-stage infection rates by reducing the attrition rate of EEFs rather than promoting the initial susceptibility of the host hepatocytes to sporozoite invasion. However, hypoxia over varying portions of the assay did not change the proportion of large EEFs 48h post-infection (**Figure 2.18C**).
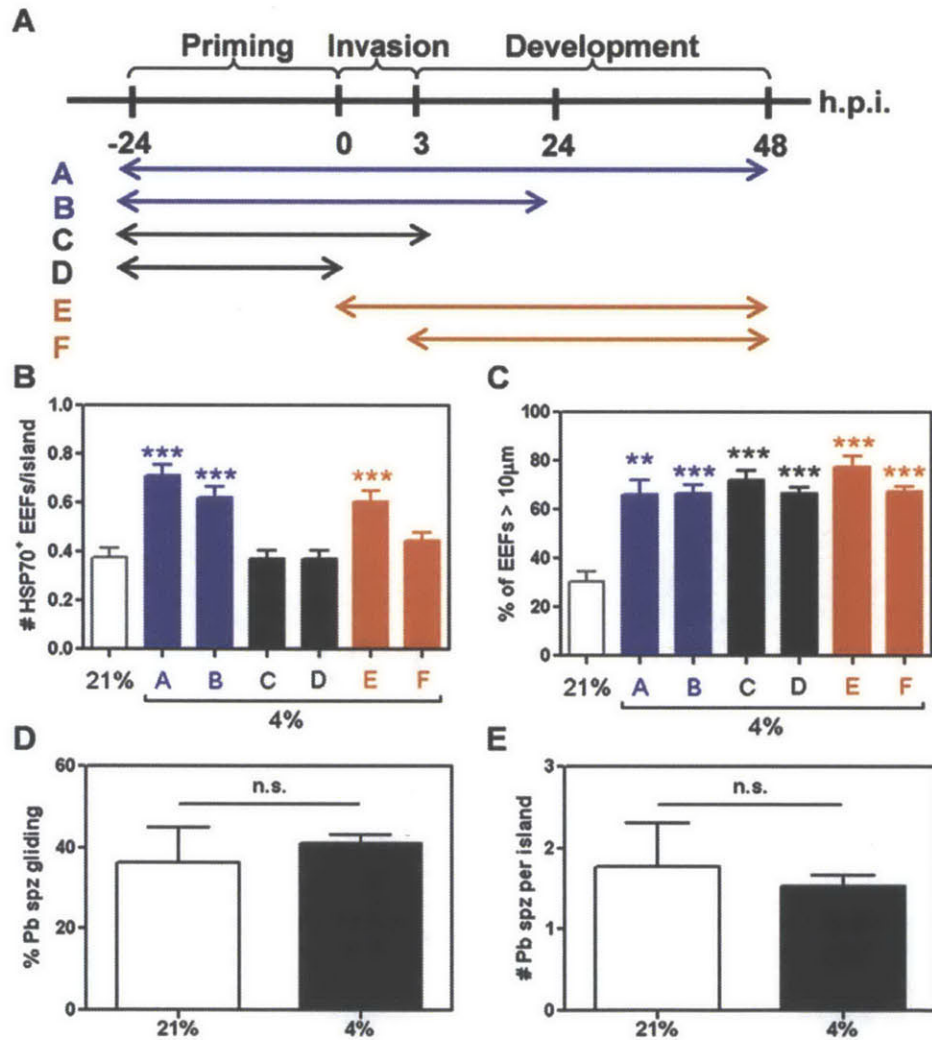
Figure 2.18. Kinetics of Hypoxic Treatment Alters Liver-stage Malaria Infection *In Vitro*. (A) Schematic of differential hypoxia treatment regimes. (B) Effect of differential hypoxia kinetic regimes on the number of *P. berghei* EEFs at 48 hours post-infection. (C) Effect of differential hypoxia kinetic regimes on *P. berghei* EEF sizes at 48 hours post-infection. (D) Effect of ambient hypoxia on *P. berghei* sporozoite gliding. (E) Effect of ambient hypoxia on *P. berghei* sporozoite entry into hepatocytes at 3 hours post-infection. **$P<0.01$, ***$P<0.001$; one way ANOVA with Tukey's multiple comparison test.

Hypoxia does not increase sporozoite-dependent or host-dependent invasion

To examine whether the hypoxia-mediated change in hepatocyte infectivity stems from an impact on sporozoite function, sporozoite gliding motility and sporozoite entry were assayed. Ambient hypoxia did not result in a significant difference in the gliding motility of *P. berghei* sporozoites (**Figure 2.18D**), and hypoxic treatment of hepatocytes did not change the number of the sporozoites that successfully entered hepatocytes (**Figure 2.18E**), suggesting that hypoxia does not improve late-stage infection efficiencies via sporozoite or host-mediated increases in the initial invasion rate, but rather by affecting the ability of the host cell to support EEF survival and growth.

Host HIF-1α induction promotes EEF survival in infected hepatocytes

The hypoxic responses of mammalian cells is largely mediated by the hypoxia-inducible factor-1 (HIF-1) pathway[210]. Consistent with the reported literature, gene set enrichment analysis (GSEA) of PHH MPCCs incubated at ambient hypoxia revealed a marked enrichment for the expression of genes that are transcriptionally regulated by HIF-1α relative to normoxic MPCCs (**Figure 2.21A**). Cobalt (II) chloride is a hypoxia mimetic which has been reported to induce the intracellular stabilization of HIF-1α and lead to the transcriptional activation of downstream hypoxia-responsive genes[211]. To determine whether ambient hypoxia promotes liver-stage malaria infection in PHH MPCCs via host HIF-1α induction, pharmacologic activation of HIF-1α in PHH MPCCs by cobalt (II) chloride was performed at normoxia in three different combinations of the priming, invasion and development phases (**Figure 2.19A**). Cobalt (II) treatment of PHH MPCCs at normoxia in any of the three combinations tested resulted in an increased number of *P. berghei* EEFs 48 hours post-infection, with the greatest effect observed if cobalt (II) was present throughout all three phases of priming, invasion and development (**Figure 2.19B**). Of note, while ambient hypoxia (4% O_2) consistently led to the emergence of a subset of larger EEFs relative to normoxic controls, cobalt (II) treatment did not fully replicate this outcome (**Figure 2.19C, Figure 2.20A**).
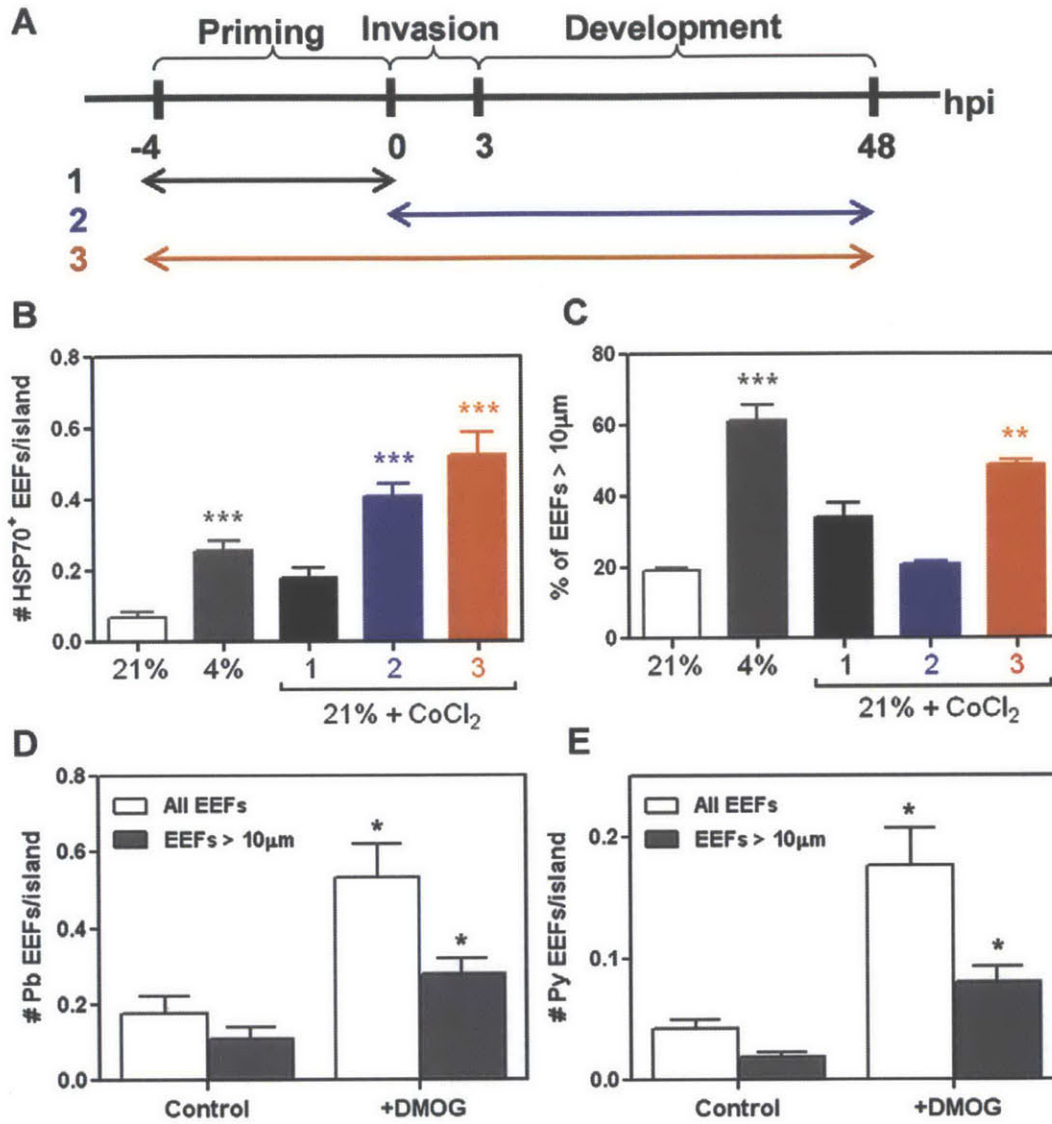
Figure 2.19: Host HIF-1α Induction Increases EEF Numbers in Infected Hepatocytes. (A) Schematic of cobalt (II) chloride treatment of primary human hepatocyte micropatterned cocultures (PHH MPCCs) during infection with *P. berghei*. (B) Effect of cobalt (II) treatment of PHH MPCCs at 21% O_2 on the number of *P. berghei* EEFs at 48h post-infection, and (C) on the percentage of *P. berghei* EEFs > 10μm at 48h post-infection. ** $p < 0.01$, *** $p < 0.001$, one way ANOVA with Tukey's Multiple Comparison Test. (D) Effect of DMOG treatment of PHH MPCCs at 21% O_2 on the numbers of *P. berghei* EEFs and (E) the number of *P. yoelii* EEFs at 48h post-infection. * $p < 0.05$, two-tailed t-test.

Under normoxia, HIF-1α is constitutively marked for proteasomal degradation by prolyl hydroxylase (PHD). Inhibition of PHD by a small molecule, dimethyloxalylglycine (DMOG), results in HIF-1α stabilization and the associated downstream host hypoxic responses[211]. GSEA of hypoxic MPCCs also shows a marked enrichment for the expression of a set of genes that are upregulated under DMOG treatment (**Figure 2.21B**)[212]. Consistent with the effect of cobalt (II) treatment on *P. berghei* infection at normoxia, PHH MPCCs that were treated with DMOG at normoxia demonstrate increased numbers of *P. berghei* and *P. yoelii* EEFs at 48h post-infection (**Figure 2.19D, E**), with the number of *P. berghei* EEFs increasing in a dose-dependent fashion with DMOG concentration (**Figure 2.20B**). However, DMOG treatment did not lead to the emergence of a subset of larger EEFs compared to the untreated control, in contrast to ambient hypoxia (**Figure 2.20C**). Further increases in DMOG concentration inhibited EEF development (**Figure 2.20C**), which is reminiscent of the effect of extremely low levels of pO_2 on the number of well-developed EEFs (**Figure 2.15D**). Together, these data suggest that intermediate levels of HIF-1α activation in the host hepatocyte support EEF survival but not EEF growth, but higher levels of HIF-1α may inhibit EEF growth and mediate the biphasic effect of pO_2 on EEF size observed in earlier experiments.
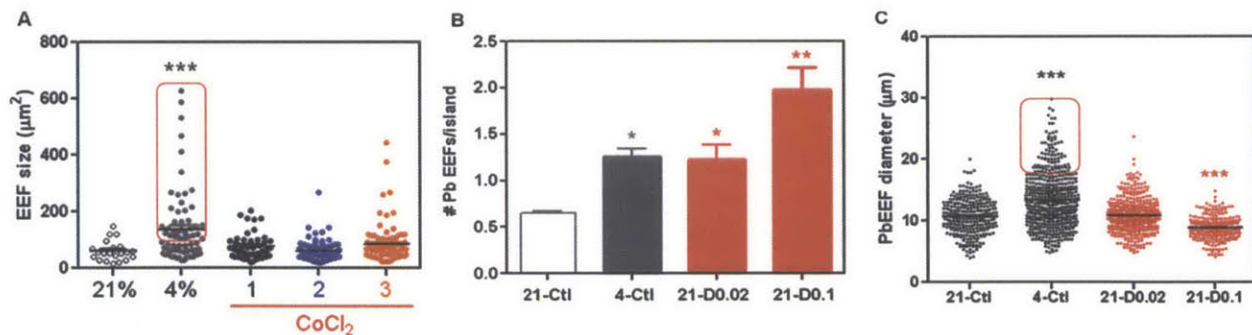
Figure 2.20: Effect of Hypoxia Mimetics on *P. berghei* Infection in PHH MPCCs. (A) Size distributions of *P. berghei* EEFs infected at normoxia, ambient hypoxia or with cobalt (II) treatment. (B) Effect of 0.02mM or 0.1mM DMOG treatment on *P. berghei* infection in MPCCs. (C) Size distributions of *P. berghei* EEFs infected at normoxia, ambient hypoxia or 0.02mM or 0.1mM DMOG. * p< 0.05, ** p < 0.01, *** p < 0.001, one way ANOVA with Tukey's Multiple Comparison Test.
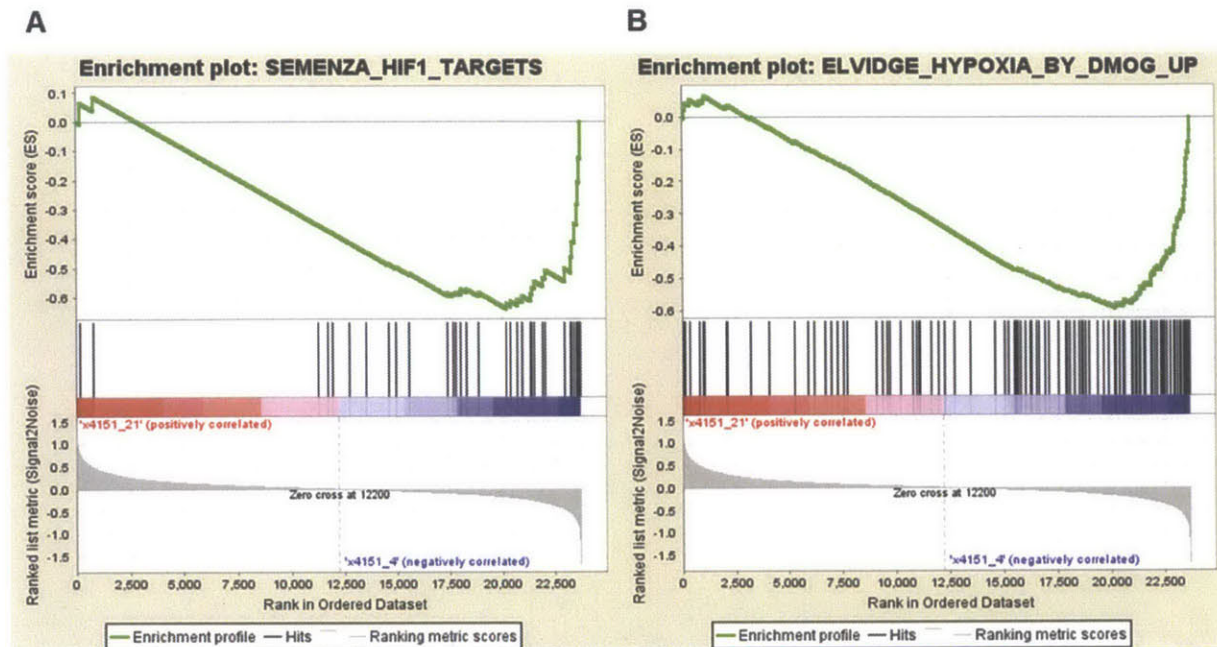
Figure 2.21: Gene Set Enrichment Analysis Comparing PHH MPCCs Incubated at Normoxia and Ambient Hypoxia. In these plots, a positive enrichment score indicates correlation of the queried gene set with the normoxic (21% O_2) condition, whereas a negative enrichment score indicates correlation of the queried gene set with the hypoxic (4% O_2) condition. The bottom portion of the plot shows the value of the ranked list metric as you move down the list of ranked genes. The ranked list metric measures a gene's correlation with a phenotype, and its value goes from positive to negative as you move down the ranked list. A positive value indicates correlation with the normoxic condition (21% O_2) and a negative value indicates correlation with the hypoxic condition (4% O2). (A) A GSEA enrichment plot shows enrichment in hypoxia (4% O_2) treated PHH MPCCs for an *a priori* defined query set of genes that is transcriptionally regulated by HIF-1α, with a negative enrichment score of -0.64, and a normalized enrichment score of -2.01. (B) A GSEA enrichment plot shows enrichment in hypoxia (4% O_2) treated PHH MPCCs for an *a priori* defined query set of genes that is upregulated by hypoxia mimetic DMOG, with a negative enrichment score of -0.63, and a normalized enrichment score of -2.49.

Exogenous and endogenous inhibitors of interferon signaling also rescue liver-stage malaria infection in MPCCs

Previous studies in our lab had shown that the infection of viral infection of MPCCs is associated with the induction of interferon stimulated gene (ISG) expression in hepatocytes and correlates with the spontaneous clearance of infection *in vitro*. To determine whether primary human hepatocytes mount an ISG response to *Plasmodium* liver-stage infection, we monitored ISG levels post-infection by *P. berghei* by RT-PCR. We found that exposure of MPCCs to *P. berghei* sporozoites obtained through the dissection of *P. berghei*-infected *Anopheles stephensi* mosquitoes resulted in a significant increase in the expression of many ISGs compared to the mock-infected controls that were exposed to salivary gland material from uninfected mosquitoes of the same species at 48 hours post-exposure (**Figure 2.22A**).

Prior MPCC infection studies with hepatitis C virus showed that persistent viral infection could be achieved in MPCCs by inhibiting the innate immune response of primary human hepatocytes with a small molecule inhibitor of the JAK family of proteins, which includes JAK1, a mediator of the cellular response to interferon by inducing dimerization and nuclear translocation of signal transducer and activator of transcription 1 (STAT1) and STAT2, ultimately leading to the expression of interferon stimulated genes (ISGs). Furthermore, these studies showed that certain immunomodulatory signals present in the liver, like IL-6, could dampen the interferon response to infection and thereby increase infection in MPCCs. Infection of MPCCs with *P. berghei* in the presence of either JAK inhibitor (JAKi) or IL-6 dramatically reduced *P. berghei*-induced ISG expression (**Figure 2.22A**). To determine whether the inhibition of interferon signaling by JAKi or IL-6 enhances *P. berghei* infection, we carried out two assays: enumeration of *P. berghei* EEFs in hepatocytes via immunostaining for *P. berghei* HSP70, and RT-PCR for *P. berghei* 18S ribosomal RNA (rRNA). Assaying infection by both assays reveals that both JAKi and IL-6 significantly enhance infection (**Figure 2.22B, Figure 2.22C**). These data demonstrate that *P. berghei* elicits an interferon-mediated elevation in ISG levels that limits infection, and this can be rescued by inhibiting the ISG response to infection.
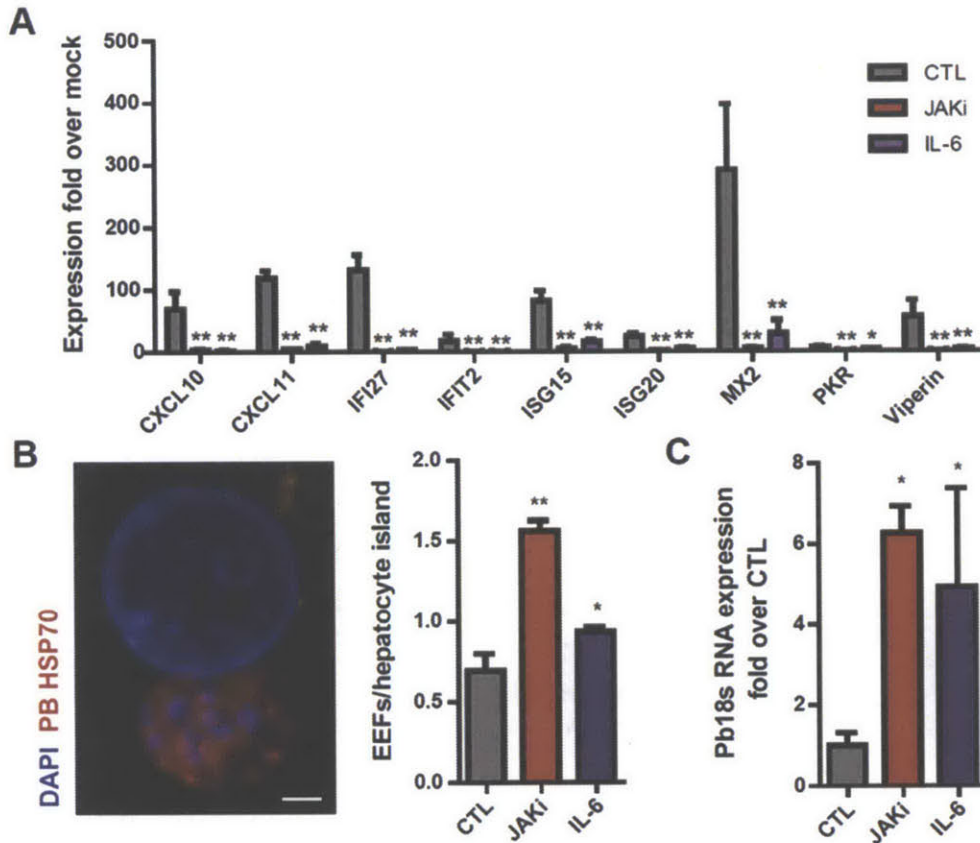
Figure 2.22: Effect of JAKi and IL-6 on Interferon Signaling Induced by Liver-stage Malaria Infection of MPCCs. (A) RT-PCR data for interferon-stimulated genes (ISGs) in response to *P. berghei* infection of MPCCs that are treated with DMSO (CTL), JAKi or IL-6, as normalized by the baseline ISG levels expressed in mock-infected MPCCs. (B) (left) Example of *P. berghei* EEF immunostained with an antibody against PbHSP70. (right) Quantification of *P. berghei* infection rates in infected MPCCs treated with either DMSO (CTL), JAKi or IL-6. (C) Quantification of *P. berghei* parasite loads in various conditions via RT-PCR analysis of *P. berghei* 18S ribosomal RNA levels.

2.3 Discussion

Platform establishment and demonstration of applications

In the first part of this chapter, we describe an *in vitro* cell-based platform that recapitulates the human liver stage of *P. falciparum* and *P. vivax* infection. Although some attempts to infect cryopreserved human primary hepatocytes have been described in the past[213,214], this source of hepatocytes has not been routinely adopted by the field, to date. The advantages of screening individual cryopreserved hepatocyte lots is paralleled by the successful production in a high compliance environment of purified, vialed, cryopreserved, well

characterized sporozoites which is a much more recent advance[18,25,215]. These cryopreserved resources overcome the donor-to-donor variability seen in primary cultured human hepatocytes as well as infectivity rate variability introduced by different batches of mosquitoes or sporozoites. In addition, the use of cryopreserved components in this platform allows for a reliable source of reagents for use in longitudinal experiments, including screening and subsequent validation. Furthermore, since cell culture of patterned hepatocytes using the MPCC platform can maintain individual patient samples for between 4 and 6 weeks[118], it is feasible to perform long-term monitoring of both liver- and blood-stage *Plasmodium* infections, analyze genetic changes acquired inside Anopheles mosquitoes, assess the safety of attenuated sporozoite vaccine candidates, and characterize *P. vivax* hypnozoites *in vitro* using this system. Notably, development of vaccines and drugs against this stage of *P. vivax* has been identified as a critically important goal for research to eradicate malaria[155,216]. Recent publications have highlighted that existing candidate vaccines continue to underperform in clinical trials, and significant "blood breakthrough" of presumably attenuated parasites formulations has been observed[217].

In our experience with disease modeling of drug-induced liver injury and hepatitis C infection, establishing platforms that better reflect host biology is an important first step to determining where existing model systems were lacking (e.g., P450 activity and interferon signaling, respectively). In this case, we have already observed three advantages over *in vitro* hepatoma cultures: (1) sporozoites appear to progress through the parasite life cycle more efficiently in MPCCs relative to infected hepatoma cells, offering the potential to improve studies of drugs and sporozoite attenuation strategies that act in the second half of the liver life cycle; (2) MPCCs are able to predict differences in infection rates of sporozoites *in vivo* that result from cryopreservation, likely reflecting the presence of critical host factors that are altered in hepatoma cells[160,192,218–220]; and (3) MPCCs fabricated from different human hepatocyte donors enable direct comparison of host factors that impact entry of different sporozoite species and strains (e.g., CD81 in *P. yoelii, P. berghei,* and *P. falciparum*), whereas hepatoma cells are limited to one or very few donor genotypes. We demonstrated that maintenance of hepatocyte function and expression of the host entry factor CD81[221] were necessary, but not sufficient, to obtain adequate levels of infection by *P. falciparum*. This

finding suggests the existence of molecular differences among donors that determine their permissiveness to *Plasmodium* infection. Furthermore, most antimalarial drug development leads identified in RBC-based high-throughput screens do not require metabolic activation. Thus, in such cases, screening via the MPCC format might yield the same, higher, or lower IC50 predictions, should the candidate compound be cleared rapidly or bioactivated via metabolic pathways[222,223].

The infection rates reported in this study using cryopreserved sporozoites are comparable or higher than those previously documented with fresh sporozoites, and they are an additional ~10-fold higher when fresh sporozoites are used in this platform[29,35,166,224]. The infection rates of hepatocytes in MPCCs are similar in comparison to the infection rates recently reported in HC04 cells, which range from 0.4% to 0.06%[18,35]. However, in our system, the progression rate from one stage of the life cycle to the other was much higher than in HC04, offering the potential for studying later stages of the liver life cycle more efficiently. Nonetheless, our MPCC infection rates remain low relative to those recorded in *in vivo* settings[23,194]. Experiments done in mice with *P. yoelii*[225] and nonhuman primates with *P. knowlesi*[226] have demonstrated that intravenous inoculation of only a few non-cryopreserved sporozoites (10 sporozoites) can lead to a productive malaria infection that results in detectable parasitemia in the blood stage. Varying hypotheses have been put forward to explain the discrepancy between model systems. For example, our *in vitro* systems do not provide the host hepatocytes with potentially necessary, physiologically relevant cellular components such as Kupffer cells or sinusoidal endothelial cells. Further, the MPCC platform conformational cues may be important for EEF growth (e.g., two-dimensional versus three-dimensional). These hypotheses will be explored further.

Hepatocyte microenvironmental optimization for liver-stage malaria infectibility

In the second part of this chapter, we used an *in vitro* model of primary hepatocyte culture that stabilizes PHH function, is oxygen-responsive, and is infectible with liver stage malaria together with a mathematical framework to estimate cell surface oxygen tensions under a variety of experimental manipulations. We show that the cell surface oxygen concentration experienced by primary adult human hepatocytes *in vitro* influences their ability

to support a productive liver-stage malaria infection by *P. berghei*, *P. yoelii* and *P. falciparum*. Moreover, we identified an optimal cell surface oxygen level (predicted cell surface pO_2 5-10 mmHg) for maximizing infection. More extreme levels of hypoxia (predicted cell surface $pO_2 < 5$ mmHg) resulted in increased late-stage parasite survival but arrested parasite development. The effects of hypoxia on late-stage EEF survival, but not EEF development, appear to be regulated in part by host-dependent HIF-1α mechanisms.

Establishing an *in vitro* model of liver stage malaria has been an ongoing challenge for the field, due in part to the relatively poor maintenance of hepatic functions by existing culture platforms. With the development of the PHH MPCC system, it is now possible to achieve robust liver-stage malaria infection *in vitro*[227], but further optimization of infection efficiency remains advantageous. Our mathematical model predicts that conventional MPCCs are hyperoxic under conventional culture conditions, with estimated cell surface pO_2 ranging from 110 – 130 mmHg (**Table 2.1**), whereas *in vivo* oxygen tensions in the liver range from 30 – 75 mmHg[171,176]. We have previously shown that achieving more physiological replication of the *in vivo* environment can improve hepatocyte function and disease modeling capacity *in vitro*[174]. Thus, we hypothesized that liver-stage malaria infection might be more robust *in vitro* in the presence of atmospheric hypoxia. Indeed, the current observations that the sizes of *P. berghei*, *P. yoelii* and *P. falciparum* EEFs increase in PHHs under hypoxia *in vitro* is consistent with previous observations that primary hepatocytes respond to physiologically relevant oxygen gradients imposed upon them *in vitro* to recapitulate *in vivo* zonation phenotypes that are otherwise not observed *in vitro*[174]. The observation that *P. berghei* and *P. yoelii* demonstrate increased numbers of EEFs under hypoxia, but not *P. falciparum*, suggests that the kinetics and extent of exposure to hypoxia for increased survival of the human malaria parasite differs from the rodent malaria species. The finding that there is an optimum cell surface pO_2 (5 – 10 mmHg) for liver-stage malaria infection *in vitro* is consistent with the histopathology findings from *P. yoelii* – infected mouse liver sections, which show that EEFs in the perivenous region, which has the lowest sinusoidal oxygen tension of 30mmHg, are larger than those in the periportal region (**Figure 2.11**). Intriguingly, this optimum range of cell surface pO_2 for primary human

hepatocyte infection *in vitro* is lower than the 30 – 75 mmHg[171] reported in hepatic sinusoids *in vivo*.

One possible reason for this discrepancy is due to a lower hepatocyte surface pO2 *in vivo* than what had been previously measured in the hepatic sinusoid. This could be due either to the unsteady perfusion of the liver which arises from the pulsatile flow that has been observed *in vivo*[228], or the significant oxygen consumption by the endothelium *in vivo*[229]. This hypothesis is supported by the observations that liver sections obtained from mice perfused with Hypoxyprobe™ show significant Hypoxyprobe™ adduct accumulation in the pericentral regions[230] and that Hypoxyprobe forms such adducts only at $pO_2 < 10$ mmHg[207].

A second possible reason is that the optimal *in vitro* pO_2 for malaria infection could simply be different from *in vivo* hepatic pO_2. This could be because our *in vitro* model is missing key *in vivo* microenvironmental cues (growth factor gradients and cycling insulin/glucagon metabolism) that may result in the necessity for more extreme pO_2 perturbations to optimize malaria infection *in vitro*. This disparity is consistent with the fact that *in vitro* infections, although improved under hypoxia, still require much higher multiplicities of infection than *in vivo* infections. It is also possible that the *in vivo* pO_2 are not necessarily optimal anyway, since blood stage malaria parasitemia in rodents can be further increased under atmospheric hypoxia that simulates high-altitude atmospheres[182].

A third reason lies in the possibility that our mathematical model underestimates cell surface pO_2 *in vitro* due to the assumption that only diffusion transports oxygen to the cell surface. Furthermore, our mathematical model assumes that hepatocytes exhibit a constant oxygen consumption rate (OCR)[206,231], which may vary with species, donor, time in culture[209,232], and culture parameters like density and coculture cell type. The finding that liver-stage malaria infection *in vitro* has an optimal oxygen tension is also consistent with the microaerophilic nature of the blood stages of *P. falciparum*, which exhibit a propensity for better growth *in vitro* under ambient hypoxia[233,234], and in fact demonstrate optimum growth at an *in vitro* pO_2 (2% – 3%, 15 – 25mmHg)[235] that is lower than *in vivo* pO_2 levels in the blood (4% – 13%, 30 – 100mmHg)[236]. To extrapolate our findings to other *in vitro* liver-stage models, the appropriate

atmospheric pO_2 should be determined within a similar mathematical framework as described for MPCCs, and take into account culture parameters such as effective hepatocyte density and oxygen diffusion distance (medium height).

The beneficial effect of hypoxia on *in vitro* liver-stage malaria infection could be due to changes in the host cell that increase host cell susceptibility to initial parasite invasion or that favor parasite survival or development, or changes in the parasite itself that promotes its own ability to survive and thrive in the host cell. Sporozoite entry assays (**Figure 2.18E**) and infection of hepatocytes exposed to hypoxia only prior to invasion but not after infection (**Figure 2.18C**) suggest that hypoxia does not increase hepatocyte susceptibility to sporozoite infection. Nonetheless, gene set enrichment analysis of PHH MPCCs incubated at ambient hypoxia versus normoxia showed a marked enrichment for the expression of HIF-1α related genes in hypoxic MPCCs (**Figure 2.21A**). HIF-1α plays a major role in the induction of cellular responses that mediate the adaptation of the host cell to hypoxic conditions. This response includes an increased expression of glucose transporters and multiple enzymes responsible for a metabolic shift towards anaerobic glycolysis (Warburg effect), as well as the downregulation of mitochondrial respiration. The latter in turn reduces mitochondrial oxygen consumption and the resultant generation of reactive oxygen species that occurs due to inefficient electron transport under hypoxic conditions[210,237]. Among other *Apicomplexan* infections, host HIF-1α has been shown to be essential for *Toxoplasma gondii* survival and growth in host cells cultured at physiological oxygen levels (3% O_2)[238], and is also necessary for the maintenance of *Leishmania amazonensis* parasitemia in human macrophages *in vitro*[239]. In fact, *Toxoplasma* and *Leishmania* infection increases HIF-1α protein levels as well as HIF-1α-regulated expression of glycolytic enzymes and glucose transporters[238,239], suggesting that these *Apicomplexan* parasites actively activate host HIF-1α presumably to favor their survival or growth.

Pharmacological activation of host HIF-1α in infected MPCCs by $CoCl_2$ and DMOG increased EEF survival (**Figure 2.19B, D**), but did not increase the EEF size distributions (**Figure 2.19C, E**), suggesting that the effects of ambient hypoxia on liver-stage malaria EEF numbers and EEF sizes may be driven by distinct mechanisms, with host HIF-1α playing a role in maintaining the survival of EEFs but not necessarily driving EEF growth. This hypothesis is

supported by the observations that the total number of EEFs increased monotonically with decreasing cell surface pO_2 (**Figure 2.15E**) but the number of well-developed EEFs exhibited a biphasic relationship with decreasing cell surface pO_2 (**Figure 2.15D**). However, in the absence of genetic perturbation of host HIF-1α, the possibility that hypoxia, $CoCl_2$ or DMOG are impacting alternative pathways in the parasite that mediate the observed infection phenotype cannot be excluded.

One possible mechanism that could explain the effect of hypoxia on EEF size is the activation of the AMPK pathway in the host cell. AMPK activation is known to induce autophagy in mammalian cells[240,241], whereas autophagy of *Plasmodium* EEFs in human hepatoma cells is known to occur and may be necessary for the growth of *Plasmodium* EEFs[242]. AMPK activation also mediates mitophagy and mitochondrial biogenesis[243], which results in increased mitochondrial renewal, and may promote *Plasmodium* EEF development. In support of this hypothesis, *Toxoplasma gondii*, another *Apicomplexan* parasite, is known to tether host mitochondria to its parasitophorous vacuole membrane[244], suggesting that host mitochondria is necessary for *Toxoplasma* growth in the host cell.

In addition to host-mediated mechanisms, the malaria parasite may contain either oxygen sensors that directly respond to hypoxia or indirect mechanisms that limit their ability to respond to oxidative stress. It is difficult to distinguish the parasite-specific and the host-specific responses to hypoxia. For example, intraerythrocytic *P. falciparum* is heavily dependent on antioxidant systems despite its almost totally fermentative lifestyle, yet it lacks significant antioxidant enzymes like catalase and glutathione peroxidase which play major protective roles in mammalian cells[245,246]. This suggests that the *Plasmodium* liver stage may also be predisposed to being overwhelmed by environmental oxidants, and that hypoxia may reduce the energy expenditure for the maintenance of redox balance in the EEF.

A caveat of our findings is that changes in atmospheric oxygen may result in modulations beyond simply adjusting cell surface oxygen levels. The modulation of hepatocyte metabolism under hypoxia may result in different rates of nutrient consumption and waste generation, which may lead to secondary effects like changes in pH. This study also does not

specifically identify the role of the coculture nonparenchymal cell type in the infection phenotype, and does not use a liver-derived nonparenchymal cell type like sinusoidal endothelial cells or Kupffer cells. The *in vivo* histopathology findings are correlative and not causal, as the presence of an oxygen gradient along the sinusoid is only one of many other gradients that simultaneously exist in the liver. Thus, it is challenging to decisively untangle the various contributions of oxygen gradients in our observations, but oxygen may be more likely to be the driver of these other sinusoidal gradients than vice versa[174]. More work is required to characterize the role of HIF-1α on *Plasmodium* infection of PHHs, including performing siRNA-mediated knockdown and overexpression of HIF-1α in primary hepatocytes *in vitro*, or using a HIF-1α knock-out mouse. Further, the target genes of HIF-1α may be host factors for *Plasmodium* EEF replication, and these downstream mechanisms of HIF-1α remain to be uncovered. These mechanisms could include increases in glycolysis or iron uptake by hepatocytes, which could lead to an elevation in intracellular glucose or iron levels that are accessible to the *Plasmodium* EEF. Other mechanisms that may contribute to the effect of hypoxia on infection could include AMPK activation in host cells leading to a starvation response that decreases intracellular ROS levels and frees up resources for the malaria EEF.

2.6 Materials and Methods

Cell culture. Cryopreserved primary human hepatocytes were purchased from vendors permitted to sell products derived from human organs procured in the United States by federally designated Organ Procurement Organizations. Vendors included CellzDirect and Celsis *In vitro* Technologies. Human hepatocyte culture medium was high glucose Dulbecco's Modified Eagle's Medium (DMEM) with 10% (v/v) fetal bovine serum (FBS), 1% (v/v) ITS™ (BD Biosciences), 7 ng/ml glucagon, 40 ng/ml dexamethasone, 15 mM HEPES, and 1% (v/v) penicillin-streptomycin. J2-3T3 murine embryonic fibroblasts (gift of Howard Green, Harvard Medical School) were cultured at <18 passages in fibroblast medium comprising of DMEM with high glucose, 10% (v/v) bovine serum, and 1% (v/v) penicillin-streptomycin. HC-04 cells were seeded in a 96-well plate (10,000 cells/well) or in a LabTek slide (40,000 cells/well).

Micropatterned co-cultures (MPCCs) of primary human hepatocytes and supportive stromal cells. 12mm coverslips that were placed into tissue culture polystyrene 24-well plates or glass-bottomed 96-

well plates were coated homogenously with rat tail type I collagen (50 μg/ml) and subjected to soft-lithographic techniques[121] to pattern the collagen into micro-domains (islands of 500 μm) that mediate selective hepatocyte adhesion. To create MPCCs, cryopreserved primary human hepatocytes were pelleted by centrifugation at 100x g for 6 min at 4 °C, assessed for viability using Trypan blue exclusion (typically 70–90%), and then seeded on collagen-micropatterned plates. The cells were washed with medium 2–3 h later and replaced with human hepatocyte culture medium. 3T3-J2 murine embryonic fibroblasts were seeded (40,000 cells in each well of 24-well plate and 10,000 cells in each well of 96-well plate) in fibroblast medium 3 days later. Fibroblast medium was replaced with human hepatocyte medium 24 h after fibroblast seeding and subsequently replaced daily.

***P. falciparum* and *P. vivax* sporozoites.** Mosquitoes were fed on Pf- and Pv- infected blood as previously described[18,163]. Briefly, *P. falciparum* and *P. vivax* sporozoites were extracted from infected mosquitoes by dissection of their salivary glands and passing the glands back and forth through a 26K G needle fitted to a 1 mL syringe. Following extraction, sporozoites were purified from mosquito salivary gland material contamination and cryopreserved in liquid nitrogen vapor phase (LNVP)[18,215]. Live-attenuated *P. falciparum* sporozoites were attenuated by exposure of PfSPZ-infected mosquitoes to 150 Gy[157,215].

***P. berghei* and *P. yoelii* sporozoites.** *P. berghei* ANKA and *P. yoelii* sporozoites were obtained by dissection of the salivary glands of infected *Anopheles stephensi* mosquitoes obtained from the insectaries at New York University (New York, New York, USA) or Harvard School of Public Health (Boston, Massachusetts, USA).

Biochemical assays. Cell culture supernatants were collected and stored at −20°C. Urea was measured by acid- and heat-catalyzed detection of diacetylmonoxime conversion to a colorimetric product (StanBio Labs). Albumin content was measured by an enzyme-linked immunosorbent assay using goat anti-human albumin antibody (Bethyl Labs) with horseradish peroxidase detection (Bethyl Labs) and 3,3',5,5'-tetramethylbenzidine (TMB, Pierce) development.

Sporozoite gliding assay. Motility of cryopreserved sporozoites was determined in each batch to define the number of infective sporozoites. Sporozoite gliding was evaluated with 20,000 sporozoites for 40 minutes in complete DMEM, at 37°C on glass cover slips covered with anti-circumsporozoite protein

(CSP) monoclonal antibody (clone 2A10 for *P. falciparum* and 210 clone NSV3 for *P. vivax*). Sporozoites were subsequently fixed in 4% paraformaldehyde (PFA) for 10 minutes and stained with anti-CSP. The percentage of sporozoites associated with CSP trails was visualized by fluorescence microscopy. Quantification was performed by counting the average percentage of sporozoites that perform at least one circle.

Infection of MPCCs with *P. falciparum* and *P. vivax* sporozoites. Cryovials containing *P. falciparum* or *P. vivax* were warmed for 30 sec at 37°C, 200 μl of human hepatocyte medium was added and the cryovials were centrifuged for 2 min at 14000x g. 200 μl of the supernatant was aspirated, and the sporozoite pellet was resuspended and diluted accordingly. Each well was infected with a ratio of 3:1 (infective sporozoites:hepatocytes). After incubation at 37°C and 5% CO_2 for 3h, the wells were washed once and fresh medium was added. Media was replaced daily. Samples were fixed on day 3 and 5 post-infection with *P. falciparum,* and days 3, 5, 12, and 21 post-infection with *P. vivax.*

Cell wounding and membrane repair assay. Sporozoite migration through cells can be quantified by the detection of sporozoite-wounded hepatocytes using a cell-impermeable fluorescent tracer macromolecule as previously described[11]. Briefly, MPCCs were infected with *P. falciparum* in the presence of 1 mg/ml tetramethylrhodamine dextran lysine fixable, 10,000 Da (Sigma). At 3h post-infection, MPCCs were washed thrice with PBS, fixed with 1% paraformaldehyde at room temperature for 20 min, and mounted on glass slides. Migration of sporozoites through cells is quantified by the number of dextran-positive hepatocytes per island.

Immunofluorescence assay. MPCC were fixed with -20°C methanol for 10 min at 4°C, washed thrice with PBS, blocked with 2% BSA in PBS and then incubated for 1h at room temperature with a primary antibody: mouse anti-CD81 (clone JS-81, BD Pharmingen; 1:100), rabbit anti-LSA-1 (Sanaria, 1:50), mouse anti-EBA-175 (Sanaria, 1:100), mouse anti-PfHsp70 (clone 4C9, Sanaria; 1:100), mouse anti-PfMSP-1 (Sanaria; 1:100), anti-rabbit PvMSP-1(MRA16; MR4) or mouse anti-PvCSP (clone NVS3, Sanaria; 1:100). Samples were washed thrice with PBS before incubation for 1 h at room temperature with secondary antibody: goat-anti-mouse Alexa Fluor 594 or Alexa 488, and goat anti-rabbit Alexa Fluor 488 (Invitrogen; 1:400). Samples were washed thrice with PBS, with nuclei counterstained with Hoechst 33258 (Invitrogen; 1:1000), and then mounted on glass slides with Fluoromount G (Southern Biotech).

For samples in 96-well plates, 50 uL of Aquamount (Thermo-Scientific) was added per well after counter-staining with Hoechst. Images were captured on a Nikon Eclipse Ti fluorescence microscope.

Double-staining assay for sporozoite entry. At 3 h post-infection, primary human hepatocytes or MPCCs were fixed and stained using a double-staining protocol as previously described[247]. Briefly, to label extracellular sporozoites, the samples were first fixed with 4% paraformaldehyde for 10min at room temperature, blocked with 2% BSA in PBS, incubated with a primary mouse anti-PfCSP (Sanaria, 1:100)[248], washed thrice in PBS and incubated with a secondary goat anti-mouse AlexaFluor488 conjugate. This was followed by a permeabilization with -20°C methanol for 10min at 4°C, incubation with the same primary mouse anti-PfCSP, washing thrice with PBS, and incubation with a secondary goat anti-mouse AlexaFluor594 conjugate. This second step labels both intracellular and extracellular sporozoites. In case of MPCCs, the samples were counterstained with Hoechst and mounted on glass slides as described above. The number of invaded sporozoites (only green) in primary human hepatocytes were counted using Acumen explorer.

Coculture with erythrocytes and merozoite invasion. To determine whether first-generation merozoites were released by infected hepatocytes, freshly prepared human O+ red blood cells (Research Blood Components) were added to each *P. falciparum*-infected well at a 2% hematocrit on day 6 after infection. Every week for two weeks, fresh red blood cells were added, and samples of the red blood cells from the previous coculture were harvested. Thin blood smears were prepared, stained with Giemsa, and examined for asexual stage parasites.

Primaquine treatment of *P. falciparum* EEFs in MPCCs. Infected MPCCs were incubated with media containing primaquine diphosphate (Sigma) ranging from 0.5-20 μM. Fresh primaquine-containing medium was added daily until the samples were fixed at days 3 and 5 post-infection.

RNA Isolation and LMA-Luminex Analysis. Total RNA from three wells per condition was purified using Trizol (Invitrogen) and Mini-RNeasy kit (Qiagen) and pooled for analysis. LMA-Luminex procedures and probes are previously described[152]. Briefly, data for triplicate loadings, expressed in mean fluorescent intensity of at least 100 beads per sample, were scaled to the human transferrin gene and row-normalized for heat map representation using Gene Pattern open software (Broad Institute).

Image Automation. Images of 96 well plates were acquired using high content screening microscopes (Molecular Devices IXM), and were then analyzed by Cell Profiler and Cell Profiler Analyst (Broad Institute)[249.] Parasites were visualized through immunofluorescent staining of the HSP70 protein, and can be distinguished from imaging artifacts by their proximity to a hepatocyte nucleus (within 30 pixels), and lack of auto fluorescence (no signal in unlabeled channels). We developed an automated image analysis pipeline to identify every infection in every image and measure hundreds of features (e.g. shape, area, texture) of each parasite. These features are then used to train machine learning algorithms to identify and count the number of parasites in each image using CellProfiler Analyst.

Gene expression microarray analysis. MPCCs established from two different donor lots of primary human hepatocytes were incubated under ambient hypoxia overnight (18-24 h), and total RNA was extracted using TRIZOL and a Qiagen RNA clean-up kit. The RNA was analyzed by a Bioanalyzer, before being labelled with Cy 3 and Cy 5 for the normoxic versus hypoxic samples respectively. The labeled RNA from biological triplicates was loaded onto an Agilent (Santa Clara, California, USA) SurePrint G3 Human Gene Expression Microarray. The microarray data was analyzed by performing a Gene Set Enrichment Analysis (GSEA), which determines whether a pre-defined set of genes shows statistically significant differences between two biological conditions[250], applying a false discovery rate of 25%.

Mathematical model. To estimate the cell surface oxygen tensions in micropatterned cocultures, the transport and consumption of oxygen was modeled as a one-dimensional reaction-diffusion system, which was described previously[206]. The average number of hepatocytes per hepatocyte island in the MPCCs was determined by manual counts with light microscopy. The following assumptions were made in applying this model. Firstly, the oxygen consumption rate of primary rat hepatocytes was used, due to absence of the oxygen consumption rates of primary human hepatocytes. Secondly, as the oxygen consumption rate of fibroblasts is only one-tenth that of primary rat hepatocytes, and the oxygen consumption rate of random cocultures of hepatocytes and fibroblasts was similar to that of hepatocytes alone[174], the oxygen consumption of MPCCs was assumed to be that of hepatocytes alone. Thirdly, the oxygen consumption rates were assumed to be independent of culture format and constant throughout the infection experiments.

Hypoxyprobe assay. Hypoxyprobe™ (pimonidazole hydrochloride, Burlington, Massachusetts, USA) forms covalent adducts in hypoxic cells at cell surface $pO_2 < 10$ mmHg[207], and was used as a hypoxia

marker in primary human hepatocytes. Hypoxia was first induced in primary hepatocytes by atmospheric hypoxia, variation of medium heights or variation in hepatocyte island densities. Pimonidazole hydrochloride was then added from a 200mM stock solution (constituted in PBS) into the culture medium (without changing medium to avoid disturbing the steady state oxygen gradient) at a 1:1000 dilution to achieve a final working concentration of 200μM. Cells were incubated at 37°C for 2h, washed twice with PBS, and fixed with chilled methanol for 10min at 4°C. Adduct formation was detected by direct immunofluorescence using the HP-Red549 antibody (Hypoxyprobe™) at a 1:100 dilution.

Histological analysis. 50-μm liver slices were obtained from C57BL/6 mice (Charles River, Wilmington, Massachusetts, USA), 46h post-infection with GFP-expressing *P. yoelii* sporozoites. Maximal EEF size of EEFs in the periportal area (up to 8 hepatocytes wide, from portal vein) and in the centrilobular area (up to 8 hepatocytes wide, from central vein) were measured using z stacks of these EEFs acquired via confocal imaging (Olympus, Center Valley, Pennsylvania, USA).

Statistical analysis. Experiments were repeated at least 2–3 times with duplicate or triplicate samples for each condition. Data from representative experiments are presented, whereas similar trends were seen in multiple trials. All error bars represent s.e.m.

2.7 Conclusion

In an era of a renewed effort towards global malaria eradication, the ability to support the liver stages of *P. falciparum and P. vivax* parasites in a medium-throughput format offers promise to improve our fundamental understanding of the liver stages of human malaria as well as accelerate the development of drugs and vaccines to aid eradication. The findings that oxygen levels and hepatocyte innate immune status influence *in vitro Plasmodium* liver stage infection of PHHs, highlights the importance of optimizing oxygen levels experienced by PHHs *in vitro* and dampening hepatocyte innate immunity so as to develop improved *in vitro* models of liver-stage malaria for antimalarial drug development.

Chapter 3: Personalizing the Study of Liver-Stage Malaria Infection

3.1 Introduction

Due to their better maintenance of hepatic drug metabolism enzymes compared to cell lines and the fact that they are the natural host for malarial sporozoites, primary human hepatocytes are a preferable cell type to model liver-stage malaria *in vitro* for the purposes of antimalarial drug development, since they may offer better predictive value in *in vitro* liver-stage malaria phenotypic drug screens and may more accurately recapitulate host-pathogen interactions *in vitro* than other cell lines that are typically used for modeling liver-stage malaria *in vitro*[227]. However, the genetic diversity of primary human hepatocytes is limited due to the sourcing of these cells from a small population of donors that may not represent the genetic variation inherent in the human population. Pluripotent stem cell sourced hepatocytes overcome some of the drawbacks of cell lines, fetal tissue and adult human sources and may be considered an alternative source of primary human hepatocytes. Compared to primary human hepatocytes, stem cell-derived hepatocytes can represent more diverse genotypes, can be personalized for rare genotypes, and are renewable. Human pluripotent embryonic stem cells were first isolated from human blastocysts [251], but embryonic stem cells face considerable ethical issues with regards to their availability and use.

More recently, the enforced expression of various factors in a variety of differentiated cell types led to the generation of induced pluripotent stem cells (iPSCs) [252]. In particular, iPSCs can, in a reliable and step-wise manner, differentiate through the developmentally appropriate stages (ie. endoderm, hepatic specified endoderm, hepatoblasts) to produce hepatocyte-like cells (iHLCs) *in vitro* [106]. The ability to generate iHLCs from different donors provides an opportunity to assess donor-specific drug responses *in vitro*, akin to conducting an *in vitro* clinical trial. Our prior work has shown that iHLCs are susceptible to hepatotropic pathogens such as hepatitis C infection [253]. To establish the feasibility of using iHLCs as an alternate source of primary human hepatocytes for liver-stage malaria assays, it is necessary to characterize the infectibility of iHLCs with liver-stage malaria. Furthermore, it is crucial to characterize the responses of malaria-infected iHLCs to known antimalarial drugs in order to establish the utility

of using iHLCs in *in vitro* liver-stage malaria phenotypic drug screens. This is especially important considering that iHLCs generated using current state of the art protocols are immature and more closely resemble fetal hepatocytes in cytochrome P450 expression and activity as well as in antigen expression[254]. However, recent promising attempts to mature iHLCs to a more adult phenotype, including the identification of small molecules [255], may ultimately contribute to the generation of appropriately mature iHLCs for such antimalarial drug screens. Isogenic iHLCs that are more developmentally mature may also be applied to host factor discovery for the *Plasmodium* liver stages.

In this study, we show the feasibility of infecting iHLCs with *Plasmodium* sporozoites *in vitro*, and demonstrate *Plasmodium* parasite development over time in culture. We identify the stage at which cells acquire permissiveness to liver-stage malaria infection during the differentiation process. We hypothesized and showed that iHLCs are not responsive to the antimalarial, primaquine, due to a lack of bioactivation of the drug by hepatic cytochrome P450 drug metabolism enzymes, and demonstrate that chemical maturation of iHLCs improves the potential for using iHLCs for antimalarial drug testing.

3.2 Results

iPSC-derived hepatocyte-like cells (iHLCs) support liver stage malaria infection *in vitro*

iHLCs were generated using a 20-day *in vitro* differentiation protocol that recapitulates the different stages of hepatic development[254]. During this differentiation process, iPSCs become endoderm cells at 5 days, hepatic-specified endoderm cells at 10 days, hepatoblasts at 15 days and iHLCs at 20 days after the initiation of differentiation respectively (**Figure 3.2A**). iHLCs express the two known host entry factors for liver-stage malaria, CD81 and SR-B1 at the genetic and protein levels and are appropriately localized on the cell surface as observed via immunofluorescence assays (data not shown).

iHLCs were initially exposed to *P. berghei* sporozoites for 3 hours, and fixed at 24 or 48 hours post-exposure for immunofluorescence assays against *P. berghei* HSP70. Because *P. berghei* has been observed to infect non-hepatic cell types *in vitro*, iHLCs were separately

infected with *P. yoelii* sporozoites, which have a more hepatocyte-specific tropism *in vitro*[32]. iHLCs supported infection with *P. berghei* and *P. yoelii* exoerythrocytic forms (EEFs) over time (**Figure 3.1A, B**), and the EEFs were observed to grow over time. *P. berghei* EEFs (PbEEFs) at 3 days post-infection were also regularly observed to express *P. berghei* MSP-1 (**Figure 3.1A**), suggesting that PbEEF maturation occurred along with PbEEF replication. iHLCs also exhibited *P. falciparum* HSP70-expressing EEFs at 3 and 6 days post-exposure to *P. falciparum* sporozoites, suggesting that iHLC infectibility with *Plasmodium* sporozoites is not restricted to the rodent malaria species (**Figure 3.1C**). Moreover, *P. falciparum* EEFs (PfEEFs) at 6 days post-exposure also expressed *P. falciparum* MSP-1 (but at lower frequencies than *P. berghei* EEFs) (**Figure 3.1C**), indicating PfEEF maturation occurred in a subset of the PfEEFs.
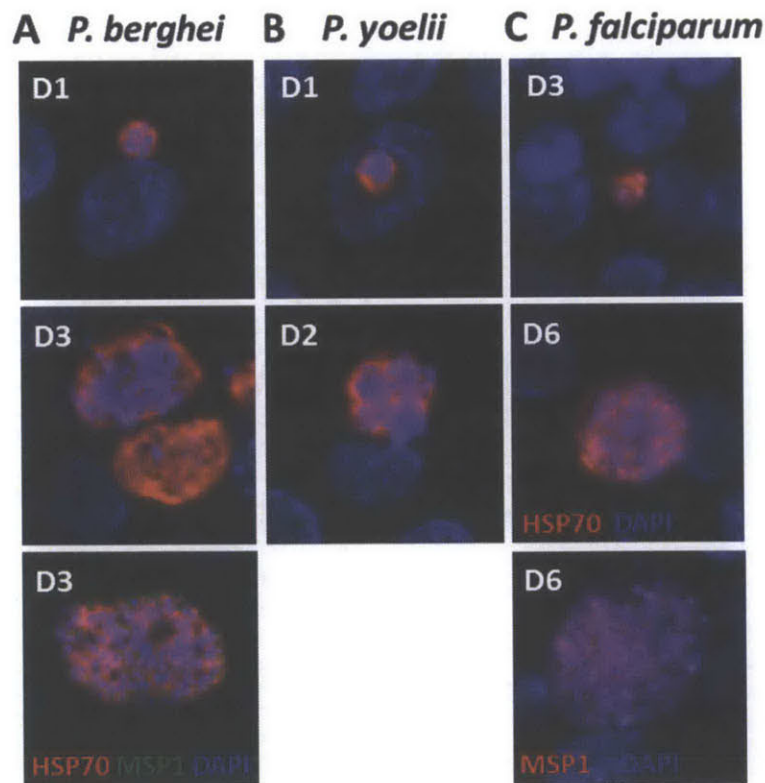
Figure 3.1. iHLCs Are Susceptible to Liver Stage Malaria. (A) Representative *P. berghei* EEFs at D1 or D3 post-infection. (B) Representative *P. yoelii* EEFs at D1 or D2 post-infection. (C) Representative *P. falciparum* EEFs at D3 or D6 post-infection.

Permissiveness to _Plasmodium_ infectibility appears at hepatic-specified endoderm stage but peaks at hepatoblast stage during _in vitro_ hepatic differentiation of iPSCs into iHLCs

Earlier experiments sought to determine whether susceptibility to liver-stage malaria infection of iHLCs was acquired only at the end of the 20-day _in vitro_ differentiation protocol. In this experiment, incompletely differentiated hepatoblasts (D16 post-initiation of differentiation) and iHLCs at the end of the differentiation were exposed to _P. yoelii_ sporozoites from the same batch of _P. yoelii_-infected _A. stephensi_ mosquitoes. iHLCs retained susceptibility to _P. yoelii_ infection for at least 33 days after the initiation of differentiation from iPSCs, whereas hepatoblasts were surprisingly infectible at even higher levels than differentiated iHLCs at 48 h post-infection (**Figure 3.3A**). This suggested that the incompletely differentiated D15 hepatoblasts had acquired sufficient host factors to both allow the invasion of _Plasmodium_ sporozoites as well as support the growth of the _Plasmodium_ EEFs upon invasion.

To determine the specific stage during the _in vitro_ differentiation of iPSCs to iHLCs at which the cells acquire permissiveness to liver-stage malaria infection, cells at different stages of differentiation (iPS cells, endoderm, hepatic-specified endoderm, hepatoblast, and iHLCs) were infected with _P. falciparum_ sporozoites obtained from the same batch of _P. falciparum_-infected _A. gambiae_ mosquitoes. At 4 days post-infection, no PfEEFs were observed in iPSCs, whereas a small number were observed in endoderm (D5) cells and hepatic-specified endoderm (D10) cells (**Figure 3.3C**). However, the number of PfEEFs 4 days post-infection significantly increased in hepatoblasts (D15) compared to hepatic-specified endoderm (D10) cells (**Figure 3.3C**), whereas differentiated iHLCs (D20) had similar numbers of PfEEFs as hepatoblasts (**Figure 3.2C**). The size distributions of the PfEEFs at 4 days post-infection in all stages at which infection was observed (D5, D10, D15, D20 post-differentiation) were not significantly different (**Figure 3.2B, 3.2D, 3.3D**), suggesting that the cells that had acquired permissiveness to malaria sporozoite infection at the earlier stages of differentiation were still capable of supporting parasite survival and growth to 4 days post-infection. Importantly, the D15 hepatoblasts supported late-stage EEF growth as well as D20 iHLCs, as shown by the similar EEF size distributions measured at 6 days post-infection (**Figure 3.3B**), but surprisingly and in

accordance with late-stage *P. yoelii* infections (**Figure 3.3A**), there was a trend towards more *P. falciparum* EEFs at 6 days post-infection in D15 hepatoblasts than in D20 iHLCs (**Figure 3.3B**).
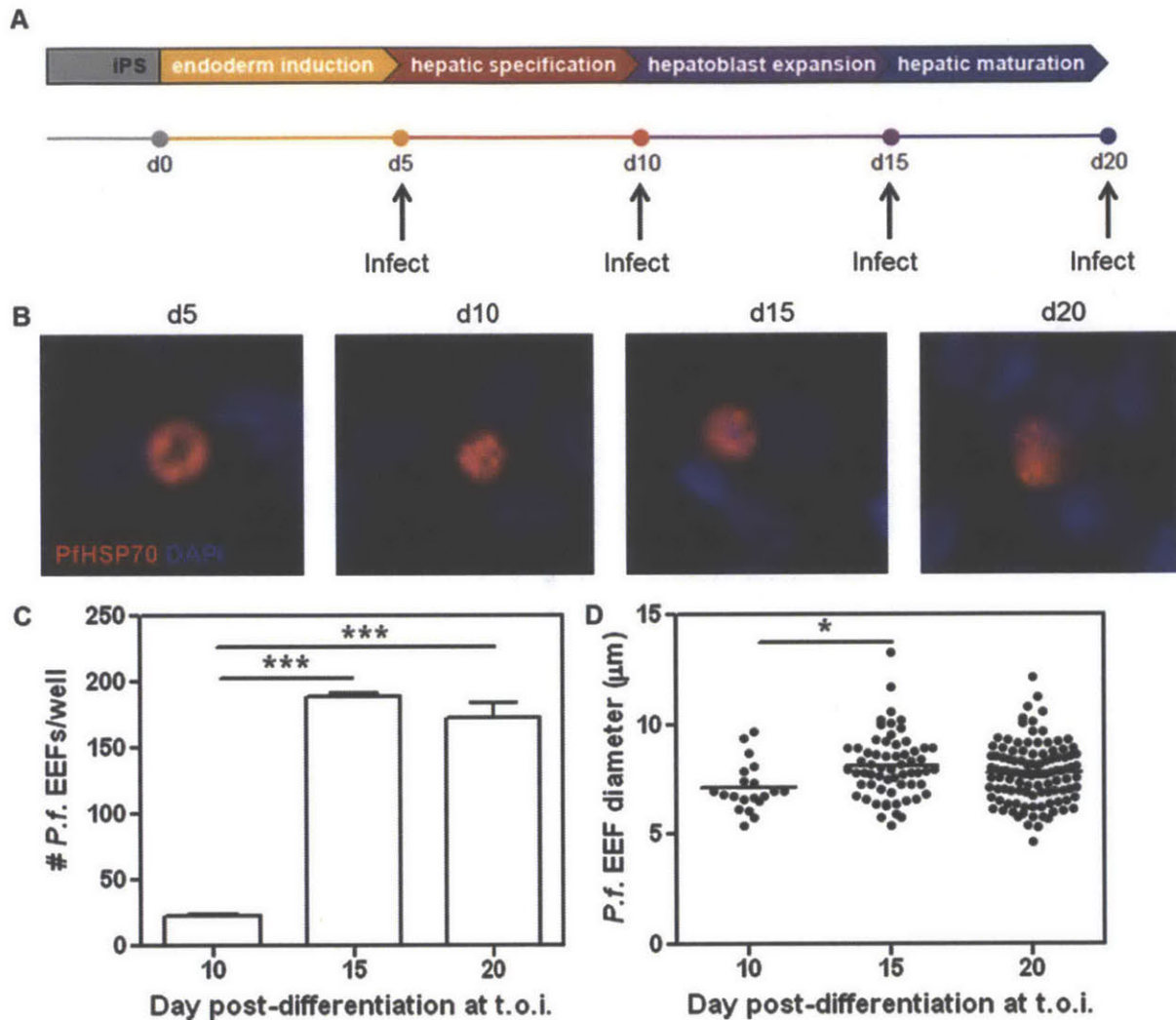
Figure 3.2. iHLCs Gain Permissiveness to Liver Stage Malaria Infection at Hepatoblast Stage.
(A) Schematic of differentiation of iPSCs into iHLCs over a 20-day period. (B) Representative *P. falciparum* EEFs from cells infected at various stages after the initiation of iPSC differentiation at D4 post-infection. (C) Peak susceptibility to infection with *P. falciparum* is attained at D15 after the initiation of differentiation, at the hepatoblast stage. (D) Size distributions of *P. falciparum* EEFs obtained from an infection of cells at the hepatic-specified endoderm (D10), hepatoblast (D15) or iHLC (D20) stage. *$P<0.05$, ***$P<0.001$; one way ANOVA with Tukey's multiple comparison test.
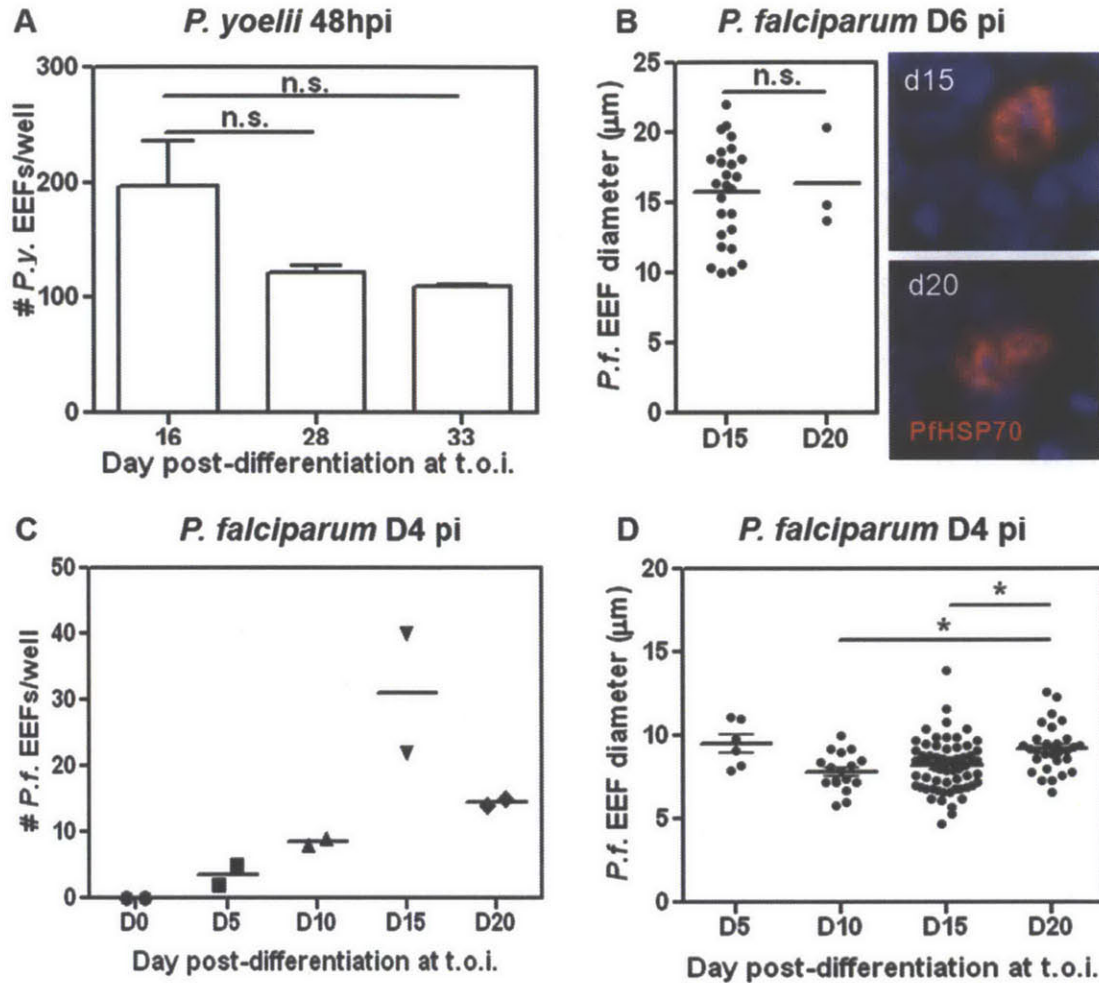
Figure 3.3. Hepatoblasts and iHLCs Support Late-stage *P. yoelii* and *P. falciparum* Infections.
(A) Number of *P. yoelii* EEFs at 48h post-infection in cells infected at various time points (16, 28, 33) after the start of the differentiation process. D16 cells are hepatoblasts, whereas D28 and D33 cells are iHLCs. (B) Similar size distributions of *P. falciparum* EEFs at D6 post-infection in D15 hepatoblasts and D20 iHLCs, although D15 hepatoblasts supported a larger number of D6 P.f. EEFs than D20 iHLCs in this experiment. (C) Number of *P. falciparum* EEFs at 4 days post-infection in cells infected at various time points (day 0, 5, 10, 15, 20) after the start of the differentiation process. (D) Size distributions of *P. falciparum* EEFs at D4 post-infection are similar in D5 endoderm cells, D10 hepatic-specified endoderm cells, D15 hepatoblasts and D20 iHLCs. *$P < 0.05$, one way ANOVA with Tukey's multiple comparison test.

Plasmodium-infected iHLCs are insensitive to primaquine but not atovaquone

As a preliminary demonstration of the potential utility of iHLCs in phenotypic screens for potential antimalarial drugs *in vitro*, iHLCs were infected with *P. yoelii* sporozoites at various time points upon the completion of the *in vitro* differentiation protocol. After the initial 3 hours allowed for the sporozoites to invade the cells, the cultures were washed and replaced with either regular medium or regular medium containing 10μM primaquine. 10μM primaquine (PQ) was chosen because it resulted in a 90% reduction in the number of *Plasmodium* EEFs in *P. falciparum*-infected primary human hepatocytes [227] and also did not cause toxicity to iHLCs, which was confirmed by comparing the morphology of the PQ-treated iHLCs to untreated iHLCs (data not shown). Surprisingly, at 48 hours post-infection, no differences in the number of *P. yoelii* EEFs were observed in PQ-treated versus untreated iHLCs infected at either 23 or 28 days post-initiation of differentiation (**Figure 3.4A**). Since some antimalarial compounds may affect *Plasmodium* EEF development rather than survival and hence cause reductions in EEF size rather the number of EEFs[256], the size distributions of *P. yoelii* EEFs in PQ-treated and untreated samples were measured, and found to be similar (**Figure 3.4B**), suggesting that primaquine neither affected the number nor the growth of EEFs. Primaquine is known to be inactive in its parent form, and becomes active only upon metabolism by specific drug metabolism enzymes expressed only in primary adult hepatocytes, including CYP2D6, CYP3A4, CYP2C19 and MAO-A [197,257,258]. This suggests that while iHLCs express sufficient host factors to support *P. yoelii* invasion and EEF growth over time, they do not yet express the appropriate hepatic drug metabolism enzymes that are necessary for the bioactivation of primaquine into an active form that can then act on *Plasmodium* EEFs. As a control, *P. yoelii*-infected iHLCs were exposed to a atovaquone, an antimalarial drug that acts directly on the parasite without the need for bioactivation by hepatic drug metabolism enzymes. Atovaquone treatment eliminated *P. yoelii* EEFs from infected iHLCs (**Figure 3.4C**) at a concentration (10 nM) that is known to eliminate a majority of *Plasmodium* EEFs from primary human hepatocytes[259].

To confirm that the absence of primaquine sensitivity of infected iHLCs extends to the human *Plasmodium* species, iHLCs were infected with *P. falciparum* sporozoites, and primaquine treatment was started 3 hours post-exposure to sporozoites. In a similar fashion to *P. yoelii*, primaquine treatment of *P. falciparum*-infected iHLCs did not reduce the number of *P. falciparum* EEFs (**Figure 3.4D**) and did not alter the PfEEF size distribution (**Figure 3.4E**).
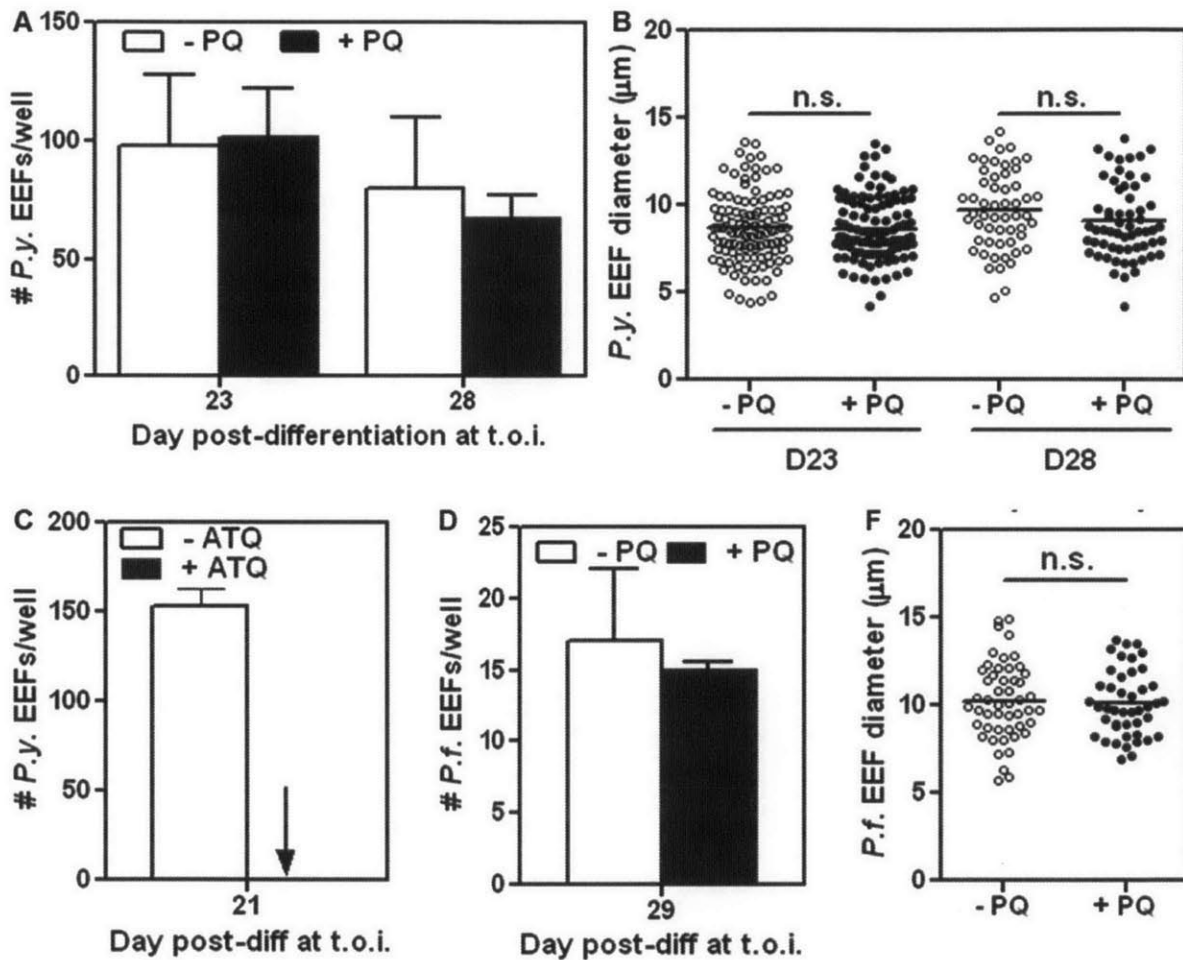
Figure 3.4. iHLCs Infected with Liver-Stage Malaria Do Not Respond to Primaquine . (A) Number of *P. yoelii* EEFs per well in iHLCs that were infected at 23 or 28 days post-differentiation in the presence or absence of 10μM primaquine. (B) Size distributions of *P. yoelii* EEFs in iHLCs that were infected at 23 or 28 days post-differentiation in the presence or absence of 10μM primaquine. (C) Number of *P. yoelii EEFs* per well in iHLCs that were infected at 23 or 28 days post-differentiation in the presence or absence of 10 nM atovaquone. (D) Number of *P. falciparum* EEFs per well in iHLCs that were infected at 29 days post-differentiation in the presence or absence of 10μM primaquine. (E) Size distributions of *P.*

94

falciparum EEFs in iHLCs that were infected at 29 days post-differentiation in the presence or absence of 10µM primaquine.

Further maturation of iHLCs with small molecules confer primaquine sensitivity on iHLCs

A previous study had compared the gene expression of 83 human hepatic drug metabolism enzymes (DMEs) in iHLCs with that of primary human hepatocytes [255], and found iHLCs to express a relatively low level of many of these genes. Specifically, the transcript levels of CYP2D6, CYP3A4, CYP2C19 and MAO-A [197,257] were all expressed at less than 5% of the levels at which they are expressed in primary human adult hepatocytes [255]. Since drug metabolism is largely regulated at the transcript level, this low level of expression of adult human hepatic DMEs suggests that the iHLCs are unlikely to be able to bioactive primaquine. The same study had identified two small molecules that resulted in a transcriptional upregulation of many adult human hepatic DMEs, and resulted in increased adult human hepatocyte-specific CYP3A4 activity and a corresponding loss of fetal hepatocyte markers such as alpha-fetal protein [255].

To test whether further maturation of iHLCs with either of these two small molecules (FH1, FPH1) can confer primaquine sensitivity to iHLCs, D20 iHLCs were exposed to either FH1, FPH1 or the DMSO carrier for a total of 6 days (treatment phase, D21-26). The iHLCs were subsequently incubated without FH1 or FPH1 for a period of 1 – 2 days (wash-out phase, D27-28) before they were exposed to *Plasmodium* sporozoites, in order to avoid any direct effects of the small molecules (or the DMSO carrier) on sporozoite infectivity or eventual drug sensitivity during the liver-stage (**Figure 3.5A**).

Due to the large number of wells involved in the following experiments, and the relatively high levels of infection with *P. yoelii* sporozoites, a luciferase-expressing strain of *P. yoelii* (Py-luc) sporozoites was used in order to allow the infection to be quantified by bioluminescence imaging (BLI)[260]. The bioluminescence of the liver-stages of the Py-luc strain is directly proportional to the total liver-stage load as measured by RT-PCR [260,261], and is also a function of the total number of EEFs per well and the mean EEF diameter in that well (**Figure 3.6**). While Py-luc infection (as measured by BLI) in DMSO-treated iHLCs did not decrease upon

primaquine treatment, iHLCs pre-treated with either FH1 or FPH1 resulted in a significant decrease in Py-luc infection (**Figure 3.5B**).
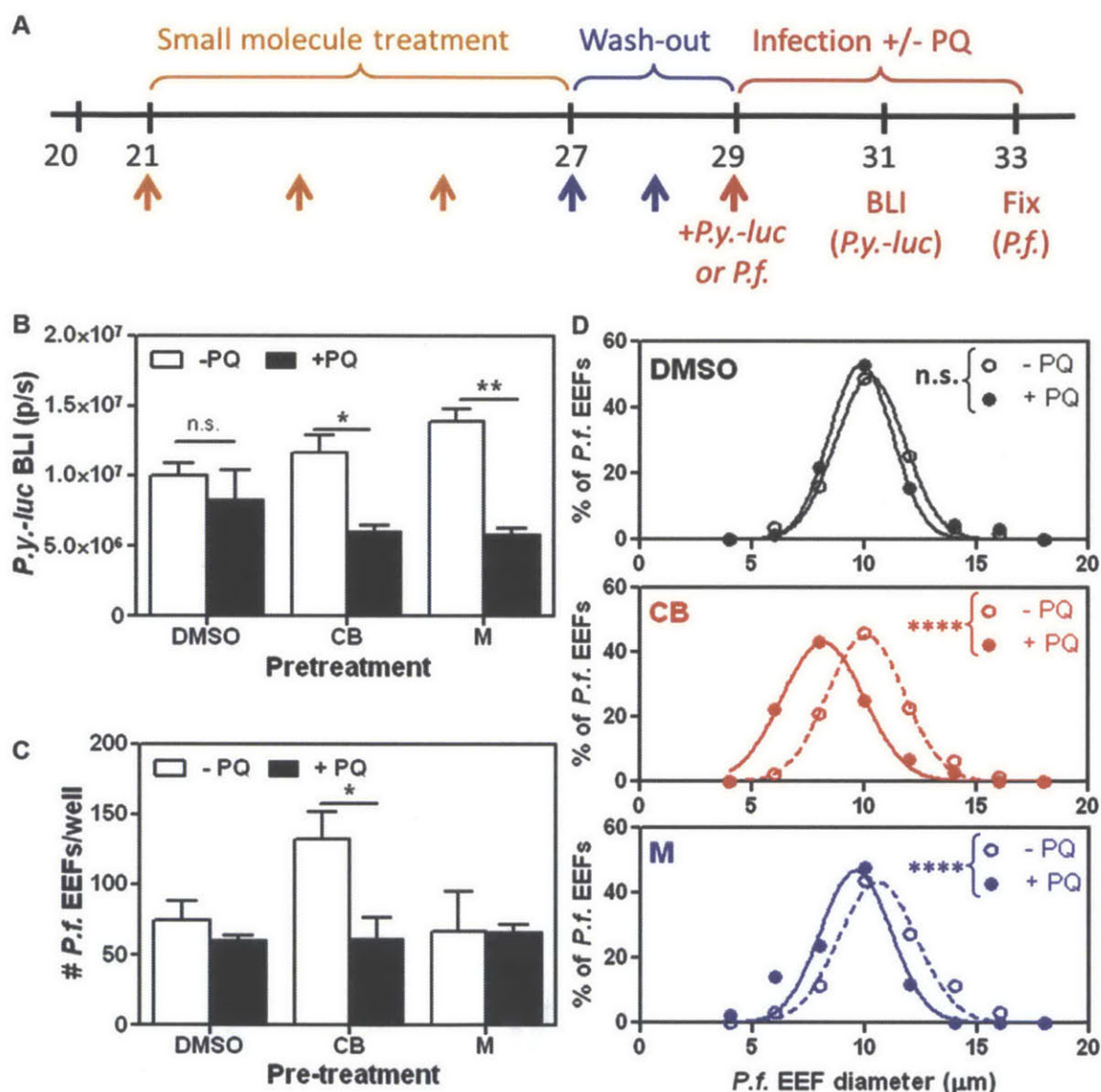
Figure 3.5 Small-Molecule Maturation of iHLCs Confers Primaquine Sensitivity to iHLCs Infected with Liver-Stage Malaria. (A) Schematic of small molecule dosing of iHLCs before infection with *P. yoelii-luciferase* (*P.y.-luc*) or *P. falciparum (P.f.)*. (B) Effect of FH1 or FPH1 pretreatment on primaquine sensitivity of iHLCs infected with *P.y.-luc*. Infection was measured by bioluminescence imaging of infected iHLCs. (C) Effect of FH1 or FPH1 pre-treatment on primaquine sensitivity of iHLCs infected with *P.f.* Infection was measured by counting the number of *P.f.*EEFs per well. (D) Size distributions of *P.f.* EEFs in *P.f.*-infected iHLCs that were treated before infection with DMSO, FH1 or FPH1 and treated after infection with or without 10μM primaquine. *$P<0.05$, ** $P<0.01$, **** $P<0.0001$, two-tailed t-test.

To determine whether primaquine sensitivity was also achieved in *P. falciparum* infected iHLCs, iHLCs were pre-treated with FH1, FPH1 or DMSO, and exposed to *P. falciparum* sporozoites. At 4 days post-infection, the infected cultures were fixed and *P. falciparum* infection was quantified by manual counts of PfEEFs immunostained for PfHSP70. As expected, iHLCs pre-treated with DMSO did not exhibit a decrease in the number of PfEEFs or the PfEEF size distribution in the presence of primaquine during infection. However, iHLCs pre-treated with FH1 exhibited a significant decrease in the number of PfEEFs in the presence of primaquine during infection (**Figure 3.5C**). It is noteworthy that although the primaquine response in iHLCs pre-treated with FH1 was incomplete, other primary human hepatocyte models of *P. falciparum* treated with the same primaquine concentration (10μM) also exhibit an incomplete response, with about 10-20% of the number of PfEEFs remaining [227,262]. Importantly, among the remaining PfEEFs in iHLCs pre-treated with FH1, there was a significant decrease in the PfEEF size distribution (**Figure 3.5D**). Interestingly, FH1 pre-treatment increased the baseline number of PfEEFs in the absence of primaquine treatment compared to DMSO pre-treatment (**Figure 3.5C**). In contrast to Py-luc infections, pre-treatment of iHLCs with FPH1 had no effect on the number of PfEEFs under primaquine treatment, but resulted in a significant decrease in the PfEEF size distribution under primaquine treatment (**Figure 3.5C, D**).

A — $R^2 = 0.8486$
P. berghei BLI at 48hpi (p/s)

B — $R^2 = 0.9767$
P. berghei BLI at 48hpi (p/s)
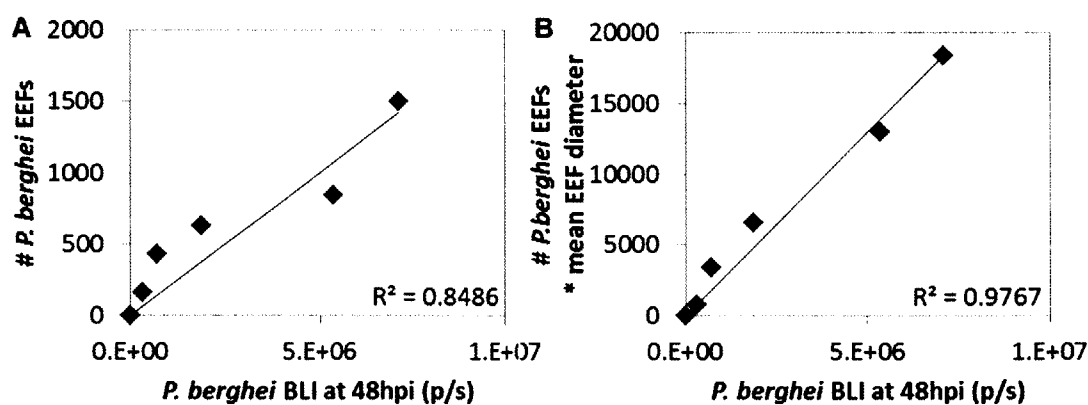
Figure 3.6 Bioluminescent *Plasmodium* strains are a good proxy of total parasite load. Luciferase-expressing *P. berghei* sporozoites were added to different wells of iHLCs from the same batch of differentiation, and the infection was imaged in an IVIS bioluminescence (BLI) imaging system at 48h post-infection. A range of BLI values were obtained, suggesting a range of infection levels was obtained. The samples were fixed and stained for PbHSP70, and the number of *P. berghei* EEFs in each well was counted. In addition the sizes of about 50 randomly

chosen EEFs in each well were quantified by ImageJ. (A) shows the correlation between the number of *P. berghei* EEFs versus the *P. berghei* BLI, whereas (B) shows the correlation between the product of the number of *P. berghei* EEFs and the mean EEF diameter versus the *P. berghei* BLI.

3.3 Discussion

In this study, we show the feasibility of infecting iHLCs with *P. berghei*, *P. yoelii* and *P. falciparum*. Liver-stage *Plasmodium* EEFs grow in size over time, and express MSP-1 which is typically expressed in more mature EEFs. While iPS cells and definitive endoderm cells are generally not infectible with *P. falciparum*, some degree of *P. falciparum* infectibility is acquired by the time the cells are further differentiated to a hepatic-specified endoderm lineage. Notably, hepatoblasts are equally or more infectible than the resulting iHLCs at the end of the *in vitro* differentiation protocol. iHLCs generated by the existing differentiation protocol do not respond to primaquine, a malaria drug that requires bioactivation by mature hepatic cytochrome P450 (CYP450) enzymes, but further maturation of iHLCs using a previously described small molecule results in the acquisition of primaquine sensitivity that was confirmed with *P. yoelii* and *P. falciparum* infection studies.

Liver-stage malaria biology is conventionally studied in *in vivo* and *in vitro* using rodent malaria models and using human hepatoma cells infected with rodent *Plasmodium* sporozoites respectively [13]. In the context of drug development, there has been a shift from the traditional paradigm of testing drugs in immortalized cell lines to the use of primary cells, which have been increasingly recognized to offer better physiological relevance to drug screening and disease modeling *in vitro* [263]. A key goal of early-stage drug discovery platforms is the elimination of drug candidates that generate toxic metabolites that can cause *in vivo* drug-induced liver injury (DILI), a key cause of drug removal from the market [264]. To this end, a hepatic cell type that accurately recapitulates the native cellular physiology of an adult human hepatocyte is advantageous, but most hepatic cell lines lack the expression of a wide array of such key adult hepatic metabolism activity[227] since they are largely tumor-derived (HepG2) or tumor-associated (HC04). A second major goal of drug discovery platforms is the ability to identify non-toxic compounds that demonstrate differential efficacy in a phenotypic screen relevant to a disease. In the case of drug discovery against the malarial liver stages, it is therefore highly

advantageous to utilize a cell type that best represents the primary adult hepatocyte. At the same time, it is also ideal to represent highly polymorphic genetic variants in drug metabolism and different ethnic groups in such drug screens, as these factors may influence the efficacy of potential antimalarial drug candidates. For example, genetic polymorphisms in CYP2D6 metabolism which stratified *P. vivax* patients into poor, intermediate or extensive CYP2D6 metabolizers were recently reported to correlate with the risk of a failure of primaquine to prevent malaria relapse due to *P. vivax*[265]. Several alternative sources other than primary human hepatocytes have been proposed to augment the genetic variation and supply of adult human hepatocytes, including xenogenic or fetal human tissue, or embryonic stem cell-derived hepatocytes, but these sources are hampered by safety, ethical, or sourcing issues.

iPSC-derived iHLCs offer a unique advantage in that they can be generated from any donor, which allows a broad spectrum of the human population to be represented in *in vitro* drug screens and provides an opportunity to assess donor-specific drug responses *in vitro*. High profile collaborations between drug discovery companies and service providers of leading academic stem cell laboratories have been struck[263], marking the development of an infrastructure that will benefit future personalized models of human diseases, including hepatotropic diseases like the relapsing forms of malaria.

iPSCs can also be engineered using DNA editing techniques to incorporate any genetic abnormality or modification to enable the exploration of the role that host genetics plays in liver-stage malaria infection. Although clinically-relevant host factors that influence hepatic susceptibility to liver-stage malaria infection have not been documented, the study of potential host factors may benefit from the larger pool of genetic variation that is accessible with the use of iPS cells. This may have implications in drug discovery against the liver stages of malaria species that present with large genetic heterogeneities in different parts of the world, especially the relapsing malaria species like *P. vivax* (e.g. temperate versus tropical strains) which may have co-evolved to infect geographically distinct human populations [266,267,268,269]. Even with a single donor, the ability to study liver-stage malaria infection at different developmental stages during their *in vitro* directed differentiation into hepatocyte-like cells

may facilitate the identification of host factors required for permissiveness to sporozoite infection and the elucidation of the roles that these host factors play in malaria pathogenesis.

The observation that iHLCs are infectible with malaria before their *in vitro* differentiation is complete could reflect the acquisition of some liver-stage malaria host entry factors during the iPSC differentiation process, or could suggest the possibility of some promiscuity in the host entry factors that are required for *Plasmodium* sporozoite entry. Further studies are required to determine whether the EEFs observed in incompletely differentiated iPSCs reflect fully replication-competent EEFs, or whether such EEFs are prone to developmental arrest due to the absence (or presence) of some host factor that promotes (or inhibits) parasite development. It is intriguing that hepatoblasts appear to support similar *P. falciparum* infection rates as iHLCs, and support similar degrees of parasite growth, with some experiments even exhibiting a trend of increased numbers of PfEEFs and PyEEFs in hepatoblasts compared to iHLCs (**Figure 3.3A, B, C**.) This slight difference in infectibility could suggest the acquisition of sufficient host entry factors that support parasite infection and development by D15 post-initiation of differentiation from iPSCs, but that further maturation beyond the hepatoblast stage results in the acquisition of other host factors that henceforth limit EEF development and survival. As the cells in different stages of *in vitro* differentiation arise from the same donor, these observations also offer a clean comparative system in which to systematically probe and identify host factors that are essential for liver-stage malaria parasite infections, using proteomics or gene expression technologies, in a donor-independent manner.

A common shortcoming of iHLCs and other iPSC-derived cells lies in the fact that they often resemble a developmentally immature state compared to the fully differentiated adult counterpart[263]. In the field of iHLCs, current *in vitro* differentiation protocols result in the production of a hepatic cell type that is biologically closer to fetal hepatocytes than adult hepatocytes, due to the incomplete abrogation of the expression of fetal markers such as alpha-fetal protein (AFP)[254,270], and the incomplete acquisition of an adult-like levels of key adult hepatocyte secretory, detoxification and metabolic activity[255]. Our data shows that further chemical maturation of iHLCs allows the acquisition of primaquine sensitivity,

presumably via the acquisition of a drug metabolism enzyme (DME) expression profile that better resembles the adult human hepatocyte. This advance decreases the biological gap between iHLCs and primary adult hepatocytes, and increases the potential utility of iHLCs in drug development efforts for malaria and other diseases. The expression of a developmentally mature repertoire of hepatic DMEs is particularly important considering that current drug development efforts towards malaria eradication revolves around the 8-aminoquinoline family, which is currently the only class of drugs that is efficacious against the cryptic hypnozoite stage of *P. vivax* liver stage infections[271], and the fact that many existing antimalarial drugs like proguanil, artemether, lumefantrine and halofantrine are known to undergo metabolism in the liver by hepatic DMEs [272] and whose *in vitro* efficacy will therefore likely be predictive of *in vivo* efficacy only if the *in vitro* hepatocyte model exhibits a DME expression profile that is reminiscent of that of primary adult hepatocytes *in vivo*.

3.4 Materials and Methods

iPSC Culture and Hepatocyte-Like Cell (iHLC) Generation. Undifferentiated iPSC were maintained and differentiated into iHLCs as described[254]. In brief, iPSCs were cultured in monolayer on Matrigel (Becton Dickinson), and directed differentiation was achieved by sequential exposure to Activin A, bone morphogenic protein 4, basic FGF, HGF, and oncostatin M (OSM).

Sporozoites. *P. berghei* ANKA and *P. yoelii* sporozoites were obtained by dissection of the salivary glands of infected Anopheles stephensi mosquitoes obtained from the insectaries at New York University (New York, New York, USA) or Harvard School of Public Health (Boston, Massachusetts, USA). *P. falciparum* sporozoites were obtained by dissection of the salivary glands of infected Anopheles gambiae mosquitoes obtained from the insectary at Johns Hopkins School of Public Health (Baltimore, Maryland, USA).

Infection of iHLCs. *P. berghei, P. yoelii* or *P. falciparum* sporozoites from dissected mosquito glands were centrifuged at 3000rpm for 5 min on to iHLCs at a multiplicity of infection of 0.1 − 1 in the presence of 2% fetal bovine serum. After incubation at 37°C and 5% CO_2 for 2-3h, the wells were washed twice before serum-free culture medium was added. Media was replaced daily. Samples were fixed 24h, 48h, or 65h post-infection with *P. berghei* and *P. yoelii*, and 4 days or 6 days post-infection with *P. falciparum*.

Immunofluorescence assay. Infected cultures were fixed with -20°C methanol for 10 min at 4°C, washed thrice with PBS, blocked with 2% BSA in PBS overnight at 4°C and then incubated overnight at 4°C with a primary antibody mouse anti-PbHSP70 (clone 2E6; 1:200 for *P. berghei* and *P. yoelii*), rabbit anti-PbMSP1 (1:500 for *P. berghei*), mouse anti-PfHSP70 (clone 4C9, Sanaria; 1:200 for *P. falciparum*), or mouse anti-PfMSP1 (1:200 for *P. falciparum*). Samples were washed thrice with PBS before incubation for 1-3h at room temperature with secondary antibody: goat anti-mouse Alexa Fluor 594 or Alexa Fluor 488 or donkey anti-rabbit-Alexa Fluor 488 (Invitrogen; 1:400). Nuclei were then counterstained with Hoechst 33258 (Invitrogen; 1:1000), samples were washed thrice with PBS, and 1mL of Aquamount (Thermo-Scientific, West Palm Beach, Florida, USA) was added per well. Images were captured on a Nikon Eclipse Ti fluorescence microscope.

Biochemical assays. Cell culture supernatants were collected and stored at −20°C. Urea was measured by acid- and heat-catalyzed detection of diacetylmonoxime conversion to a colorimetric product (StanBio Labs). Albumin content was measured by an enzyme-linked immunosorbent assay using goat anti-human albumin antibody (Bethyl Labs) with horseradish peroxidase detection (Bethyl Labs) and 3,3',5,5'-tetramethylbenzidine (TMB, Pierce) development.

3.5 Conclusion

In conclusion, the establishment of *Plasmodium* liver-stage infections in induced pluripotent stem cell-derived hepatocyte-like cells lays the foundation for their use in antimalarial drug discovery as well as paves the way to study the genetic basis of host-*Plasmodium* interactions.

Acknowledgements

Chapter 4: Engineering an Implantable Model of Liver-Stage Malaria

4.1 Introduction

Malaria affects 210 million people and causes more than half a million deaths each year[2]. As an obligatory stage of the malaria life cycle that occurs soon after infection of the human host, the *Plasmodium* liver stage is an attractive target for the development of antimalarial drugs and vaccines, especially with the current goal of malaria eradication. A major factor impeding the discovery of new and efficacious antimalarial drugs is the lack of experimental models that sufficiently recapitulate host-pathogen interactions in a physiologically relevant microenvironment. Recent advances in the development of *in vitro* models of liver-stage malaria have increased the prospects of rapidly identifying potential drugs with activity against the liver stages [227,273]. However, preclinical *in vivo* models for liver-stage malaria are sorely lacking[14,271], and such models are needed to characterize hits from *in vitro* antimalarial phenotypic drug screens in terms of pharmacokinetics, pharmacodynamics, adverse drug-drug interactions and toxicology. Due to differences in drug metabolism profiles between mouse and human hepatocytes which had often led to a lack of predictivity of adverse drug-drug interactions in humans[57], the narrow species and cellular tropism of liver-stage *Plasmodium* species that afflict humans (e.g. *P. falciparum* and *P. vivax*)[14], and a strong preference for small animal models over conventional non-human primate models due to ethical and logistical issues, humanized mouse models have emerged as an important route for the preclinical testing of potential antimalarial drugs[76,271,274].

Humanized mouse models containing a human liver component have been generated using a combination of genetic engineering and xenotransplantation approaches[76,97]. These typically involve the transplantation of primary human hepatocytes into genetically engineered immunocompromised mice that exhibits either a spontaneous liver injury due to urokinase plasminogen activator overexpression (uPA+/+/SCID) or an inducible liver injury due to a genetically targeted FAH disruption (FAH-/-) to create human liver chimeric mice. uPA+/+/SCID mice are infectible by *P. falciparum* [93,94], whereas FAH-/- mice are infectible with *P. falciparum*[96]. However, existing liver injury models are characterized by a long engraftment

time, low and variable engraftment efficiencies, an ongoing mouse liver injury during human hepatic reconstitution and high costs ($12,000 per mouse)[76,97]. In contrast, a recently described approach to creating human liver chimeric mice that circumvents some of these issues involves the implantation of human ectopic artificial livers (HEALs), biomaterial-based engineered hepatic tissues which can be fabricated in a relatively low-cost, rapid and scalable fashion [275]. Poly(ethylene glycol) (PEG)-based HEALs have been engineered to sustain primary human hepatocyte survival and functional maintenance, and have been shown to engraft ectopically *in vivo*, resulting in the presence of human proteins in the mouse serum, and allowing the modeling of human-specific drug metabolism in a mouse [275]. However, the HEALs model has not been engineered for infectibility with a hepatotropic pathogen like *Plasmodium* sporozoites. As the mechanism of sporozoite infection of hepatocytes once they arrive in the hepatic sinusoid *in vivo* is poorly understood, it is difficult to extract design principles from the natural infection process that would guide the engineering of human hepatic tissue with the suitable microenvironment that would fully recapitulate the *in vivo* infection process.

In this study, we sought to establish an implantable model of liver-stage *Plasmodium* infection in primary human hepatocytes using PEG-based HEALs. Working towards an eventual goal of infection via an intraperitoneal injection of *Plasmodium* sporozoites, we first redesigned the biomaterial scaffold to support sporozoite entry *in vitro* by creating macroporous PEG cryogels. We determined the minimal microenvironment needed to support primary human hepatocyte survival and functional maintenance in PEG cryogels *in vitro*. We further demonstrated the feasibility of establishing liver-stage *Plasmodium* infection in these PEG cryogel-based human ectopic artificial livers (PC-HEALs) with three *Plasmodium* species, and observed primaquine sensitivity of infected PC-HEALs. Lastly, we implanted PC-HEALs intraperitoneally in nude mice, characterized their survival *in vivo*, and successfully infected them with *Plasmodium* sporozoites.

4.2 Results

Fabrication of PEG cryogels and characterization of sporozoite accessibility to encapsulated cells

The fabrication of previously described PEG-based HEALs involved the co-encapsulation of primary human hepatocytes and mouse fibroblasts that were stabilized for a week in random two-dimensional coculture prior to encapsulation and a human liver endothelial cell line in poly(ethylene glycol)-diacrylate (PEGDA, MW 20kDa) that is photopolymerized in the presence of a photoinitiator and ultraviolet light to form a transparent hydrogel[275]. Due to the nanoporous network structure of conventionally photopolymerized PEGDA hydrogels (7nm for 20kDa PEGDA at 10% w/v)[276] and the non-biodegradable nature of the PEGDA hydrogels, it was hypothesized that *Plasmodium* sporozoites (1 by 10 μm) may not be able to access hepatocytes that are encapsulated within the hydrogels. Indeed, when human hepatoma Huh7.5 cells, known to be highly infectible with *P. berghei* sporozoites *in vitro*[48], were encapsulated in 20kDa PEGDA hydrogels and exposed to *P. berghei* sporozoites that express firefly luciferase (Pb-luc), no bioluminescence was observed at 48h post-exposure (**Figure 4.1B**). In contrast, when Huh7.5 cells were encapsulated in 20kDa PEGDA hydrogels and exposed to hepatitis C virus (HCV) expressing firefly luciferase, robust bioluminescence was observed within 24h post-exposure (data not shown). Since HCV has a diameter of 55nm[277], it was previously hypothesized that the pore size of 20kDa PEGDA hydrogel would increase from 7nm in a cell-free hydrogel to at least 55nm in a cell-containing hydrogel due to gelation defects introduced by the cells [278], thus allowing HCV to access the Huh7.5 cells encapsulated within the hydrogel.

To increase sporozoite accessibility to hepatocytes encapsulated within PEGDA-based hydrogels, a cryogelation protocol was adapted to introduce macroporosity into PEGDA hydrogels[279] (**Figure 4.1A**). This procedure involved the gelation of PEGDA using chemical redox initiators, ammonium persulfate (0.5% w/v) and TEMED (0.05% w/v) at -20°C, and resulted in the formation of macroporous PEG cryogels with pore sizes between 30 – 60μm. When Huh7.5 cells were seeded on to lyophilized PEG cryogels, and exposed to Pb-luc sporozoites, robust

bioluminescence was observed at 48h post-exposure (**Figure 4.1B**), suggesting that Pb-luc sporozoites can access the cells encapsulated within PEG cryogels.
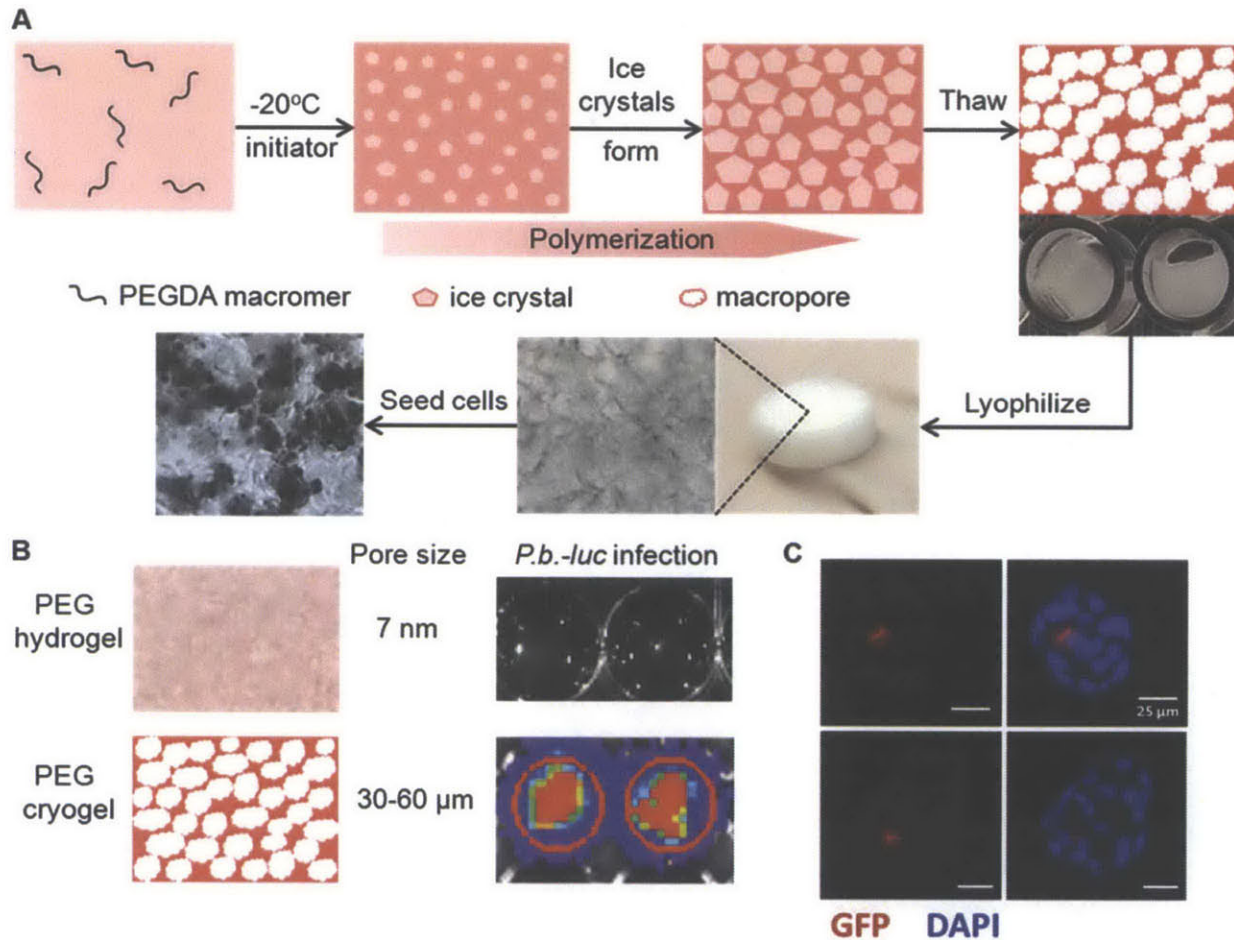
Figure 4.1. Introducing Macroporosity into PEG Hydrogel Confers Sporozoite Accessibility to Hepatocytes. (A) Schematic of cryogelation process during the synthesis of PEG cryogels. (B) Comparison of pore sizes of conventional PEG hydrogel versus PEG cryogels. Huh7.5 cells were encapsulated in PEG hydrogels or PEG cryogels, and exposed to P.b.-GFP-luc sporozoites for 3h. Bioluminescence of samples was captured at 48h post-exposure. (C) Immunostaining of GFP expressed by P.b-GFP-luc parasites.

Fabrication of PEG cryogel-based human ectopic artificial livers (PC-HEALs) and characterization of primary human hepatocyte phenotypic maintenance

Having resolved the transport of *Plasmodium* sporozoites into a cell-laden biomaterial, the next goal was to establish primary human hepatocyte survival in PEG cryogels, since primary human hepatocytes are a preferable cell type to model liver-stage malaria for several reasons that will be discussed later[227]. The poor survival of primary hepatocytes ex vivo has been a key obstacle to their utility in cell transplantation for therapeutic purposes as well as in current *in vitro* liver-stage malaria models. A common method to stabilize primary hepatocyte function is to culture the hepatocytes in three-dimensional (3D) spheroids[280–284], which can be achieved by encapsulating hepatocytes in macroporous biomaterials such as alginate[128,129]. The aggregation of hepatocytes into spheroids is a key contributing factor to hepatic phenotypic maintenance. Moreover, the introduction of a coculture cell type is another strategy that has been extensively shown to promote hepatic functional maintenance through the provision of appropriate heterotypic paracrine and juxtacrine cellular interactions[129] and, in the case of 3D culture systems, the facilitation of spheroid formation[128].

When primary human hepatocytes (PHHs) were seeded on to lyophilized PEG cryogels, the hepatocytes remained largely unicellular with limited aggregation (**Figure 4.2A**). In the presence of a coculture cell type, J2-3T3 mouse embryonic fibroblasts (J2s), which has been shown to phenotypically rescue PHHs in both two-dimensional micropatterned cocultures [118] and three-dimensional PEG-based artificial livers [275], primary human hepatocytes formed cellular aggregates whose diameters are limited by the cryogel pores (**Figure 4.2B**). PHH/J2 cocultures in PEG cryogels maintained cell surface expression of CD81 in a hepatocyte-specific manner, as determined by the differential nuclear morphologies of PHHs and J2s (**Figure 4.2C**). CD81 is a tetraspannin that has been implicated as a host entry for *Plasmodium* sporozoites[221], and has been observed to be necessary but insufficient for *Plasmodium* sporozoite invasion of PHHs *in vitro*[227]. Importantly, coculture of PHHs with J2s was essential for maintaining PHH albumin secretion, a proxy for hepatocyte survival, for 15 days *in vitro* (**Figure 4.2D**), and also better supported the maintenance of CYP3A4 drug metabolism activity compared to monocultures of PHHs alone (**Figure 4.2E**). These data suggest that PEG cryogel-based human

ectopic artificial livers (PC-HEALs) that comprise PHH/J2 cocultures successfully maintain PHH survival and function *in vitro*.
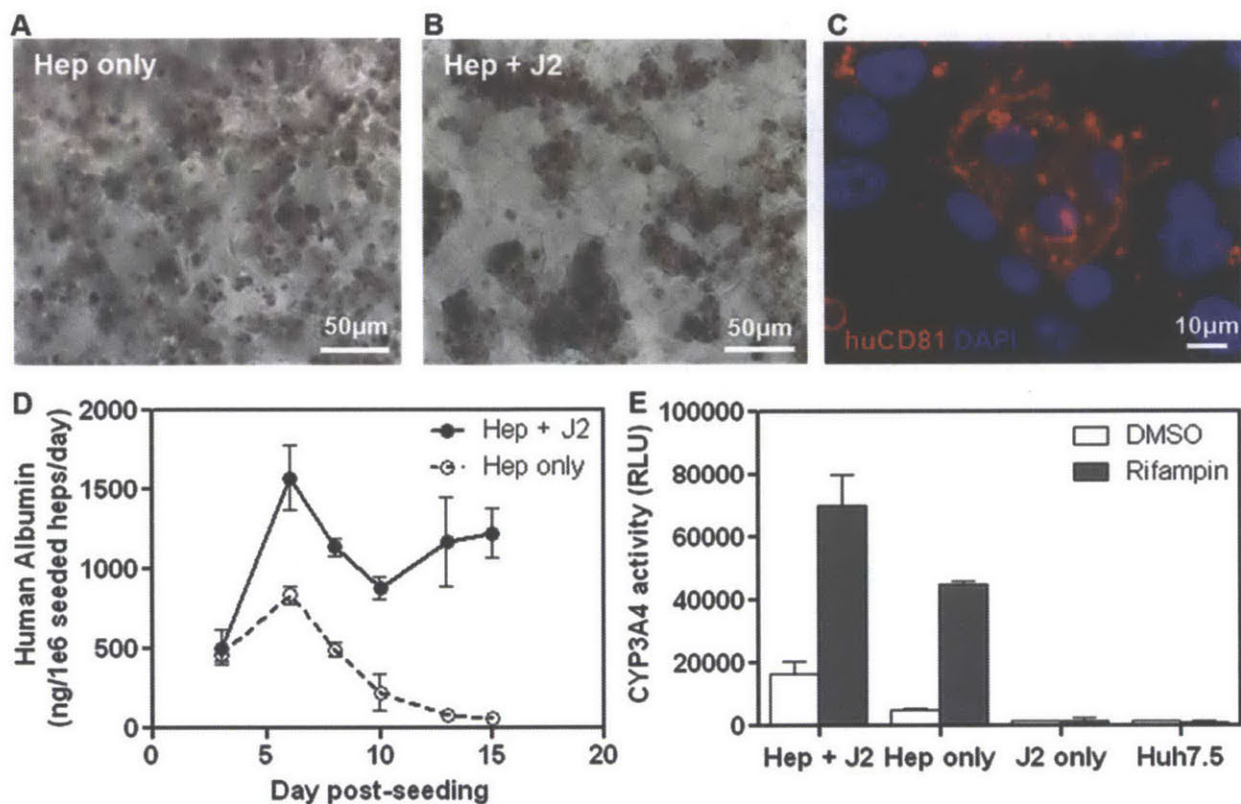
Figure 4.2. Hepatic Functional Characterization of 3D PEG Cryogel-based Artificial Human Liver *In Vitro*. (A) Monocultures of primary human hepatocytes (PHH) in PEG cryogels remain unicellular and do not aggregate. (B) PHH and J2-3T3 fibroblasts cocultures in PEG cryogels (PC-HEALs) form cellular aggregates within the first 2 – 3 days post-seeding. (C) Multiphoton imaging of PC-HEALs shows retention of cell surface expression of malaria host entry factor human CD81 in PHH. (D) PC-HEALs maintain human hepatocyte-specific albumin production better than PHH monocultures and human hepatoma cells, Huh7.5.

Establishment of liver-stage *Plasmodium* berghei infections in PC-HEALs *in vitro*

To determine whether PC-HEALs were susceptible to *Plasmodium* sporozoite infection *in vitro*, PC-HEALs were exposed to GFP- and luciferase-expressing *P. berghei* sporozoites (Pb-GFP-luc)[285] at 2 days post-seeding and imaged by IVIS bioluminescence imaging (BLI). BLI signals were observed in PC-HEALs (Hep + J2) at 24h and 48h post-exposure to Pb-GFP-luc, but not in PEG cryogels seeded with an equivalent total number of J2s alone (**Figure 4.3A, B**).

Interestingly, PHHs seeded in monoculture (Hep only) and infected with Pb-luc 2 days post-seeding were also infectible to similar levels as PHH/J2 cocultures (Hep + J2) (**Figure 4.3C**), which is consistent with their survival kinetics based on albumin secretion *in vitro* (**Figure 4.2D**). However, PHHs seeded in monoculture (Hep only) were less infectible if exposed to Pb-GFP-luc sporozoites 7 days post-seeding, whereas PC-HEALs (Hep + J2) maintained similar levels of infectibility as determined by Pb-GFP-luc BLI 48h post-exposure. This suggests that functional maintenance of PHHs in PC-HEALs also contributes to the maintenance of hepatocyte infectibility with Pb-GFP-luc sporozoites.

To confirm that *Plasmodium* exoerythrocytic forms (EEFs) were found in hepatocytes and not fibroblasts, infected PC-HEALs were fixed at 48h post-infection, and stained for human CD81 and GFP expressed in Pb-GFP-luc EEFs using a whole-mount immunostaining protocol and imaged on a multiphoton microscope. Pb-GFP-luc EEFs were observed mostly in human CD81-expressing cells containing a nucleus characteristic of hepatocytes (**Figure 4.3D**), and rarely in CD81-negative cells, validating the BLI measurements that suggest that Pb-GFP-luc infection of PC-HEALs was largely hepatocyte-specific.

To illustrate the potential utility of PC-HEALs as a model for antimalarial drug testing, PC-HEALs were exposed to Pb-GFP-luc sporozoites for 3h, after which the sporozoites were washed off, and the infected PC-HEALs were treated with or without two doses of primaquine. At 48h post-infection, Pb-GFP-luc BLI decreased in a dose-dependent manner with increasing primaquine concentrations (**Figure 4.3E, F**), suggesting that primaquine treatment inhibited the growth of Pb-GFP-luc EEFs in PC-HEALs. This is consistent with the PHHs maintaining their drug metabolism activity as measured by CYP3A4 activity (**Figure 4.2E**).

Establishment of liver-stage *Plasmodium* yoelii infections in PC-HEALs and mechanistic insights on hepatocyte infectibility *in vitro*

In addition to Pb-GFP-luc, PC-HEALs were also infected with luciferase-expressing *P. yoelii* (Py-luc)[260] two days post-seeding. Interestingly, as opposed to earlier observations where PHHs were infectible with Pb-GFP-luc 2 days post-seeding either in monoculture or in coculture with J2s, PHHs seeded in monoculture in PEG cryogels at the cell density (350,000/cryogel) used in earlier experiments were not infectible with Py-luc (**Figure 4.3G**). However, doubling this PHH seeding density to 700,000/cryogel conferred infectiblity as measured by Py-luc BLI 48h post-infection (**Figure 4.3G**). The apparent contribution of increased hepatocyte concentration alone to hepatocyte infectibility by *Plasmodium* sporozoites is consistent with previous reports that suggest that higher hepatocyte seeding densities in macroporous alginate sponges promote the formation of larger hepatic spheroids with a concomitant increase in hepatic function[128], and the observation described earlier that better hepatic functional maintenance (albumin secretion) correlated with better maintenance of hepatocyte infectibility with Pb-GFP-luc (**Figure 4.2D, 4.3C**).

Effect of coculture. Since the coculture of PHHs with J2s in PC-HEALs maintained hepatocyte infectibility with Pb-GFP-luc at higher levels over time compared to the monoculture of PHHs, the effect of coculture with J2s on PHH infectibility with Py-luc at 2 days post-seeding was tested. The addition of increasing densities of J2s to the same number of PHHs (350,000/cryogel) resulted in increasing Py-luc BLI levels measured 48h post-infection (**Figure 4.3G**). This suggests that even though coculture of PHHs with J2s had not yet resulted in a significant increase in hepatocyte function (as measured by albumin secretion) at 2 days post-seeding (**Figure 4.2D**), the presence of coculture had already substantially prevented a loss of hepatocyte infectibility with Py-luc, which is generally more restrictive than Pb-GFP-luc[161].

Effect of J2 feeder layer. As PHH/J2 cocultures in PC-HEALs result in cellular aggregation, the contribution of J2s to PHH infectibility with *Plasmodium* sporozoites could be mediated by either soluble factor or physical cell-cell interactions between the two cell types. To determine whether the contribution of J2s to hepatocyte infectibility with Py-luc occurred at the paracrine

or juxtacrine level, an additional condition was introduced where PHHs were seeded in monoculture (350,000/cryogel), and cultured over a confluent feeder layer of J2s. Surprisingly, PHHs monocultures in PEG cryogels over a feeder layer of J2s had the same levels of Py-luc BLI at 48h post-infection as the PHH/J2 cocultures (**Figure 4.3G**), suggesting that the J2s boost hepatocyte infectibility with Py-luc in a largely paracrine, and not necessarily juxtacrine fashion, at least for short-term (2 day) infections like *P. yoelii*.

Establishment of liver-stage *Plasmodium falciparum* infections in PC-HEALs *in vitro*

PC-HEALs were earlier infected with luciferase-expressing rodent malarial sporozoites to optimize their infectibility *in vitro* due to the relative scarcity of *P. falciparum* sporozoites, as well as a lack of a luciferase-expressing strain to ease platform optimization. To extend the above findings to the human malaria species, PC-HEALs were exposed to *P. falciparum* (Pf) sporozoites at 2 days post-seeding. A positive parasite load, as determined by RT-PCR using Pf18S rRNA-specific primers, was detected at 4 days post-exposure, but not in uninfected PC-HEALs and PEG cryogels containing only J2s, suggesting that Pf infection was hepatocyte-specific (**Figure 4.3H**). Furthermore, primaquine treatment of PC-HEALs at 3h post-infection resulted in a decrease in Pf parasite load (**Figure 4.3H**), suggesting that PHHs in PC-HEALs retained their ability to bioactivate primaquine into its active form, which is consistent with the maintenance of hepatic drug metabolism activity in PC-HEALs (**Figure 4.2E**) and the requirement for primaquine to be activated by hepatic drug metabolism enzymes to exert its antimalarial activity[197,257,265]. Interestingly, PHHs monocultures in PEG cryogels over a feeder layer of J2s resulted in some Pf infection compared to the absence of the J2 feeder layer, but did not recapitulate the infection levels observed in the PHH/J2 cocultures (**Figure 4.3H**). This suggests that juxtacrine interactions between PHH and J2s, which were dispensable for shorter-term infections with *P. yoelii* (**Figure 4.3G**), are important in maintaining longer-term infections with *P. falciparum*.
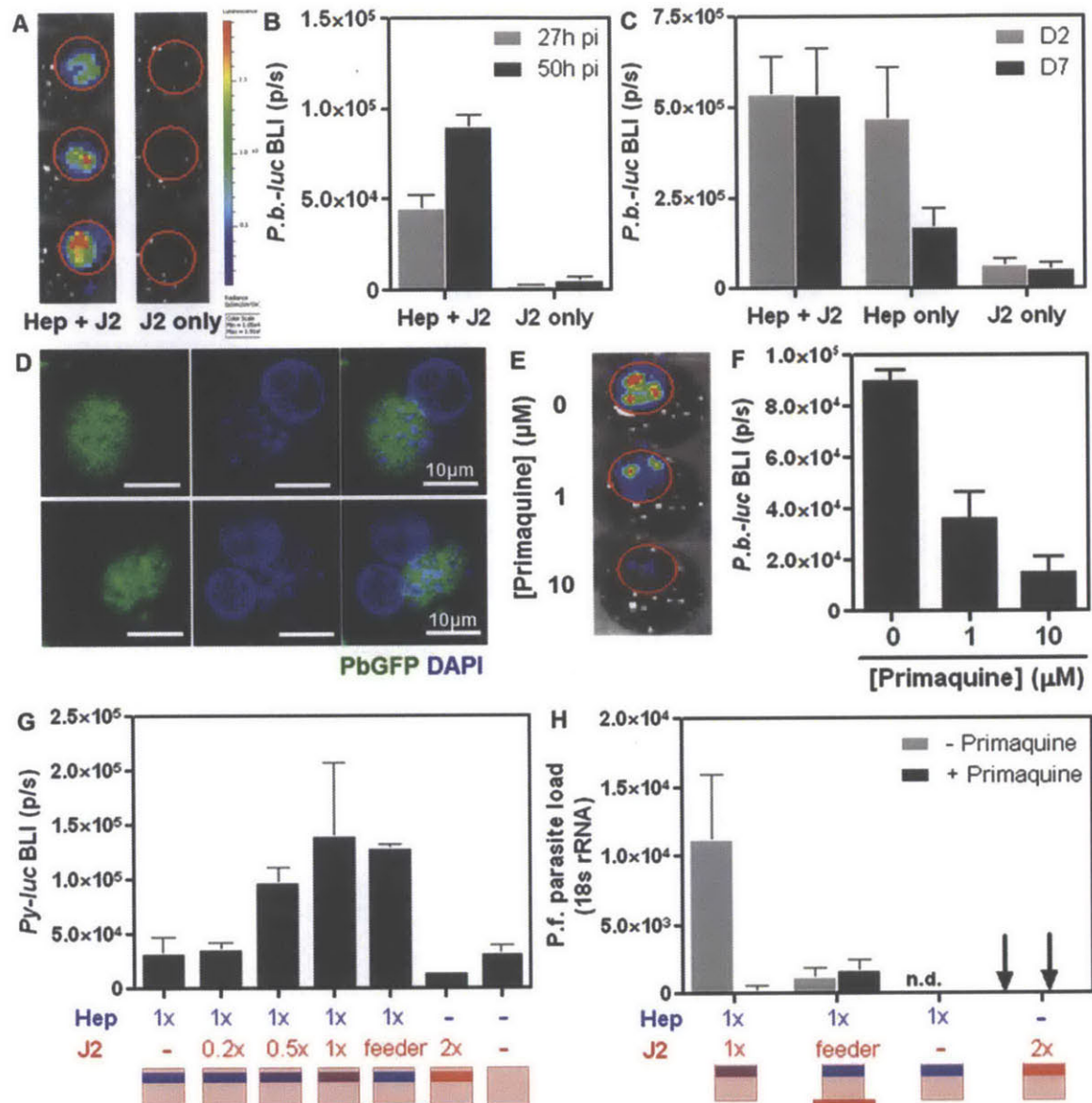
Figure 4.3. *Plasmodium* Infection of PEG Cryogel-based Human Liver *In vitro*. (A) Hepatocyte-specific infection of PC-HEALs with luciferase-expressing *P. berghei* (P.b.-GFP-luc) *in vitro*, measured by bioluminescence imaging (BLI) at 48h post-infection. (B) Quantification of P.b.-GFP-luc infection of PC-HEALs over time in terms of parasite bioluminescence (BLI). (C) Coculture with J2s maintains hepatocyte infectivity to P.b.-luc over time. (D) Multiphoton imaging of PC-HEALs infected with P.b.-GFP-luc, fixed and stained at 48h post infection using a whole mount protocol for GFP and human CD81. (E,F) Dose response of P.b.-luc-infected PC-HEALs to antimalarial drug, primaquine. (G) Infection of hepatocytes with luciferase-expressing *P. yoelii* (P.y.-luc) is dependent on paracrine, but not juxtacrine, interactions with J2s. (H) Infection of PC-HEALs with *P. falciparum* is dependent on both paracrine and juxtacrine interactions with J2s. Infection is measured by RT-PCR for *P. falciparum* 18S rRNA and is normalized to human beta actin.

Implantation of PC-HEALs and characterization of *in vivo* survival and liver-stage *Plasmodium* infection

To determine whether PC-HEALs can be implanted and functionally maintained *in vivo*, PC-HEALs were fabricated as earlier described and transduced with a lentivirus reporter that expresses firefly luciferase under the human albumin promoter (**Figure 4.4A**), and then implanted intraperitoneally in athymic nude mice[275]. Whole-animal bioluminescence imaging and quantification of luciferase production suggested that the intraperitoneal implantation site supported PHH survival and albumin promoter activity for 2-3 weeks after implantation (**Figure 4.4B**).

To assess the potential for using mice implanted with PC-HEALs (PC-HEAL humanized mice) to model liver-stage malaria *in vivo*, PC-HEAL humanized mice were challenged with Pb-GFP-luc or Py-luc sporozoites via an intraperitoneal injection, and imaged 24h and 48h post-injection in an IVIS whole animal bioluminescence imaging (BLI) system. In 83% of PC-HEALs mice (15 out of 18 mice) injected with Pb-GFP-luc sporozoites, a BLI signal at the site of the implanted PC-HEAL is seen (**Figure 4.4C, E**) at levels above mock-infected mice, suggesting that the PC-HEALs were infected with Pb-GFP-luc. This was confirmed by explanting the PC-HEALs from the mice 48h after infection and determining the parasite loads by RT-PCR against *P. berghei* 18s rRNA (data not shown). As a control, mice implanted with blank cryogels and injected with Pb-GFP-luc sporozoites demonstrated only BLI signals in the mouse liver, and not in the site of the cryogel implant. A scattered BLI signal in the mouse livers of mice injected with sporozoites was also observed at levels higher than the mock-infected mice (**Figure 4.4C**), which reflects the infectivity of Pb-GFP-luc sporozoites to mouse hepatocytes. Similarly, when PC-HEALs mice were injected with Py-luc sporozoites, a BLI signal higher than the baseline level in mock-injected animals was measured in 57% of mice (4 out of 7 mice) (**Figure 4.4D, F**).

A Lenti-Alb-Fluc transduction

BLI

Days post-thawing

0   3   4   6   25

Seed   i.p. implantation

B Hep + J2   No Hep   **C** Hep + J2   No Hep

D13 post-transduction   D12 post-implantation

D
Lenti-Alb-Fluc BLI (p/s)

2.5×10⁷
2.0×10⁷
1.5×10⁷
1.0×10⁷
5.0×10⁶
0

Hep + J2
No Hep

0   5   10   15   20   25
Days post-implantation

E   + *Pf* i.p.   RNA

Days post-thawing

0   3   8   9   10   11

BLI

Seed   i.p. implantation   + *Pb-luc* or *Py-luc*

F   Mouse liver   PC-HEAL

G *P. berghei-luc*

PC-HEAL: +   blank   +
P.b.:   mock   +   +

H *P. yoelii-luc*

PC-HEAL: +   +
P.y.:   mock   +

I *P. berghei-luc*
Pb-luc BLI (p/s)

2.3×10⁶
2.2×10⁶
4.0×10⁵
3.0×10⁵
2.0×10⁵
1.0×10⁵
0

24h   48h

PC-HEAL + Pb
PC-HEAL mock
blank + Pb

J *P. yoelii-luc*
Py-luc BLI (p/s)

5×10⁰⁶
4×10⁰⁶
3×10⁰⁶
2×10⁰⁶
1×10⁰⁶
0

+ Py-luc   Mock

K *P. falciparum*
P.f. parasite load (18S rRNA)

10000
1000
100
10
1
0.1
0.01

Hep + J2   Mock   Hep + J2 + endo

114

Figure 4.4. *In vivo* Implantation of PEG Cryogel-based Human Liver and Infection with *Plasmodium.* (A) Timeline of lentiviral transduction of PC-HEALs and *in vivo* non-invasive monitoring by bioluminescence imaging. (B) *In vitro* confirmation of lentiviral transduction of PC-HEALs. (C) Live whole animal bioluminescence imaging of lenti-Alb-Fluc-transduced PC-HEALs that are ectopically implanted in the peritoneum of NCr nude mice at D12 post-implantation. (D) Kinetics of lenti-Alb-Fluc-derived BLI in PC-HEALs *in vivo*. (E) Timeline of *Plasmodium* infection of PC-HEALs-mice. (F) Image of PC-HEALs mouse depicting the intraperitoneal location of PC-HEAL and in a spatially distinct location from the mouse liver. (G) PC-HEALs-mice were infected with *P.b.-GFP-luc* 5 days post-implantation, and infection was measured by bioluminescence imaging at 24h post-infection. (H) PC-HEALs-mice were infected with *P.y.-luc* 5 days post-implantation, and infection was measured by bioluminescence imaging at 48h post-infection. (I) Quantification of *P.b.-GFP-luc* infection by BLI imaging at 24h and 48h post-infection. (J) Quantification of *P.y.-luc* infection by BLI imaging at 48h post-infection. (K) Quantification of *P. falciparum* infection of PC-HEALs-mice as measured by RT-PCR for Pf 18S rRNA.

4.3 Discussion

In this study, we designed an implantable PEG-based artificial human liver that is amenable to liver-stage *Plasmodium* infection *in vitro* and *in vivo*. By introducing macroporosity into the PEG hydrogel via a cryogelation process, we created macroporous PEG cryogels that allow *Plasmodium* sporozoites to access hepatocytes encapsulated within the engineered human liver tissue. Furthermore, by introducing the appropriate densities of both primary human hepatocytes and stromal fibroblasts that are known to support hepatic functional maintenance, we obtained PEG cryogel-based human artificial livers that support primary human hepatocyte survival and phenotype, and more importantly, infectibility with liver-stage *Plasmodium* sporozoites *in vitro*. Importantly, we established a preliminary proof of concept that PEG cryogel-based human ectopic artificial livers survive intraperitoneal implantation and support *in vivo* infection with liver-stage *Plasmodium* parasites.

Need for in vivo models of liver-stage malaria. While *in vitro* liver-stage malaria models are an indispensable part of the antimalarial drug discovery process in terms of identifying compounds that demonstrate anti-liver-stage activity, an *in vivo* model of liver-stage malaria is equally essential for the preclinical characterization of these compounds prior to clinical testing in terms of their toxicology, pharmacokinetics, drug-drug interactions and antimalarial efficacy

in vivo. Existing *in vivo* models of liver-stage malaria range from human (controlled human malaria infections, CHMI)[37] and non-human primate models[44], which are infectible with the human *Plasmodium* species (e.g. *P. falciparum*, *P. vivax*), to rodent models which are infectible with rodent *Plasmodium* species (e.g. *P. berghei*, *P. yoelii*)[286,287]. Non-human primate models suffer from significant ethical, logistical and cost limitations that preclude them from being viable preclinical models, and although the CHMI model is increasingly utilized in early-stage clinical trials, it is unlikely to supplant other models for preclinical screening of potential antimalarial drugs and vaccines. Rodent malaria models are currently the workhorse among experimental *in vivo* malaria models[287], and rodents are widely used for the preclinical characterization of potential drugs prior to clinical testing[57]. However, the differences in the drug resistance mechanisms that have developed in rodent and human malaria species[55] present a conundrum in terms of the ability to extrapolate efficacy data that was gleaned from rodent malaria models to the human malaria species. Furthermore, the known differences in drug metabolism pathways between human and rodent livers [56] may lead to major human metabolites passing undetected in laboratory rodent models and thereby cause a lack of predictivity of rodent models for idiosyncratic drug-induced liver injury (DILI), multi-organ drug toxicity due to human-specific hepatic metabolic by-products, and adverse drug-drug interactions with existing FDA-approved drugs[57].

Humanization methods and the contribution of hepatic tissue engineering. The development of humanized mice containing a human liver compartment may overcome some of the issues associated with conventional rodent models of malaria[54]. Mice with humanized livers can be generated via various strategies, including genetic engineering, ectopic transplantation of human liver tissue or human hepatocytes, or a combination of the two[76,84,97]. The most robust approach to date for generating mice with humanized livers is the generation of transgenic mice that under mouse liver injury and thereby provide a selective advantage for human hepatocytes that are transplanted into the mouse to repopulate and engraft in the injured mouse liver[84]. These strategies generally exhibit a long engraftment time with variable engraftment efficiencies, and depending on the model, human hepatocytes are exposed to an ongoing mouse liver injury during human hepatic reconstitution. Although some of these

models are commercially available, they are associated with significant costs (e.g. $12,000 per FRG humanized mouse). An alternative approach that may complement existing human liver chimeric mouse models involves humanizing mice via the implantation of tissue-engineered artificial human livers[275]. By extending the concept of ectopic primary hepatocyte or human liver transplantation into mice, with the additional application of hepatic tissue engineering techniques to stabilize and maintain primary hepatocyte function prior to and after implantation in mice, humanized mice with human ectopic artificial livers (HEALs) were generated in a rapid (< 1 week) and scalable fashion at a significantly lower overall cost, and successfully applied to modeling human-specific drug metabolism, drug-drug interactions and drug-induced human liver injury in a small animal[275]. The ability to rapidly establish an *in vivo* model of liver-stage human malaria based on HEALs mice in a facile and scalable fashion would make it easier and faster to conduct preclinical evaluation of potential antimalarial compounds *in vivo*.

Designing HEALs for liver-stage malaria. Conceptually, there are two ways to engineer an implantable model of liver-stage *Plasmodium* infection using human ectopic artificial livers. Firstly, the artificial human liver tissue can be engineered to efficiently vascularize so as to allow the infection of the humanized mouse via an intravenous introduction of *Plasmodium* sporozoites. This requires not only an extensive engineered vasculature within the implanted tissue to maximize the chance of an interaction of a *Plasmodium* sporozoite with the hepatocytes within the implant, but also a microenvironment within the engineered vasculature that sufficiently mimics that of the hepatic sinusoids so that *Plasmodium* sporozoites will preferentially sequester in engineered vessels in implanted tissue, extravasate from these engineered vessels like they do naturally in the liver sinusoids, and invade hepatocytes. These requirements are highly challenging, as the precise mechanism of sporozoite invasion of hepatocytes after they arrive in the hepatic sinusoid *in vivo* is still poorly understood. The cumulative evidence from rodent malaria models suggest that once they arrive in the circulatory system, *Plasmodium* sporozoites are rapidly sequestered in the liver sinusoids via the electrostatic interactions between the circumsporozoite protein that is ubiquitously expressed on sporozoites and liver-expressed heparan sulfate proteoglycans (HSPGs) that

117

protrude into the liver sinusoids, the latter of which are the most highly sulfated and therefore the most negatively-charged molecules that is exposed to blood *in vivo*[5,6,288,289]. Sporozoites must then traverse the liver sinusoid, which requires their migration through sinusoidal cells in order to access the hepatocytes[290,291], and subsequently switch from a migratory to an invasive phenotype that is driven in part by the interaction of sporozoites with highly sulfated HSPGs expressed by hepatocytes[289] and in part by signals triggered by further cell traversal[11,292,293] which are still an ongoing subject of controversy within the liver-stage malaria field[5]. Before this controversy is resolved, it is difficult to distill the natural sporozoite infection process into a few design principles that would readily guide the engineering of artificial human liver tissue with the appropriate microenvironmental cues to facilitate sporozoite invasion of hepatocytes in artificial liver tissues.

In an alternative approach undertaken in this study, the artificial human liver tissue could be minimally engineered to support primary human hepatocyte survival and engraftment after implantation *in vivo* to an extent that allows the establishment of hepatocyte infection with the direct delivery of *Plasmodium* sporozoites via an intraperitoneal (or intra-implant) injection. This only requires that the implant affords sporozoite accessibility to the hepatocytes encapsulated in the implant after implantation, and overcomes the potential difficulty in recapitulating the biology of sporozoite infection in the artificial human liver tissue. Indeed, the PC-HEAL model allows *Plasmodium* sporozoites to access and infect primary human hepatocytes that are encapsulated within *in vitro* and *in vivo*, and can be established within one week. However, the infection levels are highly variable among PC-HEAL mice in which a positive ectopic bioluminescence signal was observed at the implant site, which could be due to various factors. One factor is the infectibility of PHHs, which may vary after implantation due to variable engraftment efficiencies of PC-HEALs. A second factor that contributes to variability is the delivery of sporozoites by intraperitoneal injection, which can deposit the sporozoites inside or outside the implant. Variable sporozoite delivery by injection may result in variable sporozoite accessibility to the hepatocytes within the PC-HEAL implant depending on the extent of fibrous encapsulation of the implanted PC-HEAL and the distance of the delivery site from the PC-HEAL. Later infection experiments were performed with the goal of intra-implant

sporozoite delivery, and the confidence that an intra-implant injection was achieved could be approximated using qualitative parameters such as the degree of resistance during the injection (due to the formation of a fibrous capsule around the implant) as well as the appearance of a "backflow" after injection (due to the injection of a volume larger than the volume of the PC-HEAL). Such a post-hoc analysis revealed that an animal is more likely to have a positive infection as measured by BLI signal if the above-mentioned parameters are consistent with an intra-implant injection of sporozoites. Improving the delivery of sporozoites is an area of existing work.

As this PC-HEAL model supports primary human hepatocyte survival for at least 3 weeks *in vitro* and *in vivo*, it offers the potential to model the liver-stages of *P. falciparum* and *P. vivax*, whose liver-stage development lasts 6 and 8 days respectively[294]. However, the current ability of PC-HEALs to support only short-term *P. falciparum* infections *in vitro* suggests that there is much room for improving the 3D microenvironment for *Plasmodium* infection *in vitro* and *in vivo*. This loss of infection over time could be due to the overgrowth of the stromal cell component, which could lead to extreme hypoxia which may affect hepatocyte viability or inhibit parasite growth[295], and the lack of liver-derived nonparenchymal cells or liver-specific matrix components, which could provide paracrine signals that support *Plasmodium* infection in hepatocytes[273]. More studies are needed to understand the cellular and microenvironmental determinants of hepatocyte infectibility in artificial human livers, and experiments to determine whether the *in vitro* infectibility with *P. falciparum* translates to the PC-HEAL mice are underway. If it does, the current model would allow for the testing of potential antimalarial drugs against the early stages of *P. falciparum* infection *in vivo*.

Further improvements need for other liver-stage malaria applications. To extend the potential for PC-HEALs to model *Plasmodium* species with much longer liver stages, such as the hypnozoite stage in *P. vivax* infections, a significantly longer period of hepatocyte survival *in vivo* will be needed[156]. Engineering vasculature into the artificial human livers will be essential to achieve increased hepatocyte longevity after implantation. Various strategies to achieve vascularization in tissue-engineered constructs *in vivo*, some of which have been applied to

artificial livers, include pre-vascularization via cellular self-organization[281,296] or micropatterning[297] of angiogenic and vasculogenic cell types within the engineered tissue, microfabrication of vascular units with accompanying surgical anastomosis during implantation[298,299], or incorporation of angiogenic factors, like VEGF, bFGF and PDGF, into engineered tissue[300–302]. The previously reported HEALs model involved the random co-encapsulation of a liver endothelial cell line which was vascularized after implantation[275].

To establish liver-stage *Plasmodium* infection via a more physiologically relevant infection route like via mosquito bites, a liver sinusoid-like vascularization in the implant will be required, as discussed above. Some human liver model systems have recreated liver sinusoid-like structures by cellular self-assembly[107] or through the use of decellularized liver as a scaffold for reseeding primary human liver and endothelial cells[133,303], and offer the potential for generating engineered vasculature in implantable artificial human liver tissue that are more liver-specific than achievable with other vascularization strategies.

4.4 Materials and Methods

Cell culture and reagents. Cryopreserved primary human hepatocytes were purchased from vendors permitted to sell products derived from human organs procured in the United States by federally designated Organ Procurement Organizations. Vendors included CellzDirect and Celsis *In vitro* Technologies. Human hepatocyte culture medium was high glucose Dulbecco's Modified Eagle's Medium (DMEM) with 10% (v/v) fetal bovine serum (FBS), 1% (v/v) ITS™ (BD Biosciences), 7 ng/ml glucagon, 40 ng/ml dexamethasone, 15 mM HEPES, and 1% (v/v) penicillin-streptomycin. J2-3T3 murine embryonic fibroblasts (gift of Howard Green, Harvard Medical School) were cultured at <18 passages in fibroblast medium comprising of DMEM with high glucose, 10% (v/v) bovine serum, and 1% (v/v) penicillin-streptomycin. Polyethylene glycol diacrylate (Mn 3.4kDa) was purchased from Laysan Bio Inc and used without further purification. Ammonium persulfate (APS), N,N,N′,N′-tetramethylethylenediamine (TEMED), and primaquine diphosphate were obtained from Sigma. Primaquine diphosphate was dissolved at 0.5mg/mL in deionized water, and stored as single-use aliquots at -20°C.

Synthesis of PEG cryogels. PEG cryogels (PCs) were synthesized as previously described[279]. PEGDA was dissolved in sterile phosphate buffered saline (PBS) to a working concentration of 10% w/v and kept on

ice. A final working concentration of the initiator–accelerator mixture comprising 0.5% w/v of ammonium persulfate (APS) and 0.05% w/v of N,N,N',N'-tetramethylethylenediamine (TEMED) was added to the 10% w/v PEGDA solution. 75μL or 150μL of the reaction mixture were dispensed into 96- or 48-well plates respectively and polymerized at -20°C for 20h. After gelation, PCs were rehydrated with sterile water, sterilized with three changes of 70% ethanol, and then washed extensively with fresh sterile water to remove all unreacted compounds. PCs synthesized in 96- or 48-well plates swelled to the well dimensions of 48- and 24-well plates respectively and are labeled PC96 or PC48 respectively.

Fabrication of PC-HEALs. PCs were lyophilized overnight into a sponge-like scaffold. PC96s were used for *in vitro* experiments whereas PC48s were used for *in vivo* experiments. Primary human hepatocytes were mixed with J2-3T3 mouse embryonic fibroblasts in a 1:1 ratio and seeded at 350,000 hepatocytes per PC96 sponge, and proportionately scaled up to 935,000 hepatocytes per PC48 sponge. The seeding volumes were 75μL (PC96) and 150μL (PC48). After cells were dispensed onto the lyophilized PCs, the constructs were centrifuged at 50g for 3min to encourage cellular infiltration into the pores of the PCs. The seeded PC-HEALs were then incubated at 37°C for 15min, before more hepatocyte medium was added and a second centrifugation at 50g for 3min was carried out. After that, sufficient medium was added to barely cover the PC-HEALs, and they were incubated under conventional growth conditions.

Biochemical assays. Cell culture supernatants were collected and stored at −20°C. Albumin content was measured by an enzyme-linked immunosorbent assay using goat anti-human albumin antibody (Bethyl Labs) with horseradish peroxidase detection (Bethyl Labs) and 3,3',5,5'-tetramethylbenzidine (TMB, Pierce) development. For CYP450 induction studies, *in vitro* PC-HEALs were treated daily for 3 days with CYP450 inducer rifampin (20 μM). Subsequently, CYP3A4 activity was measured using the P450-Glo™ CYP3A4 Assay with Luciferin-IPA (Promega) according to the manufacturer's instructions.

***Plasmodium* sporozoites.** *P. berghei ANKA* and *P. yoelii* sporozoites were obtained by dissection of the salivary glands of infected *Anopheles stephensi* mosquitoes obtained from the insectaries at New York University (New York, New York, USA) or Harvard School of Public Health (Boston, Massachusetts, USA). *P. falciparum* sporozoites were obtained by dissection of the salivary glands of infected *Anopheles gambiae* mosquitoes obtained from the insectary at Johns Hopkins School of Public Health (Baltimore,Maryland,USA).

Malaria infection of PC-HEALs *in vitro*. PC-HEALs (PC96s) were transferred on to sterile gauze for about 20 seconds and then transferred to a clean and dry well of a new multiwall plate. The sterile gauze

removes significant amounts of culture medium from the PC-HEAL. *Plasmodium* sporozoites were diluted in culture medium with a final concentration of 3% v/v penicillin/streptomycin and 10% v/v fetal bovine serum and dispensed on to PC-HEALs in volumes of approximately 50μL, which saturates the cryogel but ideally does not overflow down the sides of the cryogel. The sporozoite solution is readily taken up by capillary action into the semi-dry PC-HEALs, which were then incubated at 37°C for 1h to allow sporozoite invasion of hepatocytes without the addition of more culture medium (to avoid washing out the sporozoites from within the cryogel). Medium is added 1h after infection to prevent the PC-HEALs from drying out. 3h after exposure to sporozoites, the PC-HEALs were washed thrice with hepatocyte medium containing 3% v/v penicillin/streptomycin and incubated under growth conditions with hepatocyte medium containing 3% v/v penicillin/streptomycin and 0.1% v/v Fungizone® antimycotic (Gibco®).

Whole mount immunostaining and multiphoton microscopy of PC-HEALs. All the following steps were performed on an orbital shaker. PC-HEALs were washed twice with PBS for 10 min each, fixed with 4% paraformaldehyde for 30 min, washed thrice with PBS for 10min each at room temperature, then permeabilized with 0.1% Triton X-100 in PBS for 10 min at 4°C, and rinsed twice with PBS for 5 min each. The samples were blocked with 2% bovine serum albumin in PBS overnight at 4°C, and then incubated with a primary antibody diluted in 2% BSA/0.05% Tween-20/PBS: mouse anti-human CD81 (clone JS-81, BD Pharmingen; 1:100), rabbit anti-GFP-AlexaFluor488 (Invitrogen, 1:100) overnight at 4°C. The samples were washed thrice with 0.05% Tween-20/PBS for 1 – 2h each at 4°C, then incubated with a secondary antibody diluted in 2% BSA/0.05% Tween-20/PBS: donkey anti-mouse-AlexaFluor594 (Invitrogen; 1:400) overnight at 4°C. The samples were counterstained with Hoechst 33258 (Invitrogen; 1:1000) in PBS and washed thrice with PBS for 1 – 2h each at 4°C, and stored in PBS at 4°C until imaging. Immunostained samples were imaged on a multiphoton microscope (Olympus).

Implantation and monitoring of PC-HEALs. PC-HEALs were placed in the peritoneal cavity of anesthetized NCr nude mice (Taconic) following a 1-cm incision, and sutured to the mesenteric fat pads on both sides to prevent the PC-HEALs from becoming obscured by the mouse organs in the intraperitoneal space. To noninvasively monitor transplanted PC-HEALs for hepatocyte survival, HEALs were transduced with lentiviral pseudoparticles expressing firefly luciferase under the human albumin promoter (pTRIP.Alb.IVSb.IRES.tagRFP-DEST, 1:5 dilution; gift of Charles Rice, The Rockefeller University, New York) 3 days after fabrication and prior to implantation. Mice were intraperitoneally injected with 250uL of 15mg/mL D-Luciferin (in PBS) (Caliper Life Sciences) and imaged using the IVIS Spectrum

(Xenogen) system and bioluminescence was quantified using Living Image Software (Caliper Life Sciences). The Committee for Animal Care in the Department of Comparative Medicine at Massachusetts Institute of Technology approved all animal procedures.

Malaria infection of PC-HEALs mice. $1.5 \times 10^5 - 9 \times 10^5$ *P. berghei*-GFP-luc, $2.5 \times 10^5 - 1 \times 10^6$ *P. yoelii*-GFP-luc or $5 \times 10^5 - 1.5 \times 10^6$ *P. falciparum* sporozoites in $50 - 150\mu L$ of DMEM were delivered into PC-HEALs in PC-HEAL mice by intra-implant or intraperitoneal injection. An intra-implant is qualitatively noted if there is a slight resistance during the injection, whereas a typical intraperitoneal injection does not present with any resistance.

RNA isolation and RT-PCR. PC-HEALs were explanted from mice 48h after injection with *P. berghei*-GFP-luc sporozoites and $3 - 5$ days after injection with *P. falciparum* sporozoites. The fat pad is detached from the PC-HEAL, and any obvious fibrous capsule is removed. PC-HEALs explants were stored in RNAlater (Ambion) until processed. Total RNA was isolated either using the Trizol (Invitrogen) method or the RNeasy Mini Kit (Qiagen). PC-HEALs were homogenized in Trizol (Invitrogen) or RLT buffer (RNeasy Mini Kit, Qiagen) using mortar and pestle or the 'RNA 02' tissue homogenization protocol in a gentleMACS dissociator using gentleMACS M tubes (Miltenyi Biotec). For samples processed in Trizol, the lysates were used directly. For samples processed with the RNeasy Mini Kit, the lysates were first briefly centrifuged at 3500 rpm, transferred to 1.5mL Eppendorf tubes, centrifuged at 14,000 rpm to pellet the cryogel debris and only the supernatants were used. cDNA was made using the iScript cDNA synthesis kit (Biorad) according to the manufacturer's instructions. RT-PCR was carried out using the iScript one-step RT-PCR kit with SYBR® Green (Biorad) in a CFX96™ Real-Time PCR Detection System (Biorad) according to the manufacturer's instructions. The primers used to detect infections were *P. berghei* 18S rRNA (forward:, reverse:) or *P. falciparum* 18S rRNA (forward:, reverse:), and endogenous controls for human beta actin (ACTB, Applied Biosystems) were used for housekeeping purposes.

4.5 Conclusion

In summary, this study provides a proof of concept that human engineered artificial livers that support liver-stage malaria infection can be applied to the development of humanized mouse models of liver-stage human malaria in a facile, rapid and scalable fashion for preclinical drug testing *in vivo*.

Acknowledgements

Chapter 5: Summary and Conclusions

5.1 Contributions to liver-stage malaria models

Bill Gates' call for global malaria eradication in 2007[304,305] resulted in the concept becoming mainstream in the international malaria community and wholeheartedly embraced by various funding organizations such as the Bill & Melinda Gates Foundation, the US National Institutes for Health, the Wellcome Trust, Medicines for Malaria Ventures and the Roll Back Malaria Partnership. Of the 10 leading causes of death in the developing world, malaria is the only one with a real prospect for eradication[305]. This resulted in a renewed push in the malaria research community to identify the key knowledge gaps and define the tools that will bring malaria eradication from a concept to a reality, culminating in the Malaria Eradication Research Agenda (malERA) in 2011[306]. Relapsing species of malaria like *P. vivax* were identified to be a crucial target for eradication to be achievable, since eradication of *P. vivax* on a small island of Vanuatu with a population of just 718 took 5 years to achieve, compared with the almost instant elimination of *P. falciparum* through mass drug administrations of antimalarial drugs[307]. During the malERA forum, the availability of an *in vitro* model of liver-stage malaria that is amenable to screening and automation was specifically defined as a key enabling technology that would allow the discovery of potential anti-liver-stage drugs and the testing of pre-erythrocytic vaccine candidates[308]. The development of humanized mouse models engrafted with functional human cells like hepatocytes was also noted as a potentially unique tool for preclinical testing of potential drugs against liver-stage malaria in the malERA forum, while a separate group of malaria experts identified the development of simple rodent assays for testing the efficacy of new anti-liver-stage drugs *in vivo* as a key scientific challenge in current malaria drug discovery efforts, and suggested that the rebuilding of human liver tissue with stem cell-derived material could be a promising avenue for improving liver-stage malaria models [271]. Through the application of hepatic tissue engineering concepts and techniques, this thesis laid the groundwork towards achieving several of these goals.

In the first part of this work, we established liver-stage *Plasmodium* infection in a microscale human liver platform based on micropatterned cocultures of primary hepatocytes

and supportive stromal fibroblasts. This will readily enable medium-throughput phenotypic screens for potential antimalarial drugs in a more natural host cell type, as well as the testing of pre-erythrocytic malaria vaccines that are based on live-attenuated whole sporozoites. We also showed that recapitulation of a more physiologically relevant oxygen tension that is experienced by hepatocytes *in vivo* improved infection rates and *Plasmodium* parasite growth and maturation *in vitro*, which will help to improve the signal to noise ratio in *in vitro* phenotypic screens for antimalarial drugs. In the second part of this work, we established the feasibility of infecting human induced pluripotent stem cell (iPSC) -derived hepatocyte-like cells (iHLCs) with liver-stage malaria infection, thus opening up the possibility of studying the effect of host genetics on susceptibility to liver-stage malaria infection, and further demonstrated the potential for using iHLCs in the discovery of novel host factors that confer susceptibility to infection in a host-independent manner. Importantly, we induced further hepatic maturation in iHLCs using recently discovered small molecules, resulting in improved drug sensitivity of iHLCs to primaquine, thereby increasing the potential of using these cells for antimalarial drug development. In the final part of this work, we designed and provided a preliminary proof-of-concept for a humanized mouse model of liver-stage malaria that is based on the ectopic implantation of engineered human artificial livers, and that can be generated in a facile, rapid and scalable fashion for preclinical drug testing *in vivo*. The results of this research represent a three-pronged approach towards engineering scalable human liver models that recapitulate liver-stage malaria infection which may ultimately facilitate antimalarial drug discovery at various stages of the drug development pipeline.

5.2 Future directions

Drug screens against liver-stage malaria

The development of the MPCC model of liver-stage malaria infection based on primary human hepatocytes has resulted in the most physiologically relevant tool for the discovery of antimalarial compounds with efficacy against liver-stage parasites to date. In its current format, the MPCC model is ready for screening existing down-selected medium-sized antimalarial compound libraries e.g. the open access malaria box[309] against liver-stages of *P. falciparum* and

P. vivax. However, there are even larger compound libraries comprising thousands of compounds that are validated for blood-stage malaria activity[222,223] that are currently too large to be screened in the MPCC's 96-well plate format. Furthermore, since these libraries contain compounds that are validated to have antimalarial activity in their parent form, with no bioactivation or metabolism, they may not represent their true activities in the context of a human liver's substantial drug metabolism activity. As a result, there may be false negatives (and technically false positives) for antimalarial activity because they undergo bioactivation by DMEs in primary hepatocytes before becoming acquiring antimalarial activity (or get metabolized so efficiently that they lose antimalarial activity). As such, it would be ideal to carry out an unbiased high-throughput screen against liver-stage malaria in primary human hepatocytes, which would require scaling down the size of the MPCC platform to at least a 384-well plate format. Current ongoing efforts in the lab include the *in vitro* validation of specific drugs with known liver-stage activity that are currently in clinical trials, e.g. tafenoquine from GalaxoSmithKline, in MPCCs to further validate the compound's efficacy in primary hepatocytes.

The ability to infect induced pluripotent stem cell (iPSC)-derived hepatocytes (iHLCs) raises the possibility of incorporating them into a phenotypic assay that can be used for antimalarial drug discovery against the liver stages. iHLCs can be generated from any donor, which allows a broad spectrum of the human population to be represented in *in vitro* drug screens, and thereby provides an opportunity to assess the impact of donor-specific differences in hepatic drug metabolism activity profiles on drug efficacy *in vitro*. This would be akin to conducting an *in vitro* clinical trial for antimalarial efficacy, and is highly relevant for drug discovery since the efficacy of existing antimalarial drugs have been reported to be correlated with the specific genetic variant of a hepatic drug metabolism enzyme that a patient has [265]. However, iHLCs are currently most efficiently generated in 6-well plates. Differentiation of iPS cells in smaller well-plate formats results in a dramatically decreased efficiency of generating hepatocyte-like cells. The scaling down of iHLC generation will be necessary to the practical application of iHLCs towards *in vitro* antimalarial drug discovery.

In vitro culture of *P. vivax* hypnozoites for drug discovery and biological studies

The MPCC model of liver-stage malaria can potentially be used to model long term *P. vivax* hypnozoite infections, but first, it is necessary to establish that the small *P. vivax* forms previously observed in infected MPCCs are indeed hypnozoites. Ongoing studies are testing whether the small forms are preferentially sensitive to primaquine treatment but not atovaquone treatment, which is one of two major methods to prove that small forms are indeed hypnozoites, the second of which is to observe activation of the hypnozoites leading to the development of schizonts long after the primary round of schizont development have already passed. Although the stimuli needed to activate hypnozoites are not well understood, prior studies in primary macaque hepatocytes have documented that *P. cynomolgi* hypnozoites appear to activate spontaneously *in vitro*, and that hypnozoites activation can be accelerated through exposure to inhibitors of histone methyltransferases[273]. In this study by Dembele and colleagues, spontaneous activation of *P. cynomolgi* hypnozoites was demonstrated by repeatedly treating infected primary hepatocytes with a high dose of atovaquone that should kill all developing schizonts that were not hypnozoites, and observing the reappearance of growing schizonts several days after the initial atovaquone treatment. The recapitulation of these phenotypes in MPCCs would establish unequivocally the ability of MPCCs to support hypnozoite culture in primary human hepatocytes, and lead to a more physiologically relevant model of *P. vivax* hypnozoites for drug discovery.

P. vivax is a genetically heterogeneous parasite, with several notable distinct strains whose relapse frequencies vary with their geographic origin. As the MPCCs currently maintain human hepatocyte survival and function for 4 – 6 weeks, it is amenable to modeling tropical *P. vivax* strains that exhibit a high relapse rate, e.g. Chesson or Salvador strains, but not temperate *P. vivax* strains that exhibit a low relapse rate of up to a year or even nine years, e.g. North Korean or Finland strains. Whether or not a newly discovered compound against the tropical strains of *P. vivax* will have anti-hypnozoite activity against other *P. vivax* strains is a question that is open to debate. Nevertheless, the ability to model hypnozoites *in vitro* will enable the study of hypnozoite biology and the testing of hypotheses associated with hypnozoite activation[310,311], which could facilitate the discovery of novel compounds or methods to activate

hypnozoites into replicating schizonts that are susceptible to existing liver-stage drugs like atovaquone.

Pre-erythrocytic vaccine development

The MPCC liver-stage malaria model has already found utility in the safety evaluation of pre-erythrocytic malaria vaccines based on attenuated *Plasmodium* sporozoites, as demonstrated by its ability to confirm that a sub-lethally irradiated whole sporozoite vaccine candidate (PfSPZ) from Sanaria Inc was unable to develop in primary human hepatocytes *in vitro*[227], prior to the successful testing of the PfSPZ in early-stage clinical trials[312]. This model also has the potential to provide an *in vitro* correlate of protection via the collection of sera from human subjects who were previously immunized with a vaccine candidate, and the testing whether the post-vaccination sera contain antibodies that can inhibit *Plasmodium* sporozoite invasion of primary human hepatocytes *in vitro*. This can serve as an *in vitro* surrogate for clinical trial efficacy, and can help inform whether or not to carry out an *in vivo* sporozoite challenge on the immunized human subjects. As a proof of concept, ongoing experiments have preliminarily shown that MPCCs that are incubated with an antibody against *P. falciparum* CSP (the key antigen in the most advanced pre-erythrocytic malaria vaccine to date, RTS,S) during *P. falciparum* sporozoite infection are completely protected from *P. falciparum* infection in an antigen-specific manner. This paves the way for the testing of serum samples from patients who had been immunized with various pre-erythrocytic malaria vaccines[195,312–314]. Another potential application of the MPCC liver-stage malaria model is in the evaluation of the efficacy of T-cells generated in response to a candidate vaccine. In this scenario, T-cells are isolated from serum obtained from patients after immunization with the vaccine candidate, and overlaid on to *Plasmodium*-infected MPCCs, and the extent of hepatocyte death induced by T cells can theoretically be quantified.

Liver-stage malaria biology and host factor discovery

In addition to their potential utility in increasing *in vitro* infection rates to enable more statistically powerful antimalarial drug screens, the two observations that the survival and growth of *Plasmodium* liver-stage parasites in primary human hepatocytes is influenced by

oxygen tension and hepatocyte innate immune status are two examples of the multitude of biological questions that can be readily tested in a MPCC model of liver-stage malaria. Primary hepatocytes can potentially recapitulate the physiology of hepatocytes in the liver more closely than hepatic cell lines[315], and are therefore preferable for the study of host-pathogen interactions. The importance of the hepatocyte microenvironment on the development of the liver-stage parasite is highlighted by the observation that host HIF-1α activation by hypoxia is beneficial for parasite survival and development *in vitro*. This observation opens up many avenues for future investigations on the potential downstream mechanisms that underlie the effects of hypoxia on improved liver-stage malaria development, because oxygen sensors like HIF-1α play a wide-ranging role in cellular homeostasis[177,316,317], including energy conservation, redox and pH homeostasis, and autophagy[318,319].

The ability to infect stem cell-derived hepatocytes (iHLCs) will enable studies on the contribution of host genetic variation on susceptibility to liver-stage malaria infection, especially since iPSCs can also be engineered using DNA editing techniques to incorporate any genetic abnormality or modification. Such variability in host infectibility with liver-stage malaria has been observed *in vitro* in MPCCs[227]. Furthermore, iHLCs offer a clean comparative system in which to systematically probe and identify host factors that are essential for liver-stage malaria parasite infections within a *single* host genetic background, due to our observations that iHLCs are infectible with malaria to various degrees at various intermediate stages before their *in vitro* differentiation is complete. This could be achieved using modern proteomics or gene expression technologies.

Humanized mouse models of liver-stage malaria

Currently, PEG cryogel-based human ectopic artificial livers (PC-HEALs) have been engineered to support primary human hepatocyte survival and infectibility with liver-stage malaria (*P. berghei, P. yoelii, P. falciparum*) *in vitro*. At the time this thesis was written, mice humanized with PC-HEALs have also been successfully infected with luciferase-expressing *P. berghei* and *P. yoelii* sporozoites, and experiments with *P. falciparum* infections *in vivo* are ongoing. The successful extension of *P. falciparum* infections to the *in vivo* situation would

allow PC-HEALs humanized mice for the testing of potential antimalarial drugs against the early stages of *P. falciparum* infection *in vivo*. Future improvements of the PC-HEALs model could include increasing the longevity of the implanted PC-HEALs beyond the current 3 weeks, either by engineering a vascular component[281,296,297] or incorporation of angiogenic factors into the engineered livers[300–302] prior to implantation, so as to allow the modelling of longer-term liver-stage malaria infections.

To establish liver-stage *Plasmodium* infection via a more physiologically relevant infection route like via mosquito bites, and in the absence of a thorough understanding of the entire infection process *in vivo*, the requirement for a liver sinusoid-like vascular network in the engineered liver tissue has to be assumed. The use of decellularized liver[133,303] or other scaffolds that recapitulate hepatic tissue microarchitecture[107] will probably be advantageous for achieving a more liver-like vasculature in the engineered artificial liver.

References

1.   Guerra, C., Snow, R. & Hay, S. Mapping the global extent of malaria in 2005. *Trends Parasitol.* **22,** 353–358 (2006).

2.   World Health Organization. *World malaria report 2013.* *Nature* 284 (2013). doi:10.1038/nature.2013.13535

3.   Hay, S. I. *et al.* Estimating the global clinical burden of Plasmodium falciparum malaria in 2007. *PLoS Med.* **7,** e1000290 (2010).

4.   Poespoprodjo, J. R. *et al.* Vivax malaria: a major cause of morbidity in early infancy. *Clin. Infect. Dis.* **48,** 1704–12 (2009).

5.   Ejigiri, I. & Sinnis, P. Plasmodium sporozoite-host interactions from the dermis to the hepatocyte. *Curr. Opin. Microbiol.* **12,** 401–7 (2009).

6.   Cerami, C. *et al.* The basolateral domain of the hepatocyte plasma membrane bears receptors for the circumsporozoite protein of plasmodium falciparum sporozoites. *Cell* **70,** 1021–1033 (1992).

7.   Pradel, G. & Frevert, U. Malaria sporozoites actively enter and pass through rat Kupffer cells prior to hepatocyte invasion. *Hepatology* **33,** 1154–65 (2001).

8.   Frevert, U. *et al.* Intravital observation of Plasmodium berghei sporozoite infection of the liver. *PLoS Biol.* **3,** e192 (2005).

9.   Frevert, U., Usynin, I., Baer, K. & Klotz, C. Plasmodium sporozoite passage across the sinusoidal cell layer. *Subcell. Biochem.* **47,** 182–97 (2008).

10.   Ng, B. *et al.* Intravital Observation of Plasmodium berghei Sporozoite Infection of the Liver ʹ. **3,** (2005).

11.   Mota, M. M. *et al.* Migration of Plasmodium sporozoites through cells before infection. *Science* **291,** 141–4 (2001).

12.   Mota, M., Hafalla, J. & Rodriguez, A. Migration through host cells activates Plasmodium sporozoites for infection. *Nat. Med.* **8,** (2002).

13.   Prudêncio, M., Rodriguez, A. & Mota, M. M. The silent path to thousands of merozoites: the Plasmodium liver stage. *Nat. Rev. Microbiol.* **4,** 849–56 (2006).

14.   Mazier, D., Rénia, L. & Snounou, G. A pre-emptive strike against malaria's stealthy hepatic forms. *Nat. Rev. Drug Discov.* **8,** 854–64 (2009).

15.   Sturm, A. *et al.* Manipulation of host hepatocytes by the malaria parasite for delivery into liver sinusoids. *Science* **313,** 1287–90 (2006).

16.   Krotoski, W. & Collins, W. Demonstration of hypnozoites in sporozoite-transmitted Plasmodium vivax infection. *Am. J. …* (1982). at <http://europepmc.org/abstract/MED/6816080>

17.   White, N. J. *Determinants of relapse periodicity in Plasmodium vivax malaria. Malar. J.* **10,** 297 (2011).

18.   Epstein, J. E. *et al.* Live attenuated malaria vaccine designed to protect through hepatic CD8^{+} T cell immunity. *Science* **334,** 475–80 (2011).

19.   Protection against a Malaria Challenge by Sporozoite Inoculation. at <http://www.nejm.org/doi/full/10.1056/NEJMoa0805832>

20.   Butler, N. S. *et al.* Superior antimalarial immunity after vaccination with late liver stage-arresting genetically attenuated parasites. *Cell Host Microbe* **9,** 451–62 (2011).

21.   HE, S. The pre-erythrocytic stage of mammalian malaria. *Br. Med. J.* 192–194 (1948). at <http://europepmc.org/articles/PMC2089683>

22.   Shortt, H. & Garnham, P. The pre-erythrocytic development of Plasmodium cynomolgi and Plasmodium viv ax. *Trans. R. Soc. Trop. …* **41,** (1948).

23.   Shortt, H. E., Fairley, N. H., Covell, G., Shute, P. G. & Garnham, P. C. C. The pre-erythrocytic stage of plasmodium falciparum. *Trans. R. Soc. Trop. Med. Hyg.* **44,** 405–419 (1951).

24.   Hollingdale, M. R., Leef, J. L., McCullough, M. & Beaudoin, R. L. In vitro cultivation of the exoerythrocytic stage of Plasmodium berghei from sporozoites. *Science* **213,** 1021–1022 (1981).

25.   Chattopadhyay, R. *et al.* Establishment of an in vitro assay for assessing the effects of drugs on the liver stages of Plasmodium vivax malaria. *PLoS One* **5,** e14275 (2010).

26.   Hollingdale, M. R., Leland, P. & Schwartz, A. L. In vitro cultivation of the exoerythrocytic stage of Plasmodium berghei in a hepatoma cell line. *Am. J. Trop. Med. Hyg.* **32,** 682–684 (1983).

27.   Pirson, P. Culture of the exoerythrocytic liver stages of Plasmodium berghei sporozoites in rat hepatocyctes. *Trans. R. Soc. …* **76,** 1982 (1982).

28.   Lambiotte, M., Landau, I., Thierry, N. & Miltgen, F. [Development of schizonts in cultured hepatocytes of adult rats after in vitro infection with Plasmodium yoelii sporoazoites]. *C. R. Seances Acad. Sci. III.* **293,** 431–3 (1981).

29.   Mazier, D., Beaudoin, R., Mellouk, S. & Druilhe, P. Complete development of hepatic stages of Plasmodium falciparum in vitro. *Science (80-.).* **227,** 440–442 (1985).

30.   Mazier, D. *et al.* Cultivation of the liver forms of Plasmodium vivax in human hepatocytes. *Nature* **307,** 367–9

31.   Schuster, F. L. Cultivation of Plasmodium spp . Cultivation of Plasmodium spp . **15,** (2002).

32.   Silvie, O. *et al.* Expression of human CD81 differently affects host cell susceptibility to malaria sporozoites depending on the Plasmodium species. *Cell. Microbiol.* **8,** 1134–46 (2006).

33.   Hollingdale, M. R., Collins, W. E., Campbell, C. C. & Schwartz, A. L. In vitro culture of two populations (dividing and nondividing) of exoerythrocytic parasites of Plasmodium vivax. *Am. J. Trop. Med. Hyg.* **34,** 216–22 (1985).

34.   Karnasuta, C. *et al.* Complete development of the liver stage of Plasmodium falciparum in a human hepatoma cell line. *Am. J. Trop. Med. Hyg.* **53,** 607–11 (1995).

35.   Sattabongkot, J. *et al.* Establishment of a human hepatocyte line that supports in vitro development of the exo-erythrocytic stages of the malaria parasites Plasmodium falciparum and P. vivax. *Am. J. Trop. Med. Hyg.* **74,** 708–15 (2006).

36.   Roestenberg, M. *et al.* Comparison of clinical and parasitological data from controlled human malaria infection trials. *PLoS One* **7,** e38434 (2012).

37.   Laurens, M. B. *et al.* A consultation on the optimization of controlled human malaria infection by mosquito bite for evaluation of candidate malaria vaccines. *Vaccine* **30,** 5302–4 (2012).

38.   Sauerwein, R. W., Roestenberg, M. & Moorthy, V. S. Experimental human challenge infections can accelerate clinical malaria vaccine development. *Nat. Rev. Immunol.* **11,** 57–64 (2011).

39.   Roestenberg, M. *et al.* Controlled human malaria infections by intradermal injection of cryopreserved Plasmodium falciparum sporozoites. *Am. J. Trop. Med. Hyg.* **88,** 5–13 (2013).

40.   Seder, R. A. *et al.* Protection against malaria by intravenous immunization with a nonreplicating sporozoite vaccine. *Science* **341,** 1359–65 (2013).

41.   Meis, J., Ponnudurai, T. & Mons, B. Plasmodium falciparum: Studies on mature exoerythrocytic forms in the liver of the chimpanzee, Pan troglodytes. *Exp. …* **1,** (1990).

42.   Collins, W. E., McClure, H. M., Swenson, R. B., Mehaffey, P. C. & Skinner, J. C. Infection of mosquitoes with Plasmodium vivax from chimpanzees using membrane feeding. *Am. J. Trop. Med. Hyg.* **35,** 56–60 (1986).

43.   Zapata, J. C. *et al.* Reproducible infection of intact Aotus lemurinus griseimembra monkeys by Plasmodium falciparum sporozoite inoculation. *J. Parasitol.* **88,** 723–9 (2002).

44.   Herrera, S., Perlaza, B. L., Bonelo, A. & Arévalo-Herrera, M. Aotus monkeys: their great value for anti-malaria vaccines and drug testing. *Int. J. Parasitol.* **32,** 1625–1635 (2002).

45.   Collins, W. E. *et al.* The Chesson Strain of Plasmodium vivax in Humans and Different Species of Aotus Monkeys. *Am J Trop Med Hyg* **80,** 152–159 (2009).

46.   Collins, W. E. *et al.* Studies on the Salvador I strain of Plasmodium vivax in non-human primates and anopheline mosquitoes. *Am. J. Trop. Med. Hyg.* **80,** 228–35 (2009).

47. Sullivan, J. S. *et al.* Sporozoite transmission of three strains of Plasmodium knowlesi to Aotus and Saimiri monkeys. *J. Parasitol.* **82,** 268–71 (1996).

48. Prudêncio, M., Mota, M. M. & Mendes, A. M. A toolbox to study liver stage malaria. *Trends Parasitol.* **27,** 565–74 (2011).

49. Langhorne, J., Buffet, P., Galinski, M. & Good, M. The relevance of non-human primate and rodent malaria models for humans. *Malar J* (2011). doi:10.1186/1475-2875-10-23

50. Craig, A. G. *et al.* The role of animal models for research on severe malaria. *PLoS Pathog.* **8,** e1002401 (2012).

51. Brian de Souza, J. & Riley, E. M. Cerebral malaria: the contribution of studies in animal models to our understanding of immunopathogenesis. *Microbes Infect.* **4,** 291–300 (2002).

52. Lovegrove, F. E. *et al.* Parasite burden and CD36-mediated sequestration are determinants of acute lung injury in an experimental malaria model. *PLoS Pathog.* **4,** (2008).

53. Mlambo, G. & Kumar, N. Transgenic rodent Plasmodium berghei parasites as tools for assessment of functional immunogenicity and optimization of human malaria vaccines. *Eukaryot. Cell* **7,** 1875–9 (2008).

54. Kaushansky, A., Mikolajczak, S. A., Vignali, M. & Kappe, S. H. I. Of men in mice: the success and promise of humanized mouse models for human malaria parasite infections. *Cell. Microbiol.* (2014). doi:10.1111/cmi.12277

55. Carlton, J. M. *et al.* Genome sequence and comparative analysis of the model rodent malaria parasite Plasmodium yoelii yoelii. *Nature* **419,** 512–9 (2002).

56. Martignoni, M., Groothuis, G. M. M. & de Kanter, R. Species differences between mouse, rat, dog, monkey and human CYP-mediated drug metabolism, inhibition and induction. *Expert Opin. Drug Metab. Toxicol.* **2,** 875–894 (2006).

57. Leclercq, L. *et al.* Which human metabolites have we MIST? Retrospective analysis, practical aspects, and perspectives for metabolite identification and quantification in pharmaceutical development. *Chem. Res. Toxicol.* **22,** 280–293 (2009).

58. Scheer, N., Snaith, M., Wolf, C. R. & Seibler, J. Generation and utility of genetically humanized mouse models. *Drug Discov. Today* **18,** 1200–11 (2013).

59. Scheer, N. *et al.* Modeling human cytochrome P450 2D6 metabolism and drug-drug interaction by a novel panel of knockout and humanized mouse lines. *Mol. Pharmacol.* **81,** 63–72 (2012).

60. Scheer, N. *et al.* Generation and characterization of novel cytochrome P450 Cyp2c gene cluster knockout and CYP2C9 humanized mouse lines. *Mol. Pharmacol.* **82,** 1022–9 (2012).

61.   Van Herwaarden, A. E. *et al.* Midazolam and cyclosporin a metabolism in transgenic mice with liver-specific expression of human CYP3A4. *Drug Metab. Dispos.* **33,** 892–5 (2005).

62.   Scheer, N. *et al.* A novel panel of mouse models to evaluate the role of human pregnane X receptor and constitutive androstane receptor in drug response. *J. Clin. Invest.* **118,** 3228–39 (2008).

63.   Scheer, N. *et al.* Generation and characterization of a novel multidrug resistance protein 2 humanized mouse line. *Drug Metab. Dispos.* **40,** 2212–8 (2012).

64.   Hasegawa, M. *et al.* Quantitative prediction of human pregnane X receptor and cytochrome P450 3A4 mediated drug-drug interaction in a novel multiple humanized mouse line. *Mol. Pharmacol.* **80,** 518–28 (2011).

65.   Dorner, M. *et al.* A genetically humanized mouse model for hepatitis C virus infection. *Nature* **474,** 208–11 (2011).

66.   Dorner, M. *et al.* Completion of the entire hepatitis C virus life cycle in genetically humanized mice. *Nature* **501,** 237–41 (2013).

67.   Ilan, E. *et al.* The hepatitis C virus (HCV)-Trimera mouse: a model for evaluation of agents against HCV. *J. Infect. Dis.* **185,** 153–61 (2002).

68.   Eren, R. *et al.* Preclinical evaluation of two neutralizing human monoclonal antibodies against hepatitis C virus (HCV): a potential treatment to prevent HCV reinfection in liver transplant patients. *J. Virol.* **80,** 2654–64 (2006).

69.   Maeda, N. *et al.* Hepatitis C virus infection in human liver tissue engrafted in mice with an infectious molecular clone. *Liver Int.* **24,** 259–67 (2004).

70.   Sacci, J. B. *et al.* Mouse model for exoerythrocytic stages of Plasmodium falciparum malaria parasite. *Proc. Natl. Acad. Sci. U. S. A.* **89,** 3701–5 (1992).

71.   Ohashi, K. *et al.* Sustained survival of human hepatocytes in mice: A model for in vivo infection with human hepatitis B and hepatitis delta viruses. *Nat. Med.* **6,** 327–31 (2000).

72.   Sacci, J. B. & Azad, A. F. Gene expression analysis during liver stage development of Plasmodium. *Int. J. Parasitol.* **32,** 1551–1557 (2002).

73.   Sandgren, E. P. *et al.* Complete hepatic regeneration after somatic deletion of an albumin-plasminogen activator transgene. *Cell* **66,** 245–256 (1991).

74.   Rhim, J., Sandgren, E., Degen, J., Palmiter, R. & Brinster, R. Replacement of diseased mouse liver by hepatic cell transplantation. *Science (80-.).* **263,** 1149–1152 (1994).

75.   Meuleman, P. *et al.* Morphological and biochemical characterization of a human liver in a uPA-SCID mouse chimera. *Hepatology* **41,** 847–56 (2005).

76. Legrand, N. *et al.* Humanized mice for modeling human infectious disease: challenges, progress, and outlook. *Cell Host Microbe* **6,** 5–9 (2009).

77. Grompe, M. *et al.* Loss of fumarylacetoacetate hydrolase is responsible for the neonatal hepatic dysfunction phenotype of lethal albino mice. *Genes Dev.* **7,** 2298–2307 (1993).

78. Overturf, K. *et al.* Hepatocytes corrected by gene therapy are selected in vivo in a murine model of hereditary tyrosinaemia type I. *Nat. Genet.* **12,** 266–73 (1996).

79. Azuma, H. *et al.* Robust expansion of human hepatocytes in Fah-/-/Rag2-/-/Il2rg-/- mice. *Nat. Biotechnol.* **25,** 903–10 (2007).

80. Bissig, K.-D., Le, T. T., Woods, N.-B. & Verma, I. M. Repopulation of adult and neonatal mice with human hepatocytes: a chimeric animal model. *Proc. Natl. Acad. Sci. U. S. A.* **104,** 20507–11 (2007).

81. Hasegawa, M. *et al.* The reconstituted "humanized liver" in TK-NOG mice is mature and functional. *Biochem. Biophys. Res. Commun.* **405,** 405–10 (2011).

82. Washburn, M. L. *et al.* A humanized mouse model to study hepatitis C virus infection, immune response, and liver disease. *Gastroenterology* **140,** 1334–44 (2011).

83. Brehm, M. A., Jouvet, N., Greiner, D. L. & Shultz, L. D. Humanized mice for the study of infectious diseases. *Curr. Opin. Immunol.* **25,** 428–35 (2013).

84. Grompe, M. & Strom, S. Mice with human livers. *Gastroenterology* **145,** 1209–14 (2013).

85. Dandri, M. *et al.* Repopulation of mouse liver with human hepatocytes and in vivo infection with hepatitis B virus. *Hepatology* **33,** 981–8 (2001).

86. Mercer, D. F. *et al.* Hepatitis C virus replication in mice with chimeric human livers. *Nat. Med.* **7,** 927–33 (2001).

87. Kneteman, N. M. *et al.* Anti-HCV therapies in chimeric scid-Alb/uPA mice parallel outcomes in human clinical application. *Hepatology* **43,** 1346–53 (2006).

88. Kamiya, N. *et al.* Practical evaluation of a mouse with chimeric human liver model for hepatitis C virus infection using an NS3-4A protease inhibitor. *J. Gen. Virol.* **91,** 1668–77 (2010).

89. Tateno, C. *et al.* Near completely humanized liver in mice shows human-type metabolic responses to drugs. *Am. J. Pathol.* **165,** 901–12 (2004).

90. Meuleman, P. & Leroux-Roels, G. The human liver-uPA-SCID mouse: a model for the evaluation of antiviral compounds against HBV and HCV. *Antiviral Res.* **80,** 231–8 (2008).

91. Lütgehetmann, M. *et al.* Humanized chimeric uPA mouse model for the study of hepatitis B and D virus interactions and preclinical drug evaluation. *Hepatology* **55,** 685–94 (2012).

92. Kawahara, T. *et al.* Human cytomegalovirus infection in humanized liver chimeric mice. *Hepatol. Res.* **43,** 679–84 (2013).

93. Morosan, S. *et al.* Liver-stage development of Plasmodium falciparum in a humanized mouse model. *J. Infect. ...* **193,** 996–1004 (2006).

94. Sacci, J., Alam, U. & Douglas, D. Plasmodium falciparum infection and exoerythrocytic development in mice with chimeric human livers. *Int. J. ...* (2006). at <http://www.sciencedirect.com/science/article/pii/S0020751905003760>

95. Bissig, K.-D. *et al.* Human liver chimeric mice provide a model for hepatitis B and C virus infection and treatment. *J. Clin. Invest.* **120,** 924–30 (2010).

96. Vaughan, A. & Mikolajczak, S. Complete Plasmodium falciparum liver-stage development in liver-chimeric mice. *J. Clin. ...* 1–11 (2012). doi:10.1172/JCI62684.ficult

97. De Jong, Y. P., Rice, C. M. & Ploss, A. New horizons for studying human hepatotropic infections. *J. Clin. Invest.* **120,** 650–3 (2010).

98. Rämer, P. C., Chijioke, O., Meixlsperger, S., Leung, C. S. & Münz, C. Mice with human immune system components as in vivo models for infections with human pathogens. *Immunol. Cell Biol.* **89,** 408–16 (2011).

99. Ishikawa, F. *et al.* Development of functional human blood and immune systems in NOD/SCID/IL2 receptor {gamma} chain(null) mice. *Blood* **106,** 1565–73 (2005).

100. Traggiai, E. *et al.* Development of a human adaptive immune system in cord blood cell-transplanted mice. *Science* **304,** 104–7 (2004).

101. Chen, Q., Khoury, M. & Chen, J. Expression of human cytokines dramatically improves reconstitution of specific human-blood lineage cells in humanized mice. *Proc. Natl. Acad. Sci. U. S. A.* **106,** 21783–8 (2009).

102. Rongvaux, A. *et al.* Development and function of human innate immune cells in a humanized mouse model. *Nat. Biotechnol.* **32,** 364–372 (2014).

103. Lee, E.-C. *et al.* Complete humanization of the mouse immunoglobulin loci enables efficient therapeutic antibody discovery. *Nat. Biotechnol.* **32,** 356–363 (2014).

104. Bhatia, S. N., Balis, U. J., Yarmush, M. L. & Toner, M. Effect of cell-cell interactions in preservation of cellular phenotype: cocultivation of hepatocytes and nonparenchymal cells. *FASEB J* **13,** 1883–1900 (1999).

105. Guillouzo, a. Liver cell models in in vitro toxicology. *Environ. Health Perspect.* **106 Suppl ,** 511–32 (1998).

106. Schwartz, R. E., Fleming, H. E., Khetani, S. R. & Bhatia, S. N. Pluripotent stem cell-derived hepatocyte-like cells. *Biotechnol. Adv.* **32,** 504–513 (2014).

107. Nahmias, Y., Schwartz, R. E., Hu, W.-S., Verfaillie, C. M. & Odde, D. J. Endothelium-mediated hepatocyte recruitment in the establishment of liver-like tissue in vitro. *Tissue Eng.* **12,** 1627–38 (2006).

108. Moghe, P. V *et al.* Culture matrix configuration and composition in the maintenance of hepatocyte polarity and function. *Biomaterials* **17,** 373–385 (1996).

109. Lin, P., Chan, W. C. W., Badylak, S. F. & Bhatia, S. N. Assessing porcine liver-derived biomatrix for hepatic tissue engineering. *Tissue Eng.* **10,** 1046–53 (2004).

110. Flaim, C., Chien, S. & Bhatia, S. An extracellular matrix microarray for probing cellular differentiation. *Nat. Methods* **2,** 119–125 (2005).

111. Dunn, J. C., Yarmush, M. L., Koebe, H. G. & Tompkins, R. G. Hepatocyte function and extracellular matrix geometry: long-term culture in a sandwich configuration. *Faseb J.* **3,** 174–177 (1989).

112. Berthiaume, F., Moghe, P. V, Toner, M. & Yarmush, M. L. Effect of extracellular matrix topology on cell structure, function, and physiological responsiveness: hepatocytes cultured in a sandwich configuration. *Faseb J.* **10,** 1471–1484 (1996).

113. Guguen-Guillouzo, C. *et al.* Maintenance and reversibility of active albumin secretion by adult rat hepatocytes co-cultured with another liver epithelial cell type. *Exp Cell Res* **143,** 47–54 (1983).

114. Bhatia, S. N., Balis, U. J., Yarmush, M. L. & Toner, M. Effect of cell-cell interactions in preservation of cellular phenotype: cocultivation of hepatocytes and nonparenchymal cells. *FASEB J.* **13,** 1883–900 (1999).

115. Hui, E. E. & Bhatia, S. N. Micromechanical control of cell-cell interactions. *Proc. Natl. Acad. Sci. U. S. A.* **104,** 5722–6 (2007).

116. March, S., Hui, E. E., Underhill, G. H., Khetani, S. & Bhatia, S. N. Microenvironmental regulation of the sinusoidal endothelial cell phenotype in vitro. *Hepatology* **50,** 920–928 (2009).

117. Bhatia, S. N., Yarmush, M. L. & Toner, M. Micropatterning cells in tissue engineering. *Methods Mol Med* **18,** 349–363 (1999).

118. Khetani, S. R. & Bhatia, S. N. Microscale culture of human liver cells for drug development. *Nat. Biotechnol.* **26,** 120–6 (2008).

119. Wang, W. W., Khetani, S. R., Krzyzewski, S., Duignan, D. B. & Obach, R. S. Assessment of a Micropatterned Hepatocyte Coculture System to Generate Major Human Excretory and Circulating Drug Metabolites. **38,** 1900–1905 (2010).

120. Khetani, S. R. *et al.* Micropatterned Co-cultures Increase the Ability to Detect Compounds that Cause Drug induced Liver Injury in Humans Over Sandwich Cultures. 1–29

121. Ploss, A. *et al.* Persistent hepatitis C virus infection in microscale primary human hepatocyte cultures. *Proc Natl Acad Sci U S A* **107**, 3141–3145 (2010).

122. Stevenson, M. M. & Riley, E. M. Innate immunity to malaria. *Nat. Rev. Immunol.* **4**, 169–80 (2004).

123. Ranucci, C. S., Kumar, a, Batra, S. P. & Moghe, P. V. Control of hepatocyte function on collagen foams: sizing matrix pores toward selective induction of 2-D and 3-D cellular morphogenesis. *Biomaterials* **21**, 783–93 (2000).

124. Semino, C. E., Merok, J. R., Crane, G. G., Panagiotakos, G. & Zhang, S. Functional differentiation of hepatocyte-like spheroid structures from putative liver progenitor cells in three-dimensional peptide scaffolds. *Differentiation.* **71**, 262–70 (2003).

125. Bruns, H. *et al.* Injectable liver: a novel approach using fibrin gel as a matrix for culture and intrahepatic transplantation of hepatocytes. *Tissue Eng.* **11**, 1718–26 (2005).

126. Gwak, S.-J. *et al.* Stable hepatocyte transplantation using fibrin matrix. *Biotechnol. Lett.* **26**, 505–8 (2004).

127. Kim, M., Lee, J. Y., Jones, C. N., Revzin, A. & Tae, G. Heparin-based hydrogel as a matrix for encapsulation and cultivation of primary hepatocytes. *Biomaterials* **31**, 3596–603 (2010).

128. Dvir-Ginzberg, M., Gamlieli-Bonshtein, I., Agbaria, R. & Cohen, S. Liver tissue engineering within alginate scaffolds: effects of cell-seeding density on hepatocyte viability, morphology, and function. *Tissue Eng.* **9**, (2003).

129. Seo, S.-J., Kim, I.-Y., Choi, Y.-J., Akaike, T. & Cho, C.-S. Enhanced liver functions of hepatocytes cocultured with NIH 3T3 in the alginate/galactosylated chitosan scaffold. *Biomaterials* **27**, 1487–95 (2006).

130. Fan, J., Shang, Y., Yuan, Y. & Yang, J. Preparation and characterization of chitosan/galactosylated hyaluronic acid scaffolds for primary hepatocytes culture. *J. Mater. Sci. Mater. Med.* **21**, 319–27 (2010).

131. Li, K. *et al.* Chitosan/gelatin composite microcarrier for hepatocyte culture. *Biotechnol. Lett.* **26**, 879–83 (2004).

132. Kasai, S. *et al.* Cellulose microcarrier for high-density culture of hepatocytes. *Transplant. Proc.* **24**, 2933–4 (1992).

133. Uygun, B. E. *et al.* Organ reengineering through development of a transplantable recellularized liver graft using decellularized liver matrix. *Nat. Med.* **16**, 814–820 (2010).

134. Underhill, G. H., Chen, A. a, Albrecht, D. R. & Bhatia, S. N. Assessment of hepatocellular function within PEG hydrogels. *Biomaterials* **28,** 256–70 (2007).

135. Liu Tsang, V. *et al.* Fabrication of 3D hepatic tissues by additive photopatterning of cellular hydrogels. *FASEB J.* **21,** 790–801 (2007).

136. Mooney, D. J. *et al.* Long-term engraftment of hepatocytes transplanted on biodegradable polymer sponges. *J. Biomed. Mater. Res.* **37,** 413–20 (1997).

137. Hasirci, V. *et al.* Expression of liver-specific functions by rat hepatocytes seeded in treated poly(lactic-co-glycolic) acid biodegradable foams. *Tissue Eng.* **7,** 385–94 (2001).

138. Oncostatin, M. & Sulfoxide, D. Efficacy of Engineered Liver Tissue Based on Poly- L -lactic Acid Scaffolds and Fetal Mouse Liver Cells Cultured with. **10,** (2004).

139. Du, Y. *et al.* Synthetic sandwich culture of 3D hepatocyte monolayer. *Biomaterials* **29,** 290–301 (2008).

140. Janorkar, A. V. Polymeric Scaffold Materials for Two-Dimensional and Three-Dimensional in Vitro Culture of Hepatocytes. 1–32 (2010).

141. Yoon Sung Nam, Joon Jin Yoon, Jae Gwan Lee & Tae Gwan Park. Adhesion behaviours of hepatocytes cultured onto biodegradable polymer surface modified by alkali hydrolysis process. *J. Biomater. Sci. Polym. Ed.* **10,** 1145–1158 (1999).

142. Carlisle, E. S. *et al.* Enhancing hepatocyte adhesion by pulsed plasma deposition and polyethylene glycol coupling. *Tissue Eng.* **6,** 45–52 (2000).

143. Seliktar, D., Zisch, A. H., Lutolf, M. P., Wrana, J. L. & Hubbell, J. A. MMP-2 sensitive, VEGF-bearing bioactive hydrogels for promotion of vascular healing. *J. Biomed. Mater. Res. A* **68,** 704–16 (2004).

144. Gutsche, A. T., Lo, H., Zurlo, J., Yager, J. & Leong, K. W. Engineering of a sugar-derivatized porous network for hepatocyte culture. *Biomaterials* **17,** 387–393 (1996).

145. Li, J., Pan, J., Zhang, L. & Yu, Y. Culture of hepatocytes on fructose-modified chitosan scaffolds. *Biomaterials* **24,** 2317–2322 (2003).

146. Nugraha, B. *et al.* Galactosylated cellulosic sponge for multi-well drug safety testing. *Biomaterials* **32,** 6982–94 (2011).

147. Chua, K.-N. *et al.* A dual-functional fibrous scaffold enhances P450 activity of cultured primary rat hepatocytes. *Acta Biomater.* **3,** 643–50 (2007).

148. Dvir-ginzberg, M., Elkayam, T., Aflalo, E. D., Agbaria, R. & Cohen, S. Ultrastructural and Functional Investigations of Adult Hepatocyte Spheroids during. **10,** 1806–1817 (2004).

149. Stevens, K. R. *et al.* InVERT molding for scalable control of tissue microarchitecture. *Nat. Commun.* **4,** 1847 (2013).

150. Ananthanarayanan, A., Narmada, B. C., Mo, X., McMillian, M. & Yu, H. Purpose-driven biomaterials research in liver-tissue engineering. *Trends Biotechnol.* **29,** 110–118 (2011).

151. Mooney, D. J. *et al.* Biodegradable sponges for hepatocyte transplantation. *J. Biomed. Mater. Res.* **29,** 959–65 (1995).

152. Chen, A. A. *et al.* Humanized mice with ectopic artificial liver tissues. *Proc. Natl. Acad. Sci. U. S. A.* **108,** 11842–7 (2011).

153. HILL, R. S. *et al.* Immunoisolation of Adult Porcine Islets for the Treatment of Diabetes Mellitus. *Ann. N. Y. Acad. Sci.* **831,** 332–343 (2006).

154. Vaccines, T. malERA C. G. on. A Research Agenda for Malaria Eradication: Vaccines. *PLoS Med.* **8,** e1000398 (2011).

155. Alonso Djimde, A., Kremsner, P., Magill, A., Milman, J., Najera, J., Plowe, C.V., Rabinovich, R., Wells, T., and Yeung, S., P. L. A research agenda for malaria eradication: drugs. *PLoS Med* **8,** e1000402

156. Wells, T. N., Burrows, J. N. & Baird, J. K. Targeting the hypnozoite reservoir of Plasmodium vivax: the hidden obstacle to malaria elimination. *Trends Parasitol* **26,** 145–151 (2010).

157. Epstein, J. E. *et al.* Live Attenuated Malaria Vaccine Designed to Protect through Hepatic CD8+ T Cell Immunity. *Science (80-.).* (2011). doi:science.1211548 [pii] 10.1126/science.1211548

158. Plowe, C. V, Alonso, P. & Hoffman, S. L. The potential role of vaccines in the elimination of falciparum malaria and the eventual eradication of malaria. *J Infect Dis* **200,** 1646–1649 (2009).

159. Hoffman, S. L. *et al.* Sporozoite vaccine induces genetically restricted T cell elimination of malaria from hepatocytes. *Science (80-.).* **244,** 1078–1081 (1989).

160. Rodrigues, C. D. *et al.* Host scavenger receptor SR-BI plays a dual role in the establishment of malaria parasite liver infection. *Cell Host Microbe* **4,** 271–82 (2008).

161. Silvie, O., Franetich, J. F., Boucheix, C., Rubinstein, E. & Mazier, D. Alternative invasion pathways for Plasmodium berghei sporozoites. *Int J Parasitol* **37,** 173–182 (2007).

162. McCutchan, T. F. *et al.* Sequence of the immunodominant epitope for the surface protein on sporozoites of Plasmodium vivax. *Science (80-.).* **230,** 1381–1383 (1985).

163. Chattopadhyay, R. *et al.* Establishment of an in vitro assay for assessing the effects of drugs on the liver stages of Plasmodium vivax malaria. *PLoS One* **5,** e14275 (2010).

164. Sattabongkot, J. *et al.* Establishment of a human hepatocyte line that supports in vitro development of the exo-erythrocytic stages of the malaria parasites Plasmodium falciparum and P. vivax. *Am. J. Trop. Med. Hyg.* **74,** 708–715 (2006).

165. Yokoo, H. *et al.* Proteomic signature corresponding to alpha fetoprotein expression in liver cancer cells. *Hepatology* **40,** 609–17 (2004).

166. Van Schaijk, B. C. *et al.* Gene disruption of Plasmodium falciparum p52 results in attenuation of malaria liver stage development in cultured primary human hepatocytes. *PLoS One* **3,** e3549 (2008).

167. Yalaoui, S. *et al.* Scavenger receptor BI boosts hepatocyte permissiveness to Plasmodium infection. *Cell Host Microbe* **4,** 283–92 (2008).

168. Sivaraman, A. *et al.* A microscale in vitro physiological model of the liver: predictive screens for drug metabolism and enzyme induction. *Curr Drug Metab* **6,** 569–591 (2005).

169. Kidambi, S. *et al.* Oxygen-mediated enhancement of primary hepatocyte metabolism, functional polarization, gene expression, and drug clearance. *Proc Natl Acad Sci U S A* **106,** 15714–15719 (2009).

170. Jones, C. T. *et al.* Real-time imaging of hepatitis C virus infection using a fluorescent cell-based reporter system. *Nat Biotechnol* **28,** 167–171 (2010).

171. WOLFLE, D., SCHMIDT, H. & JUNGERMANN, K. Short-term modulation of glycogen metabolism, glycolysis and gluconeogenesis by physiological oxygen concentrations in hepatocyte cultures. *Eur. J. Biochem.* **135,** 405–412 (1983).

172. Jungermann, K. & Kietzmann, T. Zonation of parenchymal and nonparenchymal metabolism in liver. *Annu. Rev. Nutr.* **16,** 179–203 (1996).

173. Jungermann, K. & Kietzmann, T. Oxygen: modulator of metabolic zonation and disease of the liver. *Hepatology* **31,** 255–60 (2000).

174. Allen, J. W., Khetani, S. R. & Bhatia, S. N. In vitro zonation and toxicity in a hepatocyte bioreactor. *Toxicol. Sci.* **84,** 110–9 (2005).

175. Allen, J. W. & Bhatia, S. N. Formation of steady-state oxygen gradients in vitro: application to liver zonation. *Biotechnol. Bioeng.* **82,** 253–62 (2003).

176. Kietzmann, T. & Jungermann, K. Modulation by oxygen of zonal gene expression in liver studied in primary rat hepatocyte cultures. *Cell Biol. Toxicol.* **13,** 243–55 (1997).

177. Semenza, G. L. Oxygen sensing, homeostasis, and disease. *N. Engl. J. Med.* **365,** 537–47 (2011).

178. Park, M. K., Myers, R. A. M. & Marzella, L. Oxygen Tensions and Infections: Modulation of Microbial Growth, Activity of Antimicrobial Agents, and Immunologic Responses. *Clin. Infect. Dis.* **14,** 720–740 (1992).

179. Tsuneyoshi, I., Boyle, W. A., Kanmura, Y. & Fujimoto, T. Hyperbaric hyperoxia suppresses growth of Staphylococcus aureus, including methicillin-resistant strains. *J. Anesth.* **15,** 29–32 (2001).

180. Arrais-Silva, W. W., Pinto, E. F., Rossi-Bergmann, B. & Giorgio, S. Hyperbaric oxygen therapy reduces the size of Leishmania amazonensis-induced soft tissue lesions in mice. *Acta Trop.* **98,** 130–6 (2006).

181. Vassilaki, N. *et al.* Low oxygen tension enhances hepatitis C virus replication. *J. Virol.* **87,** 2935–48 (2013).

182. Hughes, F. & Tatum, A. Effects of hypoxia and intercurrent infections on infections by Plasmodium berghei in rats. *J. Infect. Dis.* **99,** 38–43 (1956).

183. Hughes, F. & Tatum, A. The effects of hypoxia on infections with Plasmodium cathemerium. *J. Infect. Dis.* **97,** 231–237 (1955).

184. Rencricca, N. J. *et al.* Quantification of hyperbaric oxygen-induced toxicity utilizing a malarial system. *Aviat. Space. Environ. Med.* **52,** 85–7 (1981).

185. Blanco, Y. C. *et al.* Hyperbaric oxygen prevents early death caused by experimental cerebral malaria. *PLoS One* **3,** e3126 (2008).

186. Trager, W. & Jensen, J. Human malaria parasites in continuous culture. *Science (80-.).* 673–675 (1976). at <http://www.sciencemag.org/content/193/4254/673.short>

187. Torrentino-Madamet, M. *et al.* Global response of Plasmodium falciparum to hyperoxia: a combined transcriptomic and proteomic approach. *Malar. J.* **10,** 4 (2011).

188. Lang, K. S. *et al.* Immunoprivileged status of the liver is controlled by Toll-like receptor 3 signaling. *J. Clin. Invest.* **116,** 2456–63 (2006).

189. Tiegs, G. & Lohse, A. W. Immune tolerance: what is unique about the liver. *J. Autoimmun.* **34,** 1–6 (2010).

190. Protzer, U., Maini, M. K. & Knolle, P. A. Living in the liver: hepatic infections. *Nat. Rev. Immunol.* **12,** 201–13 (2012).

191. Liehl, P. *et al.* Host-cell sensors for Plasmodium activate innate immunity against liver-stage infection. *Nat. Med.* **20,** 47–53 (2014).

192. Silvie, O. *et al.* Hepatocyte CD81 is required for Plasmodium falciparum and Plasmodium yoelii sporozoite infectivity. *Nat Med* **9,** 93–96 (2003).

193. Renia, L. *et al.* Malaria sporozoite penetration. A new approach by double staining. *J Immunol Methods* **112,** 201–205 (1988).

194. Shortt, H. E. & Garnham, P. C. The pre-erythrocytic development of Plasmodium cynomolgi and Plasmodium vivax. *Trans R Soc Trop Med Hyg* **41,** 785–795 (1948).

195. Mueller, A. K., Labaied, M., Kappe, S. H. & Matuschewski, K. Genetically modified Plasmodium parasites as a protective experimental malaria vaccine. *Nature* **433,** 164–167 (2005).

196. Ploss, A. *et al.* Persistent hepatitis C virus infection in microscale primary human hepatocyte cultures. *Proc. Natl. Acad. Sci. U. S. A.* **107,** 3141–5 (2010).

197. Pybus, B. S. *et al.* CYP450 phenotyping and accurate mass identification of metabolites of the 8-aminoquinoline, anti-malarial drug primaquine. *Malar. J.* **11,** 259 (2012).

198. Cogswell, F. B. The hypnozoite and relapse in primate malaria. *Clin. Microbiol. Rev.* **5,** 26–35 (1992).

199. Dao, N. V. H. *et al.* Vivax malaria: preliminary observations following a shorter course of treatment with artesunate plus primaquine. *Trans. R. Soc. Trop. Med. Hyg.* **101,** 534–9 (2007).

200. Durante Mangoni, E. *et al.* Case report: An unusual late relapse of Plasmodium vivax malaria. *Am. J. Trop. Med. Hyg.* **68,** 159–60 (2003).

201. Garnham, P. C. *et al.* A strain of Plasmodium vivax characterized by prolonged incubation: morphological and biological characteristics. *Bull. World Health Organ.* **52,** 21–32 (1975).

202. Hollingdale, M. R., Collins, W. E. & Campbell, C. C. In vitro culture of exoerythrocytic parasites of the North Korean strain of Plasmodium vivax in hepatoma cells. *Am. J. Trop. Med. Hyg.* **35,** 275–6 (1986).

203. Krotoski, W. & Garnham, P. and late post-sporozoite tissue stages in primate malaria. IV. Pre-erythrocytic schizonts and/or hypnozoites of Chesson and North Korean strains of Plasmodium vivax. *Am. J. …* (1986). at <http://europepmc.org/abstract/MED/3513645>

204. Douradinha, B. *et al.* Genetically attenuated P36p-deficient Plasmodium berghei sporozoites confer long-lasting and partial cross-species protection. *Int J Parasitol* **37,** 1511–1519 (2007).

205. Graewe, S. *et al.* Hostile takeover by Plasmodium: reorganization of parasite and host cell membranes during liver stage egress. *PLoS Pathog.* **7,** e1002224 (2011).

206. Yarmush, M. L. *et al.* Hepatic tissue engineering. Development of critical technologies. *Ann. N. Y. Acad. Sci.* **665,** 238–52 (1992).

207. Varghese, A. J., Gulyas, S. & Mohindra, J. K. Hypoxia-dependent reduction of 1-(2-nitro-1-imidazolyl)-3-methoxy-2-propanol by Chinese hamster ovary cells and KHT tumor cells in vitro and in vivo. *Cancer Res* **36,** 3761–3765 (1976).

208.   Siau, A. *et al.* Temperature shift and host cell contact up-regulate sporozoite expression of Plasmodium falciparum genes involved in hepatocyte infection. *PLoS Pathog.* **4,** e1000121 (2008).

209.   Bhatia SN Foy BD, Rotem A, O'Neil KM, Tompkins RG, and Yarmush ML, T. M. Zonal Liver Cell Heterogeneity: Effects of Oxygen on Metabolic Functions of Hepatocytes. *J. Cell. Eng.* **1,** 125–135 (1996).

210.   Semenza, G. L. Hypoxia-inducible factors in physiology and medicine. *Cell* **148,** 399–408 (2012).

211.   Jaakkola, P. *et al.* Targeting of HIF-alpha to the von Hippel-Lindau ubiquitylation complex by O2-regulated prolyl hydroxylation. *Science* **292,** 468–72 (2001).

212.   Elvidge, G. P. *et al.* Concordant regulation of gene expression by hypoxia and 2-oxoglutarate-dependent dioxygenase inhibition: the role of HIF-1alpha, HIF-2alpha, and other pathways. *J. Biol. Chem.* **281,** 15215–15226 (2006).

213.   Meis, J. F. *et al.* Infection of cryopreserved adult human hepatocytes with Plasmodium falciparum sporozoites. *Cell Biol. Int. Rep.* **9,** 976 (1985).

214.   Silvie, O., Franetich, J. F., Renia, L. & Mazier, D. Malaria sporozoite: migrating for a living. *Trends Mol Med* **10,** 91–97 (2004).

215.   Hoffman, S. L. *et al.* Development of a metabolically active, non-replicating sporozoite vaccine to prevent Plasmodium falciparum malaria. *Hum. Vaccin.* **6,** 97–106 (2010).

216.   Alonso Ballou, R., Brown, G., Chitnis, C., Loucq, C., Moorthy, V., Saul, A., and Wirth, D., P. L. A research agenda for malaria eradication: vaccines. *PLoS Med* **8,** e1000398

217.   Annoura, T. *et al.* Assessing the adequacy of attenuation of genetically modified malaria parasite vaccine candidates. *Vaccine* **30,** 2662–70 (2012).

218.   Albuquerque, S. S. *et al.* Host cell transcriptional profiling during malaria liver stage infection reveals a coordinated and sequential set of biological events. *BMC Genomics* **10,** 270 (2009).

219.   Epiphanio, S. *et al.* Heme oxygenase-1 is an anti-inflammatory host factor that promotes murine plasmodium liver infection. *Cell Host Microbe* **3,** 331–8 (2008).

220.   Prudêncio, M. *et al.* Kinome-wide RNAi screen implicates at least 5 host hepatocyte kinases in Plasmodium sporozoite infection. *PLoS Pathog.* **4,** e1000201 (2008).

221.   Silvie, O. *et al.* Hepatocyte CD81 is required for Plasmodium falciparum and Plasmodium yoelii sporozoite infectivity. *Nat. Med.* **9,** 93–6 (2003).

222.   Gamo, F.-J. *et al.* Thousands of chemical starting points for antimalarial lead identification. *Nature* **465,** 305–10 (2010).

223.   Guiguemde, W. A. *et al.* Chemical genetics of Plasmodium falciparum. *Nature* **465,** 311–5 (2010).

224. Mazier, D. *et al.* Cultivation of the liver forms of Plasmodium vivax in human hepatocytes. *Nature* **307,** 367–369 (1984).

225. Conteh, S., Chattopadhyay, R., Anderson, C. & Hoffman, S. L. Plasmodium yoelii-infected A. stephensi inefficiently transmit malaria compared to intravenous route. *PLoS One* **5,** e8947 (2010).

226. Jiang, G. *et al.* Sterile protection against Plasmodium knowlesi in rhesus monkeys from a malaria vaccine: comparison of heterologous prime boost strategies. *PLoS One* **4,** e6559 (2009).

227. March, S. *et al.* A microscale human liver platform that supports the hepatic stages of Plasmodium falciparum and vivax. *Cell Host Microbe* **14,** 104–15 (2013).

228. McCuskey, R. S., Vonnahme, F. J. & Grun, M. In vivo and electron microscopic observations of the hepatic microvasculature in the rat following portacaval anastomosis. *Hepatology* **3,** 96–104 (1983).

229. Santilli, S. M., Tretinyak, A. S. & Lee, E. S. Transarterial wall oxygen gradients at the deployment site of an intra-arterial stent in the rabbit. *Am. J. Physiol. Circ. Physiol.* **279,** H1518–H1525 (2000).

230. Arteel, G. E., Thurman, R. G., Yates, J. M. & Raleigh, J. A. Evidence That Hypoxia Markers Detect Oxygen Gradients in Liver - Pimonidazole and Retrograde Perfusion of Rat-Liver. *Br. J. Cancer* **72,** 889–895 (1995).

231. Rotem, a, Toner, M., Tompkins, R. G. & Yarmush, M. L. Oxygen uptake rates in cultured rat hepatocytes. *Biotechnol. Bioeng.* **40,** 1286–91 (1992).

232. Rotem, A. *et al.* Oxygen is a factor determining in vitro tissue assembly: Effects on attachment and spreading of hepatocytes. *Biotechnol. Bioeng.* **43,** 654–660 (1994).

233. Trager, W. & Jensen, J. B. Human malaria parasites in continuous culture. *Science* **193,** 673–5 (1976).

234. Briolant, S. *et al.* Influence of oxygen on asexual blood cycle and susceptibility of Plasmodium falciparum to chloroquine: requirement of a standardized in vitro assay. *Malar. J.* **6,** 44 (2007).

235. Scheibel, L. W., Ashton, S. H. & Trager, W. Plasmodium falciparum: microaerophilic requirements in human red blood cells. *Exp Parasitol* **47,** 410–418 (1979).

236. Tsai, A. G., Johnson, P. C. & Intaglietta, M. Oxygen gradients in the microcirculation. *Physiol. Rev.* **83,** 933–63 (2003).

237. Weidemann, a & Johnson, R. S. Biology of HIF-1alpha. *Cell Death Differ.* **15,** 621–7 (2008).

238. Spear, W. *et al.* The host cell transcription factor hypoxia-inducible factor 1 is required for Toxoplasma gondii growth and survival at physiological oxygen levels. *Cell. Microbiol.* **8,** 339–52 (2006).

147

239. Degrossoli, A., Bosetto, M. C., Lima, C. B. & Giorgio, S. Expression of hypoxia-inducible factor 1alpha in mononuclear phagocytes infected with Leishmania amazonensis. *Immunol Lett* **114**, 119–125 (2007).

240. Liang, J. *et al.* The energy sensing LKB1-AMPK pathway regulates p27(kip1) phosphorylation mediating the decision to enter autophagy or apoptosis. *Nat. Cell Biol.* **9**, 218–224 (2007).

241. Kim, J., Kundu, M., Viollet, B. & Guan, K. L. AMPK and mTOR regulate autophagy through direct phosphorylation of Ulk1. *Nat. Cell Biol.* **13**, 132–U71 (2011).

242. Eickel, N. *et al.* Features of autophagic cell death in Plasmodium liver-stage parasites. *Autophagy* **9**, 568–580 (2013).

243. Mihaylova, M. M. & Shaw, R. J. The AMPK signalling pathway coordinates cell growth, autophagy and metabolism. *Nat. Cell Biol.* **13**, 1016–23 (2011).

244. Sinai, A. P. & Joiner, K. A. The Toxoplasma gondii protein ROP2 mediates host organelle association with the parasitophorous vacuole membrane. *J Cell Biol* **154**, 95–108 (2001).

245. Müller, S. Redox and antioxidant systems of the malaria parasite Plasmodium falciparum. *Mol. Microbiol.* **53**, 1291–305 (2004).

246. Vonlaufen, N., Kanzok, S. M., Wek, R. C. & Sullivan, W. J. Stress response pathways in protozoan parasites. *Cell. Microbiol.* **10**, 2387–99 (2008).

247. Rénia, L., Miltgen, F. & Charoenvit, Y. Malaria sporozoite penetration A new approach by double staining. *J. …* **112**, 201–205 (1988).

248. Nardin, E. H. *et al.* Circumsporozoite proteins of human malaria parasites Plasmodium falciparum and Plasmodium vivax. *J. Exp. Med.* **156**, 20–30 (1982).

249. Carpenter, A. E. *et al.* CellProfiler: image analysis software for identifying and quantifying cell phenotypes. *Genome Biol.* **7**, R100 (2006).

250. Subramanian, A. *et al.* Gene set enrichment analysis: a knowledge-based approach for interpreting genome-wide expression profiles. *Proc Natl Acad Sci U S A* **102**, 15545–15550 (2005).

251. Thomson, J. a. Embryonic Stem Cell Lines Derived from Human Blastocysts. *Science (80-.).* **282**, 1145–1147 (1998).

252. Takahashi, K. *et al.* Induction of pluripotent stem cells from adult human fibroblasts by defined factors. *Cell* **131**, 861–72 (2007).

253. Schwartz, R. & Trehan, K. Modeling hepatitis C virus infection using human induced pluripotent stem cells. *Proc. …* (2012). doi:10.1073/pnas.1121400109/-/DCSupplemental.www.pnas.org/cgi/doi/10.1073/pnas.1121400109

254. Si-Tayeb, K. *et al.* Highly efficient generation of human hepatocyte-like cells from induced pluripotent stem cells. *Hepatology* **51,** 297–305 (2010).

255. Shan, J. *et al.* Identification of small molecules for human hepatocyte expansion and iPS differentiation. *Nat. Chem. Biol.* **9,** 514–20 (2013).

256. Meister, S. *et al.* Imaging of Plasmodium liver stages to drive next-generation antimalarial drug discovery. *Science* **334,** 1372–7 (2011).

257. Pybus, B. S. *et al.* The metabolism of primaquine to its active metabolite is dependent on CYP 2D6. *Malar. J.* **12,** 212 (2013).

258. Jin, X. *et al.* An LC-MS based study of the metabolic profile of primaquine, an 8-aminoquinoline antiparasitic drug, with an in vitro primary human hepatocyte culture model. *Eur. J. Drug Metab. Pharmacokinet.* (2013). doi:10.1007/s13318-013-0139-8

259. Gego, A., Silvie, O. & Franetich, J. New approach for high-throughput screening of drug activity on Plasmodium liver stages. *Antimicrob. agents …* **50,** 1586–1589 (2006).

260. Miller, J. L. *et al.* Quantitative bioluminescent imaging of pre-erythrocytic malaria parasite infection using luciferase-expressing Plasmodium yoelii. *PLoS One* **8,** e60820 (2013).

261. Mwakingwe, A. *et al.* Noninvasive real-time monitoring of liver-stage development of bioluminescent Plasmodium parasites. *J. Infect. Dis.* **200,** 1470–8 (2009).

262. Dembele, L. *et al.* Towards an in vitro model of Plasmodium hypnozoites suitable for drug discovery. *PLoS One* **6,** e18162 (2011).

263. Engle, S. J. & Puppala, D. Integrating human pluripotent stem cells into drug development. *Cell Stem Cell* **12,** 669–77 (2013).

264. McDonnell, M. E. & Braverman, L. E. Drug-related hepatotoxicity. *N. Engl. J. Med.* **354,** 2191–3; author reply 2191–3 (2006).

265. Bennett, J. W. *et al.* Primaquine Failure and Cytochrome P-450 2D6 in Plasmodium vivax Malaria. *N. Engl. J. Med.* **369,** 1381–2 (2013).

266. Cui, L., Escalante, A. a., Imwong, M. & Snounou, G. The genetic diversity of Plasmodium vivax populations. *Trends Parasitol.* **19,** 220–226 (2003).

267. Imwong, M. *et al.* Contrasting genetic structure in Plasmodium vivax populations from Asia and South America. *Int. J. Parasitol.* **37,** 1013–22 (2007).

268. Gunawardena, S. *et al.* Geographic structure of Plasmodium vivax: microsatellite analysis of parasite populations from Sri Lanka, Myanmar, and Ethiopia. *Am. J. Trop. Med. Hyg.* **82,** 235–42 (2010).

269. Li, J. *et al.* Geographic subdivision of the range of the malaria parasite Plasmodium vivax. *Emerg. Infect. Dis.* **7,** 35–42 (2001).

270. Song, Z. *et al.* Efficient generation of hepatocyte-like cells from human induced pluripotent stem cells. *Cell Res.* **19,** 1233–42 (2009).

271. Wells, T. N. C., Alonso, P. L. & Gutteridge, W. E. New medicines to improve control and contribute to the eradication of malaria. *Nat. Rev. Drug Discov.* **8,** 879–91 (2009).

272. Khoo, S., Back, D. & Winstanley, P. The potential for interactions between antimalarial and antiretroviral drugs. *AIDS* **19,** 995–1005 (2005).

273. Dembélé, L. *et al.* Persistence and activation of malaria hypnozoites in long-term primary hepatocyte cultures. *Nat. Med.* **20,** (2014).

274. Angulo-Barturen, I. & Ferrer, S. Humanised models of infection in the evaluation of anti-malarial drugs. *Drug Discov. Today Technol.* (2013). at <http://www.sciencedirect.com/science/article/pii/S1740674912000431>

275. Chen, A. a *et al.* Humanized mice with ectopic artificial liver tissues. *Proc. Natl. Acad. Sci. U. S. A.* **108,** 11842–7 (2011).

276. Cruise, G. M., Scharp, D. S. & Hubbell, J. a. Characterization of permeability and network structure of interfacially photopolymerized poly(ethylene glycol) diacrylate hydrogels. *Biomaterials* **19,** 1287–94 (1998).

277. Wakita, T. *et al.* Production of infectious hepatitis C virus in tissue culture from a cloned viral genome. *Nat. Med.* **11,** 791–6 (2005).

278. Cho, N.-J. *et al.* Viral infection of human progenitor and liver-derived cells encapsulated in three-dimensional PEG-based hydrogel. *Biomed. Mater.* **4,** 011001 (2009).

279. Hwang, Y., Zhang, C. & Varghese, S. Poly(ethylene glycol) cryogels as potential cell scaffolds: effect of polymerization conditions on cryogel microstructure and properties. *J. Mater. Chem.* **20,** 345 (2010).

280. Landry, J., Bernier, D., Ouellet, C., Goyette, R. & Marceau, N. Spheroidal aggregate culture of rat liver cells: histotypic reorganization, biomatrix deposition, and maintenance of functional activities. *J. Cell Biol.* **101,** 914–23 (1985).

281. Inamori, M., Mizumoto, H. & Kajiwara, T. An approach for formation of vascularized liver tissue by endothelial cell-covered hepatocyte spheroid integration. *Tissue Eng. Part A* **15,** 2029–37 (2009).

282. Abu-Absi, S. F., Friend, J. R., Hansen, L. K. & Hu, W.-S. Structural polarity and functional bile canaliculi in rat hepatocyte spheroids. *Exp. Cell Res.* **274,** 56–67 (2002).

283. Tzanakakis, E. S., Waxman, D. J., Hansen, L. K., Remmel, R. P. & Hu, W. S. Long-term enhancement of cytochrome P450 2B1/2 expression in rat hepatocyte spheroids through adenovirus-mediated gene transfer. *Cell Biol. Toxicol.* **18,** 13–27 (2002).

284. Wang, S., Nagrath, D., Chen, P. C., Berthiaume, F. & Yarmush, M. L. Three-dimensional primary hepatocyte culture in synthetic self-assembling peptide hydrogel. *Tissue Eng. Part A* **14,** 227–36 (2008).

285. Ploemen, I. H. J. *et al.* Visualisation and quantitative analysis of the rodent malaria liver stage by real time imaging. *PLoS One* **4,** e7881 (2009).

286. Langhorne, J. *et al.* The relevance of non-human primate and rodent malaria models for humans. *Malar. J.* **10,** 23 (2011).

287. Carlton, J. M. & Carucci, D. J. Rodent models of malaria in the genomics era. *Trends Parasitol* **18,** 100–102 (2002).

288. Pinzon-Ortiz, C., Friedman, J., Esko, J. & Sinnis, P. The binding of the circumsporozoite protein to cell surface heparan sulfate proteoglycans is required for plasmodium sporozoite attachment to target cells. *J. Biol. Chem.* **276,** 26784–91 (2001).

289. Coppi, A. *et al.* Heparan sulfate proteoglycans provide a signal to Plasmodium sporozoites to stop migrating and productively invade host cells. *Cell Host Microbe* **2,** 316–27 (2007).

290. Ishino, T., Yano, K., Chinzei, Y. & Yuda, M. Cell-Passage Activity Is Required for the Malarial Parasite to Cross the Liver Sinusoidal Cell Layer. **2,** 77–84 (2004).

291. Ishino, T., Chinzei, Y. & Yuda, M. A Plasmodium sporozoite protein with a membrane attack complex domain is required for breaching the liver sinusoidal cell layer prior to hepatocyte infection. *Cell. Microbiol.* **7,** 199–208 (2005).

292. Carrolo, M. *et al.* Hepatocyte growth factor and its receptor are required for malaria infection. *Nat. Med.* **9,** 1363–9 (2003).

293. Kumar, K. A. *et al.* Exposure of Plasmodium sporozoites to the intracellular concentration of potassium enhances infectivity and reduces cell passage activity. *Mol. Biochem. Parasitol.* **156,** 32–40 (2007).

294. Mazier, D., Renia, L. & Snounou, G. A pre-emptive strike against malaria's stealthy hepatic forms. *Nat Rev Drug Discov* **8,** 854–864 (2009).

295. Ng, S. *et al.* Hypoxia promotes liver-stage malaria infection in primary human hepatocytes in vitro. *Dis. Model. Mech.* **7,** 215–24 (2014).

296. Levenberg, S. *et al.* Engineering vascularized skeletal muscle tissue. *Nat. Biotechnol.* **23,** 879–84 (2005).

297. Baranski, J. D., Chaturvedi, R. R., Stevens, K. R., Eyckmans, J. & Carvalho, B. Geometric control of vascular networks to enhance engineered tissue integration and function. (2013). doi:10.1073/pnas.1217796110/-/DCSupplemental.www.pnas.org/cgi/doi/10.1073/pnas.1217796110

298. Kaihara, S. *et al.* Silicon micromachining to tissue engineer branched vascular channels for liver fabrication. *Tissue Eng.* **6**, 105–17 (2000).

299. GRIFFITH, L. G. *et al.* In Vitro Organogenesis of Liver Tissuea. *Ann. N. Y. Acad. Sci.* **831**, 382–397 (2006).

300. Smith, M. K., Peters, M. C., Richardson, T. P., Garbern, J. C. & Mooney, D. J. Locally enhanced angiogenesis promotes transplanted cell survival. *Tissue Eng.* **10**, 63–71 (2004).

301. Richardson, T. P., Peters, M. C., Ennett, A. B. & Mooney, D. J. Polymeric system for dual growth factor delivery. *Nat. Biotechnol.* **19**, 1029–34 (2001).

302. Lee, H. *et al.* Local delivery of basic fibroblast growth factor increases both angiogenesis and engraftment of hepatocytes in tissue-engineered polymer devices. *Transplantation* **73**, 1589–93 (2002).

303. Baptista, P. M. *et al.* The use of whole organ decellularization for the generation of a vascularized liver organoid. *Hepatology* **53**, 604–17 (2011).

304. B., G. Malaria forum keynote address. http://www.gatesfoundation.org/media–center/speech (2007). at <http://www.gatesfoundation.org/media-center/speeches/2007/10/bill-gates-malaria-forum>

305. Liu, J., Modrek, S., Gosling, R. D. & Feachem, R. G. Malaria eradication: is it possible? Is it worth it? Should we do it? *Lancet Glob. Heal.* **1**, e2–e3 (2013).

306. Alonso, P. L. *et al.* A research agenda to underpin malaria eradication. *PLoS Med.* **8**, e1000406 (2011).

307. Kaneko, A. *et al.* Malaria eradication on islands. *Lancet* **356**, 1560–4 (2000).

308. malERA, C. G. on B. S. and E. T. A research agenda for malaria eradication: basic science and enabling technologies. *PLoS Med* **8**, e1000399 (2011).

309. Spangenberg, T. *et al.* The open access malaria box: a drug discovery catalyst for neglected diseases. *PLoS One* **8**, e62906 (2013).

310. Shanks, G. D. & White, N. J. The activation of vivax malaria hypnozoites by infectious diseases. *Lancet Infect. Dis.* **13**, 900–6 (2013).

311. Hulden, L. & Hulden, L. Activation of the hypnozoite: a part of Plasmodium vivax life cycle and survival. *Malar. J.* **10**, 90 (2011).

312. Seder, R. a *et al.* Protection against malaria by intravenous immunization with a nonreplicating sporozoite vaccine. *Science* **341,** 1359–65 (2013).

313. Mahdi Abdel Hamid, M. *et al.* Vaccination with Plasmodium knowlesi AMA1 formulated in the novel adjuvant co-vaccine HT protects against blood-stage challenge in rhesus macaques. *PLoS One* **6,** e20547 (2011).

314. Foquet, L. *et al.* Vaccine-induced monoclonal antibodies targeting circumsporozoite protein prevent Plasmodium falciparum infection. *J. Clin. Invest.* **124,** 140–4 (2014).

315. Olsavsky, K. M. *et al.* Gene expression profiling and differentiation assessment in primary human hepatocyte cultures, established hepatoma cell lines, and human liver tissues. *Toxicol. Appl. Pharmacol.* **222,** 42–56 (2007).

316. Semenza, G. L. Hypoxia-Inducible Factors in Physiology and Medicine. *Cell* **148,** 399–408 (2012).

317. Aragonés, J., Fraisl, P., Baes, M. & Carmeliet, P. Oxygen sensors at the crossroad of metabolism. *Cell Metab.* **9,** 11–22 (2009).

318. Rzymski, T. *et al.* Regulation of autophagy by ATF4 in response to severe hypoxia. *Oncogene* **29,** 4424–35 (2010).

319. Kroemer, G., Mariño, G. & Levine, B. Autophagy and the integrated stress response. *Mol. Cell* **40,** 280–93 (2010).

Appendix

Experimental contributions for each chapter:

Chapter 2: Engineering a Microscale Human Liver Platform for Modeling Liver-Stage Malaria In vitro

This chapter was divided into two projects: the establishment of the micropatterned coculture platform as a model for liver-stage malaria and the demonstration of its applications, and the optimization of the hepatocyte microenvironment for liver-stage malaria infectibility in terms of oxygen tension and innate immunity.

For the first project, Shengyong Ng worked in a team led by Sandra March, and helped to design and perform all experiments (Figures 2.1 – 2.10) and analyze the data.

For the second project, Shengyong Ng led a team to design all experiments leading to Figures 2.11 – 2.21. Shengyong Ng, Sandra March and Ani Galstian performed the experiments and analyzed the data for Figures 2.12 – 2.21. Kirsten Hanson and Tania Carvalho performed the experiment and analyzed the data for Figure 2.11. Kartik Trehan, Shengyong Ng, Sandra March, Ani Galstian and Robert Schwartz performed the experiment and analyzed the data for Figure 2.22.

Chapter 3: Personalizing the Study of Liver-Stage Malaria Infection

Shengyong Ng led a team to design all experiments leading to Figures 3.1 – 3.6. Robert Schwartz maintained iPS cell cultures, and performed all *in vitro* directed differentiations into iHLCs. Shengyong Ng performed the malaria infection experiments for Figures 3.1 – 3.6 with the help of Sandra March and Ani Galstian, and analyzed the data for Figures 3.1 – 3.6.

Chapter 4: Engineering an Implantable Model of Liver-Stage Malaria

Shengyong Ng led a team to design all experiments leading to Figures 4.1 – 4.4. Shengyong Ng performed the experiments and analyzed the data for Figures 4.1 – 4.4, with the help of Sandra March, Ani Galstian and Kelly Stevens.

SHENGYONG NG

Massachusetts Institute of Technology, Laboratory of Multiscale Regenerative Technologies
500 Main St, Room 76-473, Cambridge, MA 02142
Email: syng@mit.edu; shengyong.ng@gmail.com

EDUCATION

2009 –   Ph.D. candidate in Bioengineering
         Massachusetts Institute of Technology
         Advisors: Sangeeta N. Bhatia, M.D., Ph.D., Robert Langer, Sc.D.

2008   BS in Biomedical Engineering, Concentration in Biomaterials & Cell/Tissue Engineering
         Johns Hopkins University, USA

2002   General Certificate of Education (GCE) Advanced Level
         Hwa Chong Junior College, Singapore

2000   General Certificate of Education (GCE) Ordinary Level
         The Chinese High School, Singapore

PROFESSIONAL EXPERIENCE

2009 –   **Massachusetts Institute of Technology**, Graduate student
         Advisors: Sangeeta N. Bhatia, M.D., Ph.D., Robert Langer, Sc.D.
         Engineered artificial human livers to develop improved in vitro and implantable models of liver-stage malaria for antimalarial drug development, and established stem-cell derived human hepatocytes as an alternative cell source for modeling liver-stage malaria.

2008 –   **Institute of Bioengineering and Nanotechnology, A*STAR, Singapore**, Lab officer
2009   Advisor: Motoichi Kurisawa, Ph.D. Injectable Hydrogels for Nanomedicine Laboratory
         Designed and synthesized nanogel complexes comprising hyaluronic acid-green tea catechin conjugates and proteins for targeted cancer therapy.

2006 –   **Johns Hopkins University**, Undergraduate research assistant
2008   Advisor: Jennifer Elisseeff, Ph.D. Biomaterials & Tissue Engineering Laboratory
         Contributed to the characterization of the potential of collagen vitrigel membranes for the reconstruction of corneal tissue in vitro and in a rabbit model of corneal injury.

2006   **Institute of Bioengineering and Nanotechnology, A*STAR, Singapore**, Research intern
         Advisor: Motoichi Kurisawa, Ph.D. Injectable Hydrogels for Nanomedicine Laboratory
         Carried out in vitro biological characterization of a novel hyaluronic acid-green tea hydrogel in terms of cell adhesion, proliferation and motility.

2005   **Institute of Bioengineering and Nanotechnology, A*STAR, Singapore**, Research intern
         Advisor: Ruan Runsheng, M.D., Ph.D., Cancer and Aging Laboratory

155

Developed a model of the in vitro transformation of normal epithelial cells into pre-malignant cells and subsequently into fully malignant cells.

2002 –
2005

Singapore Armed Forces – Administrative supervisor specialist

2001 –
2002

National University of Singapore, Research intern
Advisor: Matthew L. Whiteman, Ph.D., Free Radical Laboratory, Department of Biochemistry, Faculty of Medicine
Studied the modulation of the peroxynitrite scavenging activity (antioxidant activity) of ascorbic acid in the presence of bicarbonate.

PUBLICATIONS

Ng S., March S., Galstian A., Mota M.M., Bhatia S.N. Modelling liver stage *Plasmodium* infection in humanized mice with ectopic artificial liver tissue. *In preparation*.

Ng S., Schwartz R.E., March S., Galstian A., Bhatia S.N. Establishment of *Plasmodium* hepatic stages in human induced pluripotent stem cell-derived hepatocyte-like cells. *In preparation*.

March S., **Ng S.**, Shan J., Bhatia S.N. Blockade of PI3K Activation Sustains Primary Hepatocyte Function. *In preparation.*

Liang K. *, **Ng S.***, Lee F., Lim J., Chung J.E., Kurisawa M. Self-Assembled Nanogel Based on Hyaluronic Acid-Green Tea Catechin conjugates for Intracellular Protein Delivery. *In preparation.*

2013   **Ng S.**, March S., Galstian A., Hanson K., Carvalho T., Mota M.M., Bhatia S.N. (2013). Hypoxia Promotes Liver Stage Malaria Infection of Primary Human Hepatocytes *In Vitro*. *Disease Models & Mechanisms*, 7: 215-224.

2013   March S., **Ng S.**, Velmurugan S., Galstian A., Shan J., Logan D., Carpenter A.E., Thomas D., Sim B.K.L., Mota M.M., Hoffman S.L., Bhatia S.N. (2013). A microscale human liver platform that supports the hepatic stages of *Plasmodium falciparum* and *vivax*, *Cell Host Microbe* 14, 104–115.

2013   Stevens, KR, Ungrin, MD, Schwartz, RE, **Ng, S**, Carvalho, B, Christine, KS, Chaturvedi, R, Li, CY, Zandstra, PW, Chen, CS, and Bhatia, SN. (2013). InVERT molding for scalable control of tissue microarchitecture, *Nature Communications*. 4:1847.

2009

Ambrose W.M., Salahuddin A., So S., **Ng S.**, Ponce Marquez S., Takezawa T., Schein O. and Elisseeff J. (2009). Collagen Vitrigel Membranes for the in vitro Reconstruction of Separate

Corneal Epithelial, Stromal and Endothelial Cell Layers. *Journal of Biomedical Materials Research Part B – Applied Biomaterials.* 90B(2), 818 – 831.

CONFERENCES AND TALKS

2014   **Ng S.**, March S., Galstian A., Thomas D., Bhatia S.N.. Profiling Anti-Malarials for Loss of Efficacy in Endemic Regions. Grand Challenges Explorations Malaria Box Meeting, Tres Cantos, Spain, March 2014. (Invited Talk)

2014   **Ng S.**, March S., Bhatia S.N.. Hepatic Tissue Engineering for Modeling Liver-Stage Malaria. Novartis Institute of Tropical Diseases, Singapore, February 2014. (Invited Talk)

2013   **Ng S.**, March S., Galstian A., Hanson K., Carvalho T., Mota MM.., Bhatia S.N. Hypoxia Promotes Liver-Stage Malaria Infection in Primary Human Hepatocytes *In Vitro*. Biomedical Engineering Society Annual Meeting, Seattle, WA, USA, September 2013. (Poster + Accepted Talk)

2013   **Ng S.**, March S., Galstian A., Mota M.M., Bhatia S.N. Modeling Liver Stage Malaria in Humanized Mice with Engineered Artificial Human Livers. Gordon Research Conference - Biomaterials & Tissue Engineering, Holderness, NH, USA, August 2013. (Poster)

2013   **Ng S.**, March S., Galstian A., Bhatia S.N. *In Vitro* and *In Vivo* Human Liver Platforms for Malaria Drug Development. Broad Institute, Cambridge, MA, USA, May 2013. (Invited Talk)

2013   March S., **Ng S.**, Velmurugan S., Galstian A., Shan J., Logan D., Carpenter A.E., Thomas D., Sim B.K.L., Mota M.M., Hoffman S.L., Bhatia S.N. (2013): A microscale human liver platform that supports the hepatic stages of *Plasmodium falciparum* and *vivax*. Bill and Melinda Gates Foundation Malaria Meeting, Boston, MA, USA, March 2013. (Poster)

2013   **Ng S.**, March S., Galstian A., Mota M.M., Bhatia S.N. Hypoxia Promotes Liver-Stage Malaria Infection in Primary Human Hepatocytes *In Vitro*. Bioengineering and Toxicology Seminar Series, MIT Department of Biological Engineering, Cambridge MA, USA, March 2013.

2013   **Ng S.**, March S., Galstian A., Mota M.M., Bhatia S.N. Hypoxia Promotes Liver-Stage Malaria Infection in Primary Human Hepatocytes *In Vitro*. Keystone Symposium Malaria (A8), New Orleans, LA, USA, January 2013. (Poster + Invited Talk)

2012   **Ng S.**, March S., Galstian A., Mota M.M., Bhatia S.N. Hypoxia Promotes Liver-Stage Malaria Infection in Primary Human Hepatocytes *In Vitro*. Annual Meeting of the American Society for Tropical Medicine and Hygiene (ASTMH), Atlanta, GA, USA, November 2012. (Poster)

2011   **Ng S.**, March S., Galstian A., Mota M.M., Bhatia S.N. A Microscale Human Liver Platform for

Modeling Liver-Stage Malaria. Bioengineering and Toxicology Seminar Series, MIT Department of Biological Engineering, Cambridge MA, USA, November 2011.

2008   Ambrose W.M., Wang J., **Ng S.**, Takezawa T. and Elisseeff J. Corneal Epithelial and Neural Cell Growth Over Growth Factor/Peptide Bulk Modified Collagen Vitrigels. Annual Meeting of the Association for Research in Vision and Ophthalmology (ARVO). Ft. Lauderdale, FL, May 2008. (Poster)

2007   Ambrose W.M., So S., **Ng S.**, Zhuang W., Park C. Y., Chuck R., Takezawa T. and Elisseeff J. Collagen Vitrigel as a Substrate for Bioengineered Cell Sheet Transplantation in Rabbit Corneas. Annual Meeting of the Biomedical Engineering Society (BMES), Los Angeles, September 2007. (Poster)

PATENTS

2011   Bhatia S.N., Chen A.A., **Ng S.**. Humanized Animals Via Tissue Engineering and Uses Thereof. US Patent Application filed Oct 6, 2011 by MIT

2009   **Ng S.**, Chung J. E., Kurisawa M. Self-assembled Nanogel Complexes Comprising Hyaluronic Acid-Green Tea Catechin Conjugates and Intrabodies for Targeted Cancer Therapy. US Provisional Patent filed August 2009 by IBN, A*STAR, Singapore.

BOOK CHAPTERS

2012   Stevens K.R., Schwartz R.E., **Ng S.**, Shan J., Bhatia S.N. Hepatic Tissue Engineering, in Principles of Tissue Engineering, 4th Edition, Lanza, Langer, and Vacanti (eds). Elsevier. (2012) ISBN: 9780123983589.

TEACHING EXPERIENCE

2011   Teaching Assistant, Molecular, Cellular and Tissue Biomechanics (MIT 20.310)
2003 – Academic tutor to 5 high school students in mathematics and chemistry
2005

OTHER ACTIVITIES

2013 – Biomedical Engineering Society
2012 – American Society for Tropical Medicine and Hygiene
2007 – Tau Beta Pi Engineering Society

AWARDS

2011	MIT Department of Biological Engineering Outstanding Teaching Assistant Award
2009	A*STAR National Science Scholarship (PhD)
2009	A*STAR Roll of Honor
2008	Johns Hopkins University Richard J. Johns Award for Outstanding Academic Achievement
2008	University of San Francisco Business Plan Competition – Semifinalist
2008	Johns Hopkins University Business Plan Competition 2008 4th Place
2008	Johns Hopkins University Dean's List
2005	Best Soldier Award (Unit Level), Singapore Armed Forces
2003	A*STAR National Science Scholarship (BS)
2003	Hwa Chong Junior College Commendation Award
2002	Hwa Chong Junior College Scholarship
2001	Ministry of Education Edusave Merit Bursary
2001	2nd Singapore Biology Olympiad; Certificate of Merit
2001	The Chinese High School Distinguished Scholar Award